Averages of b-hadron Properties as of Summer 2004

Heavy Flavor Averaging Group (HFAG)*

February 7, 2008

Abstract

This article reports world averages for measurements on b-hadron properties obtained by the Heavy Flavor Averaging Group (HFAG) using the available results as of summer 2004 conferences. In the averaging, the input parameters used in the various analyses are adjusted (rescaled) to common values, and all known correlations are taken into account. The averages include b-hadron lifetimes, B-oscillation (mixing) parameters, semileptonic decay parameters, rare decay branching fractions, and CP violation measurements.

*The members of the HFAG and those involved in the subgroup activities are: J. Alexander, M. Artuso, M. Battaglia, E. Barberio, T.E. Browder, P. Chang, L. Di Ciaccio, H. Evans, T. Gershon, L. Gibbons, A. Höcker, T. Iijima, D. Kirkby, U. Langenegger, A. Limosani, O. Long, D. Lucchesi, V. Luth, T. Nozaki, Y. Sakai, O. Schneider, C. Schwanda, M. Shapiro, J. Smith, A. Stocchi, R. Van Kooten, C. Weiser, and W. Yao

Contents

1 Introduction **4**

2 Methodology **5**

3 Averages of b-hadron fractions, lifetimes and mixing parameters **10**
3.1 b-hadron production fractions . . . 11
3.1.1 b-hadron fractions in $\Upsilon(4S)$ decays . . . 11
3.1.2 b-hadron fractions at high energy . . . 13
3.2 b-hadron lifetimes . . . 15
3.2.1 Lifetime measurements, uncertainties and correlations . . . 16
3.2.2 Inclusive b-hadron lifetimes . . . 17
3.2.3 B^0 and B^+ lifetimes . . . 18
3.2.4 B_s^0 lifetime . . . 20
3.2.5 B_c^+ lifetime . . . 22
3.2.6 Λ_b^0 and b-baryon lifetimes . . . 23
3.2.7 Summary and comparison to theoretical predictions . . . 24
3.3 Neutral B-meson mixing . . . 24
3.3.1 B^0 mixing parameters . . . 26
3.3.2 B_s^0 mixing parameters . . . 29

4 Semileptonic B decays **37**
4.1 Exclusive Cabibbo-favored decays . . . 37
4.1.1 $\overline{B}^0 \to D^{*+}\ell^-\overline{\nu}$ . . . 38
4.1.2 $\overline{B}^0 \to D^+\ell^-\overline{\nu}$ . . . 40
4.2 Inclusive Cabibbo-favored decays . . . 42
4.2.1 Total semileptonic branching fraction . . . 43
4.2.2 Partial semileptonic branching fraction . . . 44
4.2.3 Determination of $|V_{cb}|$ . . . 44
4.3 Exclusive Cabibbo-suppressed decays . . . 44
4.4 Inclusive Cabibbo-suppressed decays . . . 45
4.4.1 Determination of $|V_{ub}|$ . . . 45
4.4.2 Discussion . . . 49

5 Measurements related to Unitarity Triangle angles **49**
5.1 Introduction . . . 50
5.2 Notations . . . 51
5.2.1 CP asymmetries . . . 51
5.2.2 Time-dependent CP asymmetries in decays to CP eigenstates . . . 52
5.2.3 Time-dependent CP asymmetries in decays to vector-vector final states . . . 53
5.2.4 Time-dependent CP asymmetries in decays to non-CP eigenstates . . . 53
5.2.5 Asymmetries in $B \to D^{(*)}K^{(*)}$ decays . . . 57
5.3 Common inputs and error treatment . . . 58
5.4 Time-dependent CP asymmetries in $b \to c\overline{c}s$ transitions . . . 59
5.5 Time-dependent transversity analysis of $B^0 \to J/\psi K^{*0}$ . . . 60
5.6 Time-dependent CP asymmetries in $b \to q\overline{q}s$ transitions . . . 62

5.7 Time-dependent CP asymmetries in $b \to c\bar{c}d$ transitions 64
5.8 Time-dependent asymmetries in $b \to s\gamma$ transitions 66
5.9 Time-dependent CP asymmetries in $b \to u\bar{u}d$ transitions 68
5.10 Time-dependent CP asymmetries in $b \to c\bar{u}d/u\bar{c}d$ transitions 71
5.11 Rates and asymmetries in $B^{\mp} \to D^{(*)}K^{(*)\mp}$ decays 71

6 Averages of charmless B-decay branching fractions and their asymmetries 74
6.1 Mesonic charmless decays 74
6.2 Radiative and leptonic decays 77
6.3 Baryonic decays 80
6.4 Charge asymmetries 80

7 Summary 83

1 Introduction

The flavor dynamics is one of the important elements in understanding the nature of particle physics. The accurate knowledge of properties of heavy flavor hadrons, especially b hadrons, play an essential role for determination of the Cabbibo-Kobayashi-Maskawa (CKM) matrix [1]. Since asymmetric B factories started their operation, available amounts of B meson samples has been dramatically increased and the accuracies of measurements have been improved.

The Heavy Flavor Averaging Group (HFAG) has been formed, continuing the activities of LEP Heavy Flavor Steering group [2], to provide the averages for measurements dedicated to the b-flavor related quantities. The HFAG consists of representatives and contacts from the experimental groups: *BABAR*, Belle, CDF, CLEO, DØ, and LEP.

The HFAG is currently organized into four subgroups.

- the "Lifetime and mixing" group provides averages for b-hadron lifetimes, b-hadron fractions in $\Upsilon(4S)$ decay and high energy collisions, and various parameters in B^0 and B_s^0 oscillation (mixing).

- the "Semileptonic B decays" group provides averages for inclusive and exclusive B-decay branching fractions, and best values of the CKM matrix elements $|V_{cb}|$ and $|V_{ub}|$.

- the "$CP(t)$ and Unitarity Triangle angles" group provides averages for time-dependent CP asymmetry parameters and angles of the unitarity triangles.

- the "Rare decays" group provides averages of branching fractions and their asymmetries between B and $\overline{B}$ for charmless mesonic, radiative, leptonic, and baryonic B decays.

The first two subgroups continue the activities from LEP working groups with some reorganization (merging four groups into two groups). The latter two groups are newly formed to take care of new results which are available from asymmetric B factory experiments.

In this article, we report the world averages using the available results as of summer 2004 conferences (ICHEP04 and FPCP04). All results that are publicly available, including recent preliminary results, are used in averages. We do not use preliminary results which remain unpublished for a long time or for which no publication is planned. Close contacts have been established between representatives from the experiments and members of different subgroups in charge of the averages, to ensure that the data are prepared in a form suitable for combinations.

We do not scale the error of an average (as is presently done by the Particle Data Group [3]) in case $\chi^2/\mathrm{dof} > 1$, where dof is the number of degrees of freedom in the average calculation. In this case, we examine the systematics of each measurement and try to understand them. Unless we find possible systematic discrepancies between the measurements, we do not make any special treatment for the calculated error. We provide the confidence level of the fit so that one can know the consistency of the measurements included in the average. We attach a warning message in case that some special treatment is done or the approximation used in the average calculation may not be good enough (*e.g.*, Gaussian error is used in averaging though the likelihood indicates non-Gaussian behavior).

Section 2 describes the methodology for averaging various quantities in the HFAG. In the averaging, the input parameters used in the various analyses are adjusted (rescaled) to common values, and, where possible, known correlations are taken into account. The general philosophy and tools for calculations of averages are presented.

Sections 3–6 describe the averaging of the quantities from each subgroup mentioned above. A summary of the averages described in this article is given in Sec. 7.

The complete listing of averages and plots described in this article are also available on the HFAG Web page:

`http://www.slac.stanford.edu/xorg/hfag` and
`http://belle.kek.jp/mirror/hfag` (KEK mirror site).

2 Methodology

The general averaging problem that HFAG faces is to combine the information provided by different measurements of the same parameter, to obtain our best estimate of the parameter's value and uncertainty. The methodology described here focuses on the problems of combining measurements performed with different systematic assumptions and with potentially-correlated systematic uncertainties. Our methodology relies on the close involvement of the people performing the measurements in the averaging process.

Consider two hypothetical measurements of a parameter x, which might be summarized as

$$x = x_1 \pm \delta x_1 \pm \Delta x_{1,1} \pm \Delta x_{2,1} \ldots$$
$$x = x_2 \pm \delta x_2 \pm \Delta x_{1,2} \pm \Delta x_{2,2} \ldots \ ,$$

where the δx_k are statistical uncertainties, and the $\Delta x_{i,k}$ are contributions to the systematic uncertainty. One popular approach is to combine statistical and systematic uncertainties in quadrature

$$x = x_1 \pm (\delta x_1 \oplus \Delta x_{1,1} \oplus \Delta x_{2,1} \oplus \ldots)$$
$$x = x_2 \pm (\delta x_2 \oplus \Delta x_{1,2} \oplus \Delta x_{2,2} \oplus \ldots)$$

and then perform a weighted average of x_1 and x_2, using their combined uncertainties, as if they were independent. This approach suffers from two potential problems that we attempt to address. First, the values of the x_k may have been obtained using different systematic assumptions. For example, different values of the B^0 lifetime may have been assumed in separate measurements of the oscillation frequency Δm_d. The second potential problem is that some contributions of the systematic uncertainty may be correlated between experiments. For example, separate measurements of Δm_d may both depend on an assumed Monte-Carlo branching fraction used to model a common background.

The problems mentioned above are related since, ideally, any quantity y_i that x_k depends on has a corresponding contribution $\Delta x_{i,k}$ to the systematic error which reflects the uncertainty Δy_i on y_i itself. We assume that this is the case, and use the values of y_i and Δy_i assumed by each measurement explicitly in our averaging (we refer to these values as $y_{i,k}$ and $\Delta y_{i,k}$ below). Furthermore, since we do not lump all the systematics together, we require that each measurement used in an average have a consistent definition of the various contributions to the systematic uncertainty. Different analyses often use different decompositions of their systematic uncertainties, so achieving consistent definitions for any potentially correlated contributions requires close coordination between HFAG and the experiments. In some cases, a group of systematic uncertainties must be lumped to obtain a coarser description that is consistent between measurements. Systematic uncertainties that are uncorrelated with any other sources

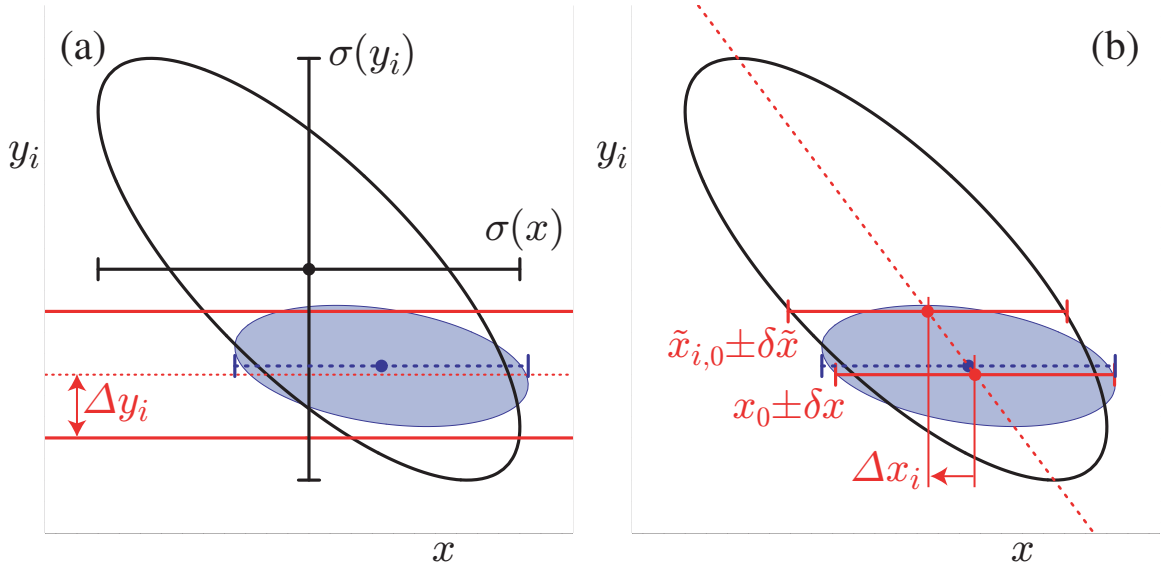

Figure 1: The left-hand plot, (a), compares the 68% confidence-level contours of a hypothetical measurement's unconstrained (large ellipse) and constrained (filled ellipse) likelihoods, using the Gaussian constraint on y_i represented by the horizontal band. The solid error bars represent the statistical uncertainties, $\sigma(x)$ and $\sigma(y_i)$, of the unconstrained likelihood. The dashed error bar shows the statistical error on x from a constrained simultaneous fit to x and y_i. The right-hand plot, (b), illustrates the method described in the text of performing fits to x only with y_i fixed at different values. The dashed diagonal line between these fit results has the slope $\rho(x, y_i)\sigma(y_i)/\sigma(x)$ in the limit of a parabolic unconstrained likelihood. The result of the constrained simultaneous fit from (a) is shown as a dashed error bar on x.

of uncertainty appearing in an average are lumped with the statistical error, so that the only systematic uncertainties treated explicitly are those that are correlated with at least one other measurement via a consistently-defined external parameter y_i. When asymmetric statistical or systematic uncertainties are quoted, we symmetrize them since our combination method implicitly assumes parabolic likelihoods for each measurement.

The fact that a measurement of x is sensitive to the value of y_i indicates that, in principle, the data used to measure x could equally-well be used for a simultaneous measurement of x and y_i, as illustrated by the large contour in Fig. 1(a) for a hypothetical measurement. However, we often have an external constraint Δy_i on the value of y_i (represented by the horizontal band in Fig. 1(a)) that is more precise than the constraint $\sigma(y_i)$ from our data alone. Ideally, in such cases we would perform a simultaneous fit to x and y_i, including the external constraint, obtaining the filled (x, y) contour and corresponding dashed one-dimensional estimate of x shown in Fig. 1(a). Throughout, we assume that the external constraint Δy_i on y_i is Gaussian.

In practice, the added technical complexity of a constrained fit with extra free parameters is not justified by the small increase in sensitivity, as long as the external constraints Δy_i are sufficiently precise when compared with the sensitivities $\sigma(y_i)$ to each y_i of the data alone. Instead, the usual procedure adopted by the experiments is to perform a baseline fit with all y_i fixed to nominal values $y_{i,0}$, obtaining $x = x_0 \pm \delta x$. This baseline fit neglects the uncertainty due to Δy_i, but this error can be mostly recovered by repeating the fit separately for each external

parameter y_i with its value fixed at $y_i = y_{i,0} + \Delta y_i$ to obtain $x = \tilde{x}_{i,0} \pm \delta\tilde{x}$, as illustrated in Fig. 1(b). The absolute shift, $|\tilde{x}_{i,0} - x_0|$, in the central value of x is what the experiments usually quote as their systematic uncertainty Δx_i on x due to the unknown value of y_i. Our procedure requires that we know not only the magnitude of this shift but also its sign. In the limit that the unconstrained data is represented by a parabolic likelihood, the signed shift is given by

$$\Delta x_i = \rho(x, y_i)\frac{\sigma(x)}{\sigma(y_i)}\,\Delta y_i \ , \tag{1}$$

where $\sigma(x)$ and $\rho(x, y_i)$ are the statistical uncertainty on x and the correlation between x and y_i in the unconstrained data. While our procedure is not equivalent to the constrained fit with extra parameters, it yields (in the limit of a parabolic unconstrained likelihood) a central value x_0 that agrees to $\mathcal{O}(\Delta y_i/\sigma(y_i))^2$ and an uncertainty $\delta x \oplus \Delta x_i$ that agrees to $\mathcal{O}(\Delta y_i/\sigma(y_i))^4$.

In order to combine two or more measurements that share systematics due to the same external parameters y_i, we would ideally perform a constrained simultaneous fit of all data samples to obtain values of x and each y_i, being careful to only apply the constraint on each y_i once. This is not practical since we generally do not have sufficient information to reconstruct the unconstrained likelihoods corresponding to each measurement. Instead, we perform the two-step approximate procedure described below.

Figs. 2(a,b) illustrate two statistically-independent measurements, $x_1 \pm (\delta x_1 \oplus \Delta x_{i,1})$ and $x_2 \pm (\delta x_i \oplus \Delta x_{i,2})$, of the same hypothetical quantity x (for simplicity, we only show the contribution of a single correlated systematic due to an external parameter y_i). As our knowledge of the external parameters y_i evolves, it is natural that the different measurements of x will assume different nominal values and ranges for each y_i. The first step of our procedure is to adjust the values of each measurement to reflect the current best knowledge of the values y_i' and ranges $\Delta y_i'$ of the external parameters y_i, as illustrated in Figs. 2(c,b). We adjust the central values x_k and correlated systematic uncertainties $\Delta x_{i,k}$ linearly for each measurement (indexed by k) and each external parameter (indexed by i):

$$x_k' = x_k + \sum_i \frac{\Delta x_{i,k}}{\Delta y_{i,k}}\,(y_i' - y_{i,k}) \tag{2}$$

$$\Delta x_{i,k}' = \Delta x_{i,k} \cdot \frac{\Delta y_i'}{\Delta y_{i,k}} \ . \tag{3}$$

This procedure is exact in the limit that the unconstrained likelihoods of each measurement is parabolic.

The second step of our procedure is to combine the adjusted measurements, $x_k' \pm (\delta x_k \oplus \Delta x_{k,1}' \oplus \Delta x_{k,2}' \oplus \ldots)$ using the chi-square

$$\chi^2_{\rm comb}(x, y_1, y_2, \ldots) \equiv \sum_k \frac{1}{\delta x_k^2}\left[x_k' - \left(x + \sum_i (y_i - y_i')\frac{\Delta x_{i,k}'}{\Delta y_i'}\right)\right]^2 + \sum_i \left(\frac{y_i - y_i'}{\Delta y_i'}\right)^2 \ , \tag{4}$$

and then minimize this χ^2 to obtain the best values of x and y_i and their uncertainties, as illustrated in Fig. 3. Although this method determines new values for the y_i, we do not report them since the $\Delta x_{i,k}$ reported by each experiment are generally not intended for this purpose (for example, they may represent a conservative upper limit rather than a true reflection of a 68% confidence level).

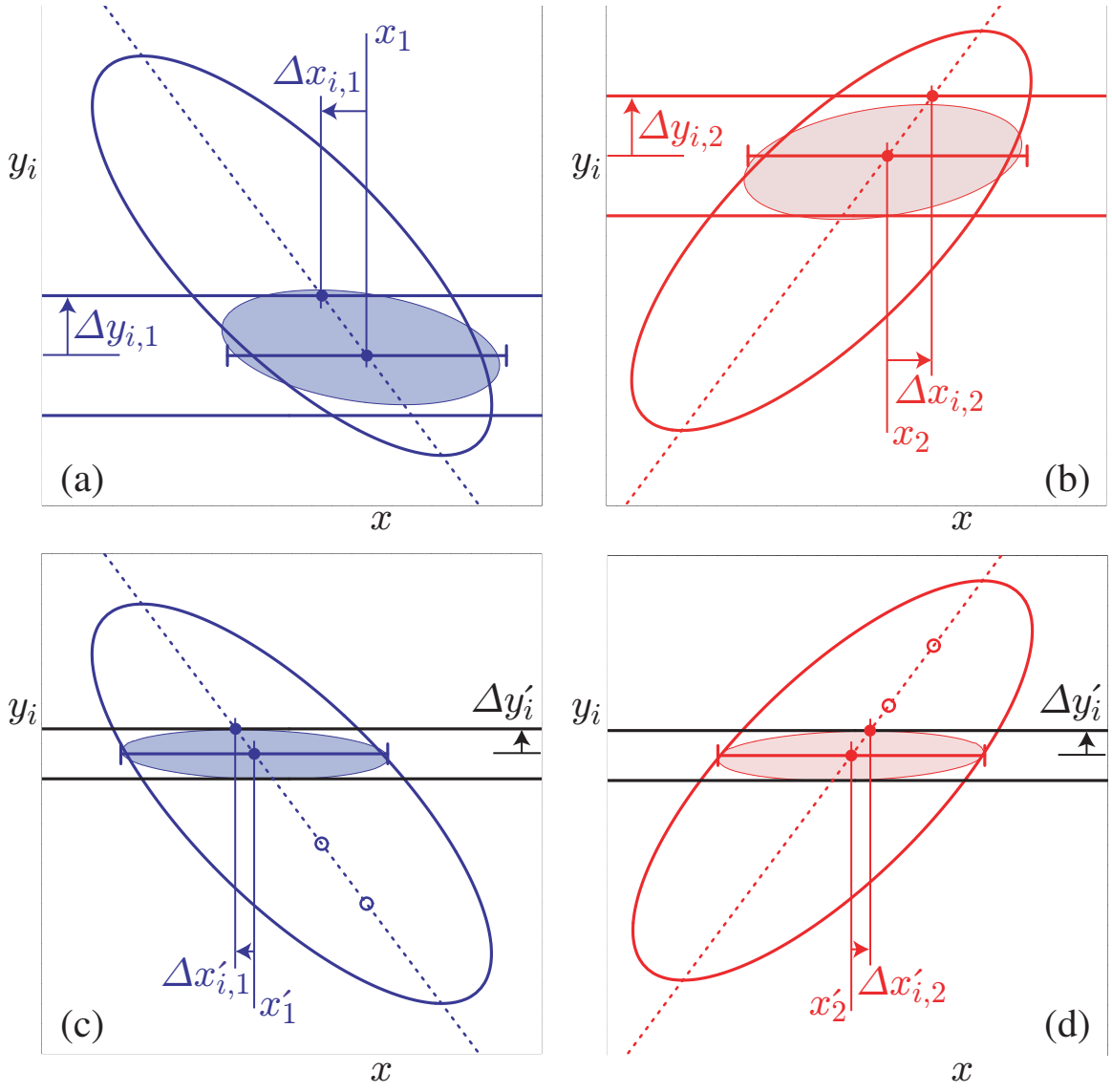

Figure 2: The upper plots, (a) and (b), show examples of two individual measurements to be combined. The large ellipses represent their unconstrained likelihoods, and the filled ellipses represent their constrained likelihoods. Horizontal bands indicate the different assumptions about the value and uncertainty of y_i used by each measurement. The error bars show the results of the approximate method described in the text for obtaining x by performing fits with y_i fixed to different values. The lower plots, (c) and (d), illustrate the adjustments to accommodate updated and consistent knowledge of y_i described in the text. Hollow circles mark the central values of the unadjusted fits to x with y fixed, which determine the dashed line used to obtain the adjusted values.

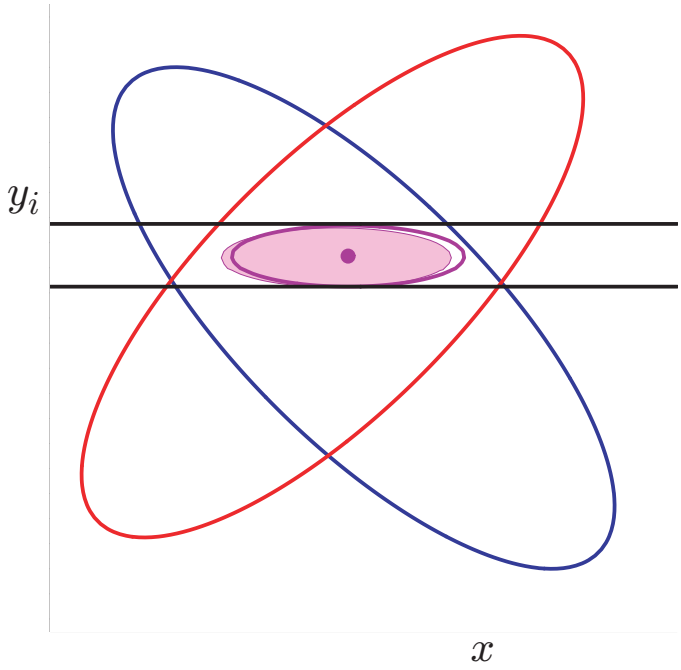

Figure 3: An illustration of the combination of two hypothetical measurements of x using the method described in the text. The ellipses represent the unconstrained likelihoods of each measurement and the horizontal band represents the latest knowledge about y_i that is used to adjust the individual measurements. The filled small ellipse shows the result of the exact method using $\mathcal{L}_{\rm comb}$ and the hollow small ellipse and dot show the result of the approximate method using $\chi^2_{\rm comb}$.

For comparison, the exact method we would perform if we had the unconstrained likelihoods $\mathcal{L}_k(x, y_1, y_2, \ldots)$ available for each measurement is to minimize the simultaneous constrained likelihood

$$\mathcal{L}_{\rm comb}(x, y_1, y_2, \ldots) \equiv \prod_k \mathcal{L}_k(x, y_1, y_2, \ldots) \prod_i \mathcal{L}_i(y_i) \ , \tag{5}$$

with an independent Gaussian external constraint on each y_i

$$\mathcal{L}_i(y_i) \equiv \exp\left[-\frac{1}{2}\left(\frac{y_i - y_i'}{\Delta y_i'}\right)^2\right] \ . \tag{6}$$

The results of this exact method are illustrated by the filled ellipses in Figs. 3(a,b), and agree with our method in the limit that each $\mathcal{L}_k$ is parabolic and that each $\Delta y_i' \ll \sigma(y_i)$. In the case of a non-parabolic unconstrained likelihood, experiments would have to provide a description of $\mathcal{L}_k$ itself to allow an improved combination. In the case of some $\sigma(y_i) \simeq \Delta y_i'$, experiments are advised to perform a simultaneous measurement of both x and y so that their data will improve the world knowledge about y.

The algorithm described above is used as a default in the averages reported in the following sections. For some cases, somewhat simplified or more complex algorithms are used and noted in the corresponding sections.

Following the prescription described above, the central values and errors are rescaled to a common set of input parameters in the averaging procedures, according to the dependency on any of these input parameters. We try to use the most up-to-date values for these common inputs and the same values among the HFAG subgroups. For the parameters whose averages are produced by the HFAG, we use the updated values in the current update cycle. For other external parameters, we use the most recent PDG values.

The parameters and values used in this update cycle are listed in each subgroup section.

3 Averages of *b*-hadron fractions, lifetimes and mixing parameters

Quantities such as b-hadron production fractions, b-hadron lifetimes, and neutral B-meson oscillation frequencies have been measured for many years at high-energy colliders, namely LEP and SLC (e^+e^- colliders at $\sqrt{s} = m_Z$) as well as Tevatron Run I ($p\overline{p}$ collider at $\sqrt{s} = 1.8$ TeV). More recently, precise measurements of the B^0 and B^+ lifetimes, as well as of the B^0 oscillation frequency, have also been performed at the asymmetric B factories, KEKB and PEPII (e^+e^- colliders at $\sqrt{s} = m_{\Upsilon(4S)}$). In most cases, these basic quantities, although interesting by themselves, can now be seen as necessary ingredients for the more complicated and refined analyses being currently performed at the asymmetric B factories and at the Tevatron Run II ($\sqrt{s} = 2$ TeV), in particular the time-dependent CP measurements. It is therefore important that the best experimental values of these quantities continue to be kept up-to-date and improved.

In several cases, the averages presented in this chapter are indeed needed and used as input for the results given in the subsequent chapters. However, within this chapter, some averages need the knowledge of other averages in a circular way. This "coupling", which appears through the b-hadron fractions whenever inclusive or semi-exclusive measurements have to be considered,

has been reduced significantly in the last years with increasingly precise exclusive measurements becoming available. To cope with this circularity, a rather involved averaging procedure had been developed, in the framework of the former LEP Heavy Flavour Steering Group. This is still in use now (details can be found in [2]), although simplifications can be envisaged in the future when even more precise exclusive measurements become available.

3.1 *b*-hadron production fractions

We consider here the relative fractions of the different b-hadron species found in an unbiased sample of weakly-decaying b hadrons produced under some specific conditions. The knowledge of these fractions is useful to characterize the signal composition in inclusive b-hadron analyses, or to predict the background composition in exclusive analyses. Many analyses in B physics need these fractions as input. We distinguish here the following two conditions: $\Upsilon(4S)$ decays and high-energy collisions.

3.1.1 *b*-hadron fractions in $\Upsilon(4S)$ decays

Only pairs of the two lightest (charged and neutral) B mesons can be produced in $\Upsilon(4S)$ decays, and it is enough to determine the following branching fractions:

$$f^{+-} = \Gamma(\Upsilon(4S) \to B^+B^-)/\Gamma_{\rm tot}(\Upsilon(4S))\,, \tag{7}$$

$$f^{00} = \Gamma(\Upsilon(4S) \to B^0\overline{B}^0)/\Gamma_{\rm tot}(\Upsilon(4S))\,. \tag{8}$$

In practice, most analyses measure their ratio

$$R^{+-/00} = f^{+-}/f^{00} = \Gamma(\Upsilon(4S) \to B^+B^-)/\Gamma(\Upsilon(4S) \to B^0\overline{B}^0)\,, \tag{9}$$

which is easier to access experimentally. Since an inclusive (but separate) reconstruction of B^+ and B^0 is difficult, specific exclusive decay modes, $B^+ \to x^+$ and $B^0 \to x^0$, are usually considered to perform a measurement of $R^{+-/00}$, whenever they can be related by isospin symmetry (for example $B^+ \to J/\psi K^+$ and $B^0 \to J/\psi K^0$). Under the assumption that $\Gamma(B^+ \to x^+) = \Gamma(B^0 \to x^0)$, *i.e.* that isospin invariance holds in these B decays, the ratio of the number of reconstructed $B^+ \to x^+$ and $B^0 \to x^0$ mesons is proportional to

$$\frac{f^{+-}\,B(B^+ \to x^+)}{f^{00}\,B(B^0 \to x^0)} = \frac{f^{+-}\,\Gamma(B^+ \to x^+)\,\tau(B^+)}{f^{00}\,\Gamma(B^0 \to x^0)\,\tau(B^0)} = \frac{f^{+-}}{f^{00}}\,\frac{\tau(B^+)}{\tau(B^0)}\,, \tag{10}$$

where $\tau(B^+)$ and $\tau(B^0)$ are the B^+ and B^0 lifetimes respectively. Hence the primary quantity measured in these analyses is $R^{+-/00}\,\tau(B^+)/\tau(B^0)$, and the extraction of $R^{+-/00}$ with this method therefore requires the knowledge of the $\tau(B^+)/\tau(B^0)$ lifetime ratio.

The published measurements of $R^{+-/00}$ are listed in Table 1 together with the corresponding assumed values of $\tau(B^+)/\tau(B^0)$. All measurements are based on the above-mentioned method, except the one from Belle, which is a by-product of the B^0 mixing frequency analysis using dilepton events (but note that it also assumes isospin invariance, namely $\Gamma(B^+ \to \ell^+{\rm X}) = \Gamma(B^0 \to \ell^+{\rm X})$). The latter is therefore treated in a slightly different manner in the following procedure used to combine these measurements:

Table 1: Published measurements of the B^+/B^0 production ratio in $\Upsilon(4S)$ decays, together with their average (see text). Systematic uncertainties due to the imperfect knowledge of $\tau(B^+)/\tau(B^0)$ are included.

Experiment and year	Ref.	Decay modes or method	Published value of $R^{+-/00} = f^{+-}/f^{00}$	Assumed value of $\tau(B^+)/\tau(B^0)$
CLEO, 2001	[4]	$J/\psi K^{(*)}$	$1.04 \pm 0.07 \pm 0.04$	1.066 ± 0.024
BABAR, 2002	[5]	$(c\overline{c})K^{(*)}$	$1.10 \pm 0.06 \pm 0.05$	1.062 ± 0.029
CLEO, 2002	[6]	$D^*\ell\nu$	$1.058 \pm 0.084 \pm 0.136$	1.074 ± 0.028
Belle, 2003	[7]	dilepton events	$1.01 \pm 0.03 \pm 0.09$	1.083 ± 0.017
BABAR, 2004	[8]	$J/\psi K$	$1.006 \pm 0.036 \pm 0.031$	1.083 ± 0.017
Average			1.010 ± 0.038 (tot)	1.081 ± 0.015

- each published value of $R^{+-/00}$ from CLEO and *BABAR* is first converted back to the original measurement of $R^{+-/00}\,\tau(B^+)/\tau(B^0)$, using the value of the lifetime ratio assumed in the corresponding analysis;
- a simple weighted average of these original measurements of $R^{+-/00}\,\tau(B^+)/\tau(B^0)$ from CLEO and *BABAR* (which do not depend on the assumed value of the lifetime ratio) is then computed, assuming no statistical or systematic correlations between them;
- the weighted average of $R^{+-/00}\,\tau(B^+)/\tau(B^0)$ is converted into a value of $R^{+-/00}$, using the latest average of the lifetime ratios, $\tau(B^+)/\tau(B^0) = 1.081 \pm 0.015$ (see Sec. 3.2.3);
- the Belle measurement of $R^{+-/00}$ is adjusted to the current values of $\tau(B^0) = 1.534 \pm 0.013$ ps and $\tau(B^+)/\tau(B^0) = 1.081 \pm 0.015$ (see Sec. 3.2.3), using the quoted systematic uncertainties due to these parameters;
- the combined value of $R^{+-/00}$ from CLEO and *BABAR* is averaged with the adjusted value of $R^{+-/00}$ from Belle, assuming a 100% correlation of the systematic uncertainty due to the limited knowledge on $\tau(B^+)/\tau(B^0)$; no other correlation is considered.

The resulting global average,

$$R^{+-/00} = \frac{f^{+-}}{f^{00}} = 1.010 \pm 0.038\,, \tag{11}$$

is consistent with an equal production of charged and neutral B mesons.

On the other hand, the *BABAR* collaboration has recently performed a direct measurement of the f^{00} fraction using a novel method, which does not rely on isospin symmetry nor requires the knowledge of $\tau(B^+)/\tau(B^0)$. Its preliminary analysis, based on a comparison between the number of events where a single $B^0 \to D^{*-}\ell^+\nu$ decay could be reconstructed and the number of events where two such decays could be reconstructed, yields [9]

$$f^{00} = 0.486 \pm 0.010\,(\text{stat}) \pm 0.009\,(\text{syst})\,. \tag{12}$$

The two results of Eqs. (11) and (12) are of very different natures and completely independent of each other. Their product is equal to $f^{+-} = 0.491 \pm 0.023$, while another combination

of them gives $f^{+-} + f^{00} = 0.977 \pm 0.033$, compatible with unity. Assuming $f^{+-} + f^{00} = 1$, also consistent with CLEO's observation that the fraction of $\Upsilon(4S)$ decays to $B\overline{B}$ pairs is larger than 0.96 at 95% CL [10], the results of Eqs. (11) and (12) can be averaged (first converting Eq. (11) into a value of $f^{00} = 1/(R^{+-/00} + 1)$) to yield the following more precise estimates:

$$f^{00} = 0.494 \pm 0.008\,, \quad f^{+-} = 1 - f^{00} = 0.506 \pm 0.008\,, \quad \frac{f^{+-}}{f^{00}} = 1.026 \pm 0.032\,. \tag{13}$$

3.1.2 *b*-hadron fractions at high energy

At high energy, all species of weakly-decaying b hadrons can be produced. We assume here that the fractions of these different species are the same in unbiased samples of high-$p_{\rm T}$ b jets originating from Z^0 decays or from $p\overline{p}$ collisions at the Tevatron, either directly or in strong and electromagnetic decays of excited b hadrons. This hypothesis is plausible considering that, in both cases, the last step of the jet hadronization is a non-perturbative QCD process occurring at a scale of order $\Lambda_{\rm QCD}$. On the other hand, there is no strong argument to claim that these fractions should be strictly equal, so this assumption should be checked experimentally. Although the available data is not quite sufficient at this time to perform a significant check, it is expected that the new data from Tevatron Run II will soon improve this situation and allow to confirm or infirm this assumption with reasonable confidence. Meanwhile, the attitude adopted here is that these fractions are assumed to be equal at all high-energy colliders until demonstrated otherwise by experiment.[1]

Contrary to what happens in the charm sector where the fractions of D^+ and D^0 are different, the relative amount of B^+ and B^0 is not affected by the electromagnetic decays of excited B^{+*} and B^{0*} states and strong decays of excited B^{+**} and B^{0**} states. Decays of the type $B_s^{0**} \to B^{(*)}K$ also contribute to the B^+ and B^0 rates, but with the same magnitude if mass effects can be neglected. We therefore assume equal production of B^+ and B^0. We also neglect the production of weakly-decaying states made of several heavy quarks (like B_c^+ and other heavy baryons) which is known to be very small. Hence, for the purpose of determining the b-hadron fractions, we use the constraints

$$f_u = f_d \quad \text{and} \quad f_u + f_d + f_s + f_{\rm baryon} = 1\,, \tag{14}$$

where f_u, f_d, f_s and $f_{\rm baryon}$ are the unbiased fractions of B^+, B^0, B_s^0 and b-baryons, respectively.

The LEP experiments have measured $f_s \times \mathcal{B}(B_s^0 \to D_s^- \ell^+ \nu_\ell X)$ [11], $\mathcal{B}(b \to \Lambda_b^0) \times \mathcal{B}(\Lambda_b^0 \to \Lambda_c^+ \ell^- \overline{\nu}_\ell X)$ [12, 13] and $\mathcal{B}(b \to \Xi_b^-) \times \mathcal{B}(\Xi_b^- \to \Xi^- \ell^- \overline{\nu}_\ell X)$ [14, 15] from partially reconstructed final states including a lepton, $f_{\rm baryon}$ from protons identified in b events [16], and the production rate of charged b hadrons [17]. The various b-hadron fractions have also been measured at CDF using electron-charm final states [18] and double semileptonic decays with $\phi\ell$ and $K^*\ell$ final states [19]. All these published results have been combined following the procedure and assumptions described in [2] to yield $f_u = f_d = 0.403 \pm 0.011$, $f_s = 0.088 \pm 0.021$ and $f_{\rm baryon} = 0.107 \pm 0.019$ under the constraints of Eq. (14). For this combination, other external inputs are used, *e.g.* the branching ratios of B mesons to final states with a D, D^* or D^{**} in semileptonic decays, which are needed to evaluate the fraction of semileptonic B_s^0 decays with a D_s^- in the final state.

[1] It is not unlikely that the b-hadron fractions in low-$p_{\rm T}$ jets at a hadronic machine be different; in particular, beam-remnant effects may enhance the b-baryon production.

Table 2: Fractions of the different b-hadron species in an unbiased sample of weakly-decaying b hadrons produced at high energy, obtained from both direct and mixing measurements.

b-hadron species	Fraction	Correlation coefficients with $f_d = f_u$	and f_s
B^0, B^+	$f_d = f_u = 0.398 \pm 0.010$		
B_s^0	$f_s = 0.104 \pm 0.015$	-0.566	
b baryons	$f_{\rm baryon} = 0.100 \pm 0.017$	-0.712	-0.176

Time-integrated mixing analyses performed with lepton pairs from $b\overline{b}$ events produced at high-energy colliders measure the quantity

$$\overline{\chi} = f'_d\,\chi_d + f'_s\,\chi_s\,, \tag{15}$$

where f'_d and f'_s are the fractions of B^0 and B_s^0 hadrons in a sample of semileptonic b-hadron decays, and where χ_d and χ_s are the B^0 and B_s^0 time-integrated mixing probabilities. Assuming that all b hadrons have the same semileptonic decay width implies $f'_i = f_i R_i$, where $R_i = \tau_i/\tau_b$ is the ratio of the lifetime τ_i of species i to the average b-hadron lifetime $\tau_b = \sum_i f_i \tau_i$. Hence measurements of the mixing probabilities $\overline{\chi}$, χ_d and χ_s can be used to improve our knowledge on the f_u, f_d, f_s and $f_{\rm baryon}$ fractions. In practice, the above relations yield another determination of f_s obtained from $f_{\rm baryon}$ and mixing information,

$$f_s = \frac{1}{R_s}\frac{(1+r)\overline{\chi} - (1 - f_{\rm baryon}R_{\rm baryon})\chi_d}{(1+r)\chi_s - \chi_d}\,, \tag{16}$$

where $r = R_u/R_d = \tau(B^+)/\tau(B^0)$.

The published measurements of $\overline{\chi}$ performed by the LEP experiments have been combined by the LEP Electroweak Working Group to yield $\overline{\chi} = 0.1257 \pm 0.0042$ [20]. This can be compared with a recent measurement from CDF, $\overline{\chi} = 0.152 \pm 0.013$ [21], obtained from an analysis of the Run I data. The two estimates deviate from each other by $1.9\,\sigma$, and could be an indication that the fractions of b hadrons produced at the Z peak or at the Tevatron are not the same. Although this discrepancy is not very significant it should be carefully monitored in the future. We choose to combine these two results in a simple weighted average, assuming no correlations, and, following the PDG prescription, we multiply the combined uncertainty by 1.9 to account for the discrepancy. Our world average is then

$$\overline{\chi} = 0.1282 \pm 0.0077\,. \tag{17}$$

Introducing the latter result in Eq. (16), together with our world average $\chi_d = 0.186 \pm 0.003$ (see Eq. (39) of Sec. 3.3.1), the assumption $\chi_s = 1/2$ (justified by the large value of Δm_s, see Eq. (43) in Sec. 3.3.2), the best knowledge of the lifetimes (see Sec. 3.2) and the estimate of $f_{\rm baryon}$ given above, yields $f_s = 0.120 \pm 0.021$, an estimate dominated by the mixing information. Taking into account all known correlations (including the one introduced by $f_{\rm baryon}$), this result is then combined with the set of fractions obtained from direct measurements (given above), to yield the improved estimates of Table 2, still under the constraints of Eq. (14). As can be seen, our knowledge on the mixing parameters substantially reduces the uncertainty on f_s, despite the rather strong deweighting introduced in the computation of the world average of $\overline{\chi}$. It should be noted that the results are correlated, as indicated in Table 2.

3.2 *b*-hadron lifetimes

In the spectator model the decay of b-flavored hadrons H_b is governed entirely by the flavor changing $b \to Wq$ transition ($q = c, u$). For this very reason, lifetimes of all b-flavored hadrons are the same in the spectator approximation regardless of the (spectator) quark content of the H_b. In the early 1990's experiments became sophisticated enough to start seeing the differences of the lifetimes among various H_b species. The first theoretical calculations of the spectator quark effects on H_b lifetime emerged only few years earlier.

Currently, most of such calculations are performed in the framework of the Heavy Quark Expansion, HQE. In the HQE, under certain assumptions (most important of which is that of quark-hadron duality), the decay rate of an H_b to an inclusive final state f is expressed as the sum of a series of expectation values of operators of increasing dimension, multiplied by the correspondingly higher powers of $\Lambda_{\rm QCD}/m_b$:

$$\Gamma_{H_b \to f} = |CKM|^2 \sum_n c_n^{(f)} \left(\frac{\Lambda_{\rm QCD}}{m_b}\right)^n \langle H_b|O_n|H_b\rangle, \tag{18}$$

where $|CKM|^2$ is the relevant combination of the CKM matrix elements. Coefficients $c_n^{(f)}$ of this expansion, known as Operator Product Expansion [22], can be calculated perturbatively. Hence, the HQE predicts $\Gamma_{H_b \to f}$ in the form of an expansion in both $\Lambda_{\rm QCD}/m_b$ and $\alpha_s(m_b)$. The precision of current experiments makes it mandatory to go to the next-to-leading order in QCD, *i.e.* to include correction of the order of $\alpha_s(m_b)$ to the $c_n^{(f)}$'s. All non-perturbative physics is shifted into the expectation values $\langle H_b|O_n|H_b\rangle$ of operators O_n. These can be calculated using lattice QCD or QCD sum rules, or can be related to other observables via the HQE [23]. One may reasonably expect that powers of $\Lambda_{\rm QCD}/m_b$ provide enough suppression that only the first few terms of the sum in Eq. (18) matter.

Theoretical predictions are usually made for the ratios of the lifetimes (with $\tau(B^0)$ chosen as the common denominator) rather than for the individual lifetimes, for this allows several calculational uncertainties to cancel. Present HQE results including next-to-leading order corrections (see Refs. [24, 25, 26] for the latest updates) are in some instances already surpassed by the experimental measurements, *e.g.* in the case of $\tau(B^+)/\tau(B^0)$. Also, HQE calculations are not assumption-free. More accurate predictions are a matter of progress in the evaluation of the non-perturbative hadronic matrix elements and verifying the assumptions that the calculations are based upon. However, the HQE, even in its present shape, draws a number of important conclusions, which are in agreement with experimental observations:

- The heavier the mass of the heavy quark the smaller is the variation in the lifetimes among different hadrons containing this quark, which is to say that as $m_b \to \infty$ we retrieve the spectator picture in which the lifetimes of all H_b's are the same. This is well illustrated by the fact that lifetimes in the b sector are all very similar, while in the c sector ($m_c < m_b$) lifetimes differ by as much as a factor of 2.

- The non-perturbative corrections arise only at the order of $\Lambda^2_{\rm QCD}/m_b^2$, which translates into differences among H_b lifetimes of only a few percent.

- It is only the difference between meson and baryon lifetimes that appears at the $\Lambda^2_{\rm QCD}/m_b^2$ level. The splitting of the meson lifetimes occurs at the $\Lambda^3_{\rm QCD}/m_b^3$ level, yet it is enhanced by a phase space factor $16\pi^2$ with respect to the leading free b decay.

To ensure that certain sources of systematic uncertainty cancel, lifetime analyses are sometimes designed to measure a ratio of lifetimes. However, because of the differences in decay topologies, abundance (or lack thereof) of decays of a certain kind, *etc.*, measurements of the individual lifetimes are more common. In the following section we review the most common types of the lifetime measurements. This discussion is followed by the presentation of the averaging of the various lifetime measurements, each with a brief description of its particularities.

3.2.1 Lifetime measurements, uncertainties and correlations

In most cases lifetime of an H_b is estimated from a flight distance and a $\beta\gamma$ factor which is used to convert the geometrical distance into the proper decay time. Methods of accessing lifetime information can roughly be divided in the following five categories:

1. ***Inclusive (flavor blind) measurements***. These measurements are aimed at extracting the lifetime from a mixture of b-hadron decays, without distinguishing the decaying species. Often the knowledge of the mixture composition is limited, which makes these measurements experiment or accelerator specific. Also, these measurements have to rely on Monte Carlo for estimating the $\beta\gamma$ factor, because the decaying hadrons are not fully reconstructed. On the bright side, these usually are the largest statistics b-hadron lifetime measurements that are accessible to a given experiment, and can, therefore, serve as an important performance benchmark.

2. ***Measurements in semileptonic decays of a specific H_b***. W from $b \to Wc$ produces $\ell\nu_l$ pair ($\ell = e, \mu$) in about 21% of the cases. Electron or muon from such decays is usually a well-detected signature, which provides for clean and efficient trigger. c quark from $b \to Wc$ transition and the other quark(s) making up the decaying H_b combine into a charm hadron, which is reconstructed in one or more exclusive decay channels. Knowing what this charmed hadron is allows one to separate, at least statistically, different H_b species. The advantage of these measurements is in statistics which is usually superior to that of the exclusively reconstructed H_b decays. Some of the main disadvantages are related to the difficulty of estimating lepton+charm sample composition and Monte Carlo reliance for the $\beta\gamma$ factor estimate.

3. ***Measurements in exclusively reconstructed decays***. These have the advantage of complete reconstruction of decaying H_b, which allows one to infer the decaying species as well as to perform precise measurement of the $\beta\gamma$ factor. Both lead to generally smaller systematic uncertainties than in the above two categories. The downsides are smaller branching ratios, larger combinatoric backgrounds, especially in $H_b \to H_c\pi(\pi\pi)$ and multi-body H_c decays, or in a hadron collider environment with non-trivial underlying event. $H_b \to J/\psi H_s$ are relatively clean and easy to trigger on $J/\psi \to \ell^+\ell^-$, but their branching fraction is only about 1%.

4. ***Measurements at asymmetric B factories***. In the $\Upsilon(4S) \to B\overline{B}$ decay, the B mesons (B^+ or B^0) are essentially at rest in the $\Upsilon(4S)$ rest frame. This makes lifetime measurements impossible with experiments, such as CLEO, in which $\Upsilon(4S)$ produced at rest. At asymmetric B factories $\Upsilon(4S)$ is boosted resulting in B and $\overline{B}$ moving nearly parallel to each other. The lifetime is inferred from the distance Δz separating B and $\overline{B}$ decay vertices and $\Upsilon(4S)$ boost known from colliding beam energies. In order to

maximize the precision of the measurement one B meson is reconstructed in the $D^{(*)}\ell\nu_\ell$ decay. The other B is typically not fully reconstructed, only position of its decay vertex is determined. These measurements benefit from very large statistics, but suffer from poor Δz resolution.

5. ***Direct measurement of lifetime ratios***. This method has so far been only applied in the measurement of $\tau(B^+)/\tau(B^0)$. The ratio of the lifetimes is extracted from the dependence of the observed relative number of B^+ and B^0 candidates (both reconstructed in semileptonic decays) on the proper decay time.

In some of the latest analyses, measurements of two (*e.g.* $\tau(B^+)$ and $\tau(B^+)/\tau(B^0)$) or three (*e.g.* $\tau(B^+)$, $\tau(B^+)/\tau(B^0)$, and Δm_d) quantities are combined. This introduces correlations among measurements. Another source of correlations among the measurements are the systematic effects, which could be common to an experiment or to an analysis technique across the experiments. When calculating the averages, such correlations are taken into account per general procedure, described in Ref. [27].

3.2.2 Inclusive *b*-hadron lifetimes

The inclusive b hadron lifetime is defined as $\tau_b = \sum_i f_i \tau_i$ where τ_i are the individual b-hadron lifetimes and f_i the fractions of the various species present in an unbiased sample of weakly-decaying b hadrons produced at a high-energy collider.[2] This quantity is certainly less fundamental than the lifetimes of the individual b hadron species, the latter being much more useful in the comparison of measurements with theoretical predictions. Nonetheless, we present the measurements of the inclusive lifetime for completeness.

In practice, an unbiased measurement of the inclusive lifetime is difficult to achieve, because it would imply an efficiency which is guaranteed to be the same across species. So most of the measurements are biased. In an attempt to group analyses which are expected to select the same mixture of b hadrons, the available results (given in Table 3) are divided into the following three sets:

1. measurements at LEP and SLD that accept any b-hadron decay, based on topological reconstruction (secondary vertex or impact parameters) using charged tracks;

2. measurements at LEP based on the identification of a lepton from a b decay; and

3. measurements at the Tevatron based on inclusive $b \to J/\psi$ reconstruction, where the J/ψ is fully reconstructed.

The measurements of the first set are generally considered as estimates of τ_b, although the efficiency to reconstruct a secondary vertex most probably depends, in an analysis-dependent way, on the number charged tracks from a b hadron decay, which in turn should depend on the type of b hadron. Even though these efficiency variations can in principle be accounted for using Monte Carlo simulations (which inevitably contain assumptions on branching fractions), the b hadron mixture in that case can remain somewhat ill-defined and could be slightly different between analyses in that set.

[2] In principle such a quantity could be slightly different in Z decays and a the Tevatron, in case the fractions of b-hadron species are not exactly the same; see the discussion in Sec. 3.1.2.

Table 3: Measurements of average b-hadron lifetimes.

Experiment	Method	Data set	τ_b (ps)	Ref.
ALEPH	Dipole	91	$1.511 \pm 0.022 \pm 0.078$	[28]
DELPHI	All track i.p. (2D)	91–92	$1.542 \pm 0.021 \pm 0.045$	[29][a]
DELPHI	Sec. vtx	91–93	$1.582 \pm 0.011 \pm 0.027$	[30][a]
DELPHI	Sec. vtx	94–95	$1.570 \pm 0.005 \pm 0.008$	[31]
L3	Sec. vtx + i.p.	91–94	$1.556 \pm 0.010 \pm 0.017$	[32][b]
OPAL	Sec. vtx	91–94	$1.611 \pm 0.010 \pm 0.027$	[33]
SLD	Sec. vtx	93	$1.564 \pm 0.030 \pm 0.036$	[34]
Average set 1 (b vertex)			1.576 ± 0.008	
ALEPH	Lepton i.p. (3D)	91–93	$1.533 \pm 0.013 \pm 0.022$	[35]
L3	Lepton i.p. (2D)	91–94	$1.544 \pm 0.016 \pm 0.021$	[32][b]
OPAL	Lepton i.p. (2D)	90–91	$1.523 \pm 0.034 \pm 0.038$	[36]
Average set 2 ($b \to \ell$)			1.537 ± 0.020	
CDF	J/ψ vtx	92–95	$1.533 \pm 0.015^{+0.035}_{-0.031}$	[37]
Average of all above			1.574 ± 0.008	

[a] The combined DELPHI result quoted in [30] is $1.575 \pm 0.010 \pm 0.026$ ps.
[b] The combined L3 result quoted in [32] is $1.549 \pm 0.009 \pm 0.015$ ps.

On the contrary, the mixtures corresponding to the other two sets of measurements are better defined, in the limit where the reconstruction and selection efficiency of a lepton or a J/ψ from a b hadron does not depend on the type of that b hadron. These mixtures are given by the production fractions and the inclusive branching fractions for each b hadron species to give a lepton or a J/ψ. In particular, under the assumption that all b hadrons have the same semileptonic decay width, the analyses of the second set should measure $\tau(b \to \ell) = (\sum_i f_i \tau_i^2)/(\sum_i f_i \tau_i)$ which is necessarily larger than τ_b if lifetime differences exist. Given the present knowledge on τ_i and f_i, $\tau(b \to \ell) - \tau_b$ is expected to be of the order of 0.01 ps.

For the averaging, correlated systematic are taken into account, which are due to b and c fragmentation, b and c decay models, $\mathcal{B}(B \to \ell)$, $\mathcal{B}(B \to c \to \ell)$, τ_c, $\mathcal{B}(c \to \ell)$, and B charged track decay multiplicity. The averages for the sets defined above (also given in Table 3) are

$$\tau(b \text{ vertex}) = 1.576 \pm 0.008 \text{ ps}, \quad (19)$$

$$\tau(b \to \ell) = 1.537 \pm 0.020 \text{ ps}, \quad (20)$$

$$\tau(b \to J/\psi) = 1.533^{+0.038}_{-0.034} \text{ ps}, \quad (21)$$

whereas an average of all measurements, ignoring mixture differences, yields 1.574 ± 0.008 ps.

3.2.3 B^0 and B^+ lifetimes

In LEP and CDF experiments, the most precise measurements of the B^0 and B^+ lifetimes have originated from two classes of partially reconstructed decays. In the first class the decay $B \to \overline{D}^{(*)} \ell^+ \nu_\ell X$ is used in which the charge of the charmed meson distinguishes between neutral and charged B mesons; the ratio B^+/B^0 lifetime ratio is usually also extracted directly, as the

Table 4: Measurements of the B^0 lifetime.

Experiment	Method	Data set	$\tau(B^0)$ (ps)	Ref.
ALEPH	$D^{(*)}\ell$	91–95	$1.518 \pm 0.053 \pm 0.034$	[39]
ALEPH	Exclusive	91–94	$1.25^{+0.15}_{-0.13} \pm 0.05$	[40]
ALEPH	Partial rec. $\pi^+\pi^-$	91–94	$1.49^{+0.17+0.08}_{-0.15-0.06}$	[40]
CDF	$D^{(*)}\ell$	92–95	$1.474 \pm 0.039^{+0.052}_{-0.051}$	[41]
CDF	Excl. $J/\psi K$	92–95	$1.497 \pm 0.073 \pm 0.032$	[42]
CDF	Excl. $J/\psi K$	02–03	$1.49 \pm 0.06 \pm 0.062$	[38]^p
DELPHI	$D^{(*)}\ell$	91–93	$1.61^{+0.14}_{-0.13} \pm 0.08$	[43]
DELPHI	Charge sec. vtx	91–93	$1.63 \pm 0.14 \pm 0.13$	[44]
DELPHI	Inclusive $D^*\ell$	91–93	$1.532 \pm 0.041 \pm 0.040$	[45]
DELPHI	Charge sec. vtx	94–95	$1.531 \pm 0.021 \pm 0.031$	[31]
L3	Charge sec. vtx	94–95	$1.52 \pm 0.06 \pm 0.04$	[46]
OPAL	$D^{(*)}\ell$	91–93	$1.53 \pm 0.12 \pm 0.08$	[47]
OPAL	Charge sec. vtx	93–95	$1.523 \pm 0.057 \pm 0.053$	[48]
OPAL	Inclusive $D^*\ell$	91–00	$1.541 \pm 0.028 \pm 0.023$	[49]
SLD	Charge sec. vtx ℓ	93–95	$1.56^{+0.14}_{-0.13} \pm 0.10$	[50]^a
SLD	Charge sec. vtx	93–95	$1.66 \pm 0.08 \pm 0.08$	[50]^a
BABAR	Exclusive	99–00	$1.546 \pm 0.032 \pm 0.022$	[51]
BABAR	Inclusive $D^*\ell$	99–01	$1.529 \pm 0.012 \pm 0.029$	[52]
BABAR	Exclusive $D^*\ell$	99–02	$1.523^{+0.024}_{-0.023} \pm 0.022$	[53]
BABAR	Incl. $D^*\pi$, $D^*\rho$	99–01	$1.533 \pm 0.034 \pm 0.038$	[54]
Belle	Exclusive	00–01	$1.554 \pm 0.030 \pm 0.019$	[55]
Average			1.534 ± 0.013	
Recent measurements not yet included in the average				
CDF	Excl. $J/\psi K$	02–04	$1.539 \pm 0.051 \pm 0.008$	[56]^{b,p}
BABAR	Inclusive $D^*\ell$	99–04	$1.501 \pm 0.008 \pm 0.030$	[57]
Belle	Exclusive	00–03	$1.534 \pm 0.008 \pm 0.010$	[58]^c

^{a} The combined SLD result quoted in [50] is $1.64 \pm 0.08 \pm 0.08$ ps.
^{b} To replace [38]. ^{c} To replace [55]. ^{p} Preliminary.

B^0 and B^+ lifetime measurements are correlated. In the second class the charge attached to the b-decay vertex is used to achieve this separation.

With the benefit from very large statistics, the asymmetric B-factory experiments, *BABAR* and Belle, now provide more precise lifetime measurements using exclusively reconstructed decays, as well as partially reconstructed decays. With increased data sample, CDF also provides improved measurements using large samples of exclusive $B^0 \to J/\psi K^{(*)0}$ and $B^+ \to J\psi K^+$ decays.

The averaging is summarized in Tables 4, 5, and 6. The following sources of correlated systematic uncertainties have been considered: D^{**} branching ratio uncertainties [2], momentum estimation of B mesons from Z^0 decays (b-quark fragmentation parameter $\langle X_E \rangle = 0.702 \pm 0.008$ [2]), B_s^0 and b-baryon lifetimes (see Secs. 3.2.4 and 3.2.6), and b-hadron fractions

Table 5: Measurements of the B^+ lifetime.

Experiment	Method	Data set	$\tau(B^+)$ (ps)	Ref.
ALEPH	$D^{(*)}\ell$	91–95	$1.648 \pm 0.049 \pm 0.035$	[39]
ALEPH	Exclusive	91–94	$1.58^{+0.21+0.04}_{-0.18-0.03}$	[40]
CDF	$D^{(*)}\ell$	92–95	$1.637 \pm 0.058^{+0.045}_{-0.043}$	[41]
CDF	Excl. $J/\psi K$	92–95	$1.636 \pm 0.058 \pm 0.025$	[42]
CDF	Excl. $(J/\psi K)$	02–03	$1.64 \pm 0.05 \pm 0.02$	[38]^p
DELPHI	$D^{(*)}\ell$	91–93	$1.61 \pm 0.16 \pm 0.12$	[43]^a
DELPHI	Charge sec. vtx	91–93	$1.72 \pm 0.08 \pm 0.06$	[44]^a
DELPHI	Charge sec. vtx	94–95	$1.624 \pm 0.014 \pm 0.018$	[31]
L3	Charge sec. vtx	94–95	$1.66 \pm 0.06 \pm 0.03$	[46]
OPAL	$D^{(*)}\ell$	91–93	$1.52 \pm 0.14 \pm 0.09$	[47]
OPAL	Charge sec. vtx	93–95	$1.643 \pm 0.037 \pm 0.025$	[48]
SLD	Charge sec. vtx ℓ	93–95	$1.61^{+0.13}_{-0.12} \pm 0.07$	[50]^b
SLD	Charge sec. vtx	93–95	$1.67 \pm 0.07 \pm 0.06$	[50]^b
BABAR	Exclusive	99–00	$1.673 \pm 0.032 \pm 0.023$	[51]
Belle	Exclusive	00–01	$1.695 \pm 0.026 \pm 0.015$	[55]
Average			1.652 ± 0.014	
Recent measurements not yet included in the average				
CDF	Excl. $J/\psi K$	02–04	$1.662 \pm 0.033 \pm 0.008$	[56]^{c,p}
Belle	Exclusive	00–03	$1.635 \pm 0.011 \pm 0.011$	[58]^d

^{a} The combined DELPHI result quoted in [44] is 1.70 ± 0.09 ps.
^{b} The combined SLD result quoted in [50] is $1.66 \pm 0.06 \pm 0.05$ ps.
^{c} To replace [38]. ^{d} To replace [55]. ^{p} Preliminary.

at high energy (see Table 2). The world averages are:

$$\tau(B^0) = 1.534 \pm 0.013 \text{ ps}, \quad (22)$$

$$\tau(B^+) = 1.653 \pm 0.014 \text{ ps}, \quad (23)$$

$$\tau(B^+)/\tau(B^0) = 1.081 \pm 0.015. \quad (24)$$

As indicated in the tables, these averages do not include recent CDF [56], DØ [59], *BABAR* [57], and Belle [58] results; it is planned to incoporate them in the next update of this report.

3.2.4 B_s^0 lifetime

Some of the more precise measurements of the B_s^0 lifetime originate from partially reconstructed decays in which a D_s^- meson has been completely reconstructed.

The following correlated systematic errors were considered: average B lifetime used in backgrounds, B_s^0 decay multiplicity, and branching ratios used to determine backgrounds (*e.g.* $\mathcal{B}(B \to D_s D)$).

A knowledge of the multiplicity of B_s^0 decays is important for measurements that partially reconstruct the final state such as $B \to D_s X$ (where X is not a lepton). The boost deduced from Monte Carlo simulation depends on the multiplicity used. Since this is not well known,

Table 6: Measurements of the ratio $\tau(B^+)/\tau(B^0)$.

Experiment	Method	Data set	Ratio $\tau(B^+)/\tau(B^0)$	Ref.
ALEPH	$D^{(*)}\ell$	91–95	$1.085 \pm 0.059 \pm 0.018$	[39]
ALEPH	Exclusive	91–94	$1.27^{+0.23+0.03}_{-0.19-0.02}$	[40]
CDF	$D^{(*)}\ell$	92–95	$1.110 \pm 0.056^{+0.033}_{-0.030}$	[41]
CDF	Excl. $J/\psi K$	92–95	$1.093 \pm 0.066 \pm 0.028$	[42]
DELPHI	$D^{(*)}\ell$	91–93	$1.00^{+0.17}_{-0.15} \pm 0.10$	[43]
DELPHI	Charge sec. vtx	91–93	$1.06^{+0.13}_{-0.11} \pm 0.10$	[44]
DELPHI	Charge sec. vtx	94–95	$1.060 \pm 0.021 \pm 0.024$	[31]
L3	Charge sec. vtx	94–95	$1.09 \pm 0.07 \pm 0.03$	[46]
OPAL	$D^{(*)}\ell$	91–93	$0.99 \pm 0.14^{+0.05}_{-0.04}$	[47]
OPAL	Charge sec. vtx	93–95	$1.079 \pm 0.064 \pm 0.041$	[48]
SLD	Charge sec. vtx ℓ	93–95	$1.03^{+0.16}_{-0.14} \pm 0.09$	[50][a]
SLD	Charge sec. vtx	93–95	$1.01^{+0.09}_{-0.08} \pm 0.05$	[50][a]
BABAR	Exclusive	99–00	$1.082 \pm 0.026 \pm 0.012$	[51]
Belle	Exclusive	00–01	$1.091 \pm 0.023 \pm 0.014$	[55]
Average			1.081 ± 0.015	
Recent measurements not yet included in the average				
DØ	$D^{*+}\mu$ $D^0\mu$ ratio	02–04	$1.080 \pm 0.016 \pm 0.014$	[59]
CDF	Excl. $J/\psi K$	02–04	1.080 ± 0.042	[56][p]
Belle	Exclusive	00–03	$1.066 \pm 0.008 \pm 0.008$	[58][b]

[a] The combined SLD result quoted in [50] is $1.01 \pm 0.07 \pm 0.06$.
[b] To replace [55]. [p] Preliminary.

the multiplicity in the simulation is varied and this range of values observed is taken to be a systematic.

Similarly not all the branching ratios for the potential background processes are measured. Where they are available, the PDG values are used for the error estimate. Where no measurements are available estimates can usually be made by using measured branching ratios of related processes and using some reasonable extrapolation.

The inputs used to form the average B_s^0 lifetime are given in Table 7.

It is important to note that similar to the kaon system, neutral B mesons contain short- and long-lived components, since the two mass eigenstates B_L and B_H differ not only in their masses, but also in their widths with $\Delta\Gamma = \Gamma_L - \Gamma_H$. In the Standard Model for the B_s^0 system, this difference can be large, *i.e.*, $\Delta\Gamma_s/\Gamma_s = 0.12 \pm 0.06$ [69]. Specific measurements of this parameter are explained in more detail in Sec. 3.3.2.

Flavor-specific decays, such as semileptonic $B_s \to D_s\ell\nu$ will have equal contributions of $\tau_H = 1/\Gamma_H$ and $\tau_L = 1/\Gamma_L$. For this reason, lifetime measurements via these decays are broken out separately as given in Table 7, and their world average is:

$$\tau(B_s^0)_{D_s\ell} = 1.442 \pm 0.066 \text{ ps}\,. \tag{25}$$

Any final state can be decomposed into its *CP*-even and *CP*-odd component, and in the Standard Model, $\Delta\Gamma_{sCP} = \Delta\Gamma_s$. Fully exclusive decays of B_s^0 into $B_s^0 \to J/\psi\phi$ are expected to

Table 7: Measurements of the B_s^0 lifetime.

Experiment	Method	Data set	$\tau(B_s^0)$ (ps)	Ref.
ALEPH	$D_s\ell$	91–95	$1.54^{+0.14}_{-0.13} \pm 0.04$	[60]
CDF	$D_s\ell$	92–96	$1.36 \pm 0.09^{+0.06}_{-0.05}$	[61]
DELPHI	$D_s\ell$	91–95	$1.42^{+0.14}_{-0.13} \pm 0.03$	[62]
OPAL	$D_s\ell$	90–95	$1.50^{+0.16}_{-0.15} \pm 0.04$	[63]
Average of $D_s\ell$ measurements			1.442 ± 0.066	
ALEPH	D_sh	91–95	$1.47 \pm 0.14 \pm 0.08$	[64]
DELPHI	D_sh	91–95	$1.53^{+0.16}_{-0.15} \pm 0.07$	[65]
DELPHI	D_s incl.	91–94	$1.60 \pm 0.26^{+0.13}_{-0.15}$	[66]
OPAL	D_s incl.	90–95	$1.72^{+0.20+0.18}_{-0.19-0.17}$	[67]
Average of all above D_s measurements			1.469 ± 0.059	
CDF	$J/\psi\phi$	92–95	$1.34^{+0.23}_{-0.19} \pm 0.05$	[37]
CDF	$J/\psi\phi$	02–04	$1.369 \pm 0.100^{+0.008}_{-0.010}$	[56][p]
DØ	$J/\psi\phi$	02–04	$1.444^{+0.098}_{-0.090} \pm 0.02$	[68]
Average of $J/\psi\phi$ measurements			1.404 ± 0.066	

[p] Preliminary.

be dominated by the *CP*-even state and its lifetime. First measurements of the *CP* mix for this decay mode are outlined in Sec. 3.3.2. CDF and DØ measurements from this particular mode $B_s^0 \to J/\psi\phi$ are combined into an average given in Table 7. There are no correlations between the measurements for this fully exclusive channel, and the world average for this specific decay is:

$$\tau(B_s^0)_{J/\psi\phi} = 1.404 \pm 0.066 \text{ ps}\,. \tag{26}$$

Finally, the remaining measurements are variations of lifetimes determined more inclusively via D_s plus hadrons, and hence into a more unknown mixture of flavors and/or *CP*-states. A lifetime weighted this way can still be a useful input for analyses examining such an inclusive sample. These are separated in Table 7 and combined with the semileptonic lifetime to obtain:

$$\tau(B_s^0)_{D_s\mathrm{X}} = 1.469 \pm 0.059 \text{ ps}\,. \tag{27}$$

3.2.5 B_c^+ lifetime

There are currently two measurements of the lifetime of the B_c^+ meson from CDF [70] and DØ [71] using the semileptonic decay mode $B_c^+ \to J/\psi\ell$ and fitting simultaneously to the mass and lifetime using the vertex formed from the leptons from the decay of the J/ψ and the third lepton. Correction factors to estimate the boost due to the missing neutrino are used. Mass values of $6.40 \pm 0.39 \pm 0.13$ GeV/c^2 and $5.95^{+0.14}_{-0.13} \pm 0.34$ GeV/c^2, respectively, are found by fitting to the tri-lepton invariant mass spectrum. These mass measurements are consistent to within errors, and no adjustments to the lifetimes are made. Correlated systematic errors include the impact of the uncertainty of the B_c^+ p_T spectrum on the correction factors, the level of feed-down from $\psi(2S)$, MC modeling of the decay model varying from phase space to

Table 8: Measurements of the B_c^+ lifetime.

Experiment	Method	Data set	$\tau(B_c^+)$ (ps)	Ref.
CDF	$J/\psi\ell$	92–95	$0.46^{+0.18}_{-0.16}\pm 0.03$	[70]
DØ	$J/\psi\mu$	02–04	$0.448^{+0.123}_{-0.096}\pm 0.121$	[71]^p
Average			0.45 ± 0.12	

^{p} Preliminary.

the ISGW model, and mass variations. Inputs are given in Table 8 and the world average is determined to be:

$$\tau(B_c^+) = 0.45 \pm 0.12 \text{ ps}\,. \tag{28}$$

3.2.6 Λ_b^0 and b-baryon lifetimes

The most precise measurements of the b-baryon lifetime originate from two classes of partially reconstructed decays. In the first class, decays with an exclusively reconstructed Λ_c^+ baryon and a lepton of opposite charge are used. These products are more likely to occur in the decay of Λ_b^0 baryons. In the second class, more inclusive final states with a baryon (p, $\overline{p}$, Λ, or $\overline{\Lambda}$) and a lepton have been used, and these final states can generally arise from any b baryon.

The following sources of correlated systematic uncertainties have been considered: experimental time resolution within a given experiment, b-quark fragmentation distribution into weakly decaying b baryons, Λ_b^0 polarization, decay model, and evaluation of the b-baryon purity in the selected event samples. In computing the averages the central values of the masses are scaled to $M(\Lambda_b^0) = 5624 \pm 9$ MeV/c^2 [72] and $M(b\text{-baryon}) = 5670 \pm 100$ MeV/c^2.

The meaning of decay model and the correlations are not always clear. Uncertainties related to the decay model are dominated by assumptions on the fraction of n-body decays. To be conservative it is assumed that it is correlated whenever given as an error. DELPHI varies the fraction of 4-body decays from 0.0 to 0.3. In computing the average, the DELPHI result is corrected for 0.2 ± 0.2.

Furthermore, in computing the average, the semileptonic decay results are corrected for a polarization of $-0.45^{+0.19}_{-0.17}$ [2] and a Λ_b^0 fragmentation parameter $\langle X_E \rangle = 0.70 \pm 0.03$ [73].

Inputs to the averages are given in Table 9. The world average lifetime of b baryons is then:

$$\langle \tau(b\text{-baryon}) \rangle = 1.210 \pm 0.048 \text{ ps}\,. \tag{29}$$

Keeping only $\Lambda_c^\pm \ell^\mp$ and $\Lambda \ell^- \ell^+$ final states, as representative of the Λ_b^0 baryon, the following lifetime is obtained:

$$\tau(\Lambda_b^0) = 1.232 \pm 0.072 \text{ ps}\,. \tag{30}$$

Averaging the measurements based on the $\Xi^\mp \ell^\mp$ final states [15, 14] gives a lifetime value for a sample of events containing Ξ_b^0 and Ξ_b^- baryons:

$$\langle \tau(\Xi_b) \rangle = 1.39^{+0.34}_{-0.28} \text{ ps}\,. \tag{31}$$

Table 9: Measurements of the b-baryon lifetimes.

Experiment	Method	Data set	Lifetime (ps)	Ref.
ALEPH	$\Lambda_c^+\ell$	91–95	$1.18^{+0.13}_{-0.12} \pm 0.03$	[13]
ALEPH	$\Lambda\ell^-\ell^+$	91–95	$1.30^{+0.26}_{-0.21} \pm 0.04$	[13]
CDF	$\Lambda_c^+\ell$	91–95	$1.32 \pm 0.15 \pm 0.06$	[74]
CDF	$J/\psi\Lambda$	02–03	$1.25 \pm 0.26 \pm 0.10$	[75][p]
DØ	$J/\psi\Lambda$	02–04	$1.22^{+0.22}_{-0.18} \pm 0.04$	[76]
DELPHI	$\Lambda_c^+\ell$	91–94	$1.11^{+0.19}_{-0.18} \pm 0.05$	[77][a]
OPAL	$\Lambda_c^+\ell$, $\Lambda\ell^-\ell^+$	90–95	$1.29^{+0.24}_{-0.22} \pm 0.06$	[63]
Average of above 7 (Λ_b^0 lifetime)			1.232 ± 0.072	
ALEPH	$\Lambda\ell$	91–95	$1.20^{+0.08}_{-0.08} \pm 0.06$	[13]
DELPHI	$\Lambda\ell\pi$ vtx	91–94	$1.16 \pm 0.20 \pm 0.08$	[77][a]
DELPHI	$\Lambda\mu$ i.p.	91–94	$1.10^{+0.19}_{-0.17} \pm 0.09$	[78][a]
DELPHI	$p\ell$	91–94	$1.19 \pm 0.14 \pm 0.07$	[77][a]
OPAL	$\Lambda\ell$ i.p.	90–94	$1.21^{+0.15}_{-0.13} \pm 0.10$	[79][b]
OPAL	$\Lambda\ell$ vtx	90–94	$1.15 \pm 0.12 \pm 0.06$	[79][b]
Average of above 13 (b-baryon lifetime)			1.210 ± 0.048	
ALEPH	$\Xi\ell$	90–95	$1.35^{+0.37+0.15}_{-0.28-0.17}$	[15]
DELPHI	$\Xi\ell$	91–93	$1.5^{+0.7}_{-0.4} \pm 0.3$	[14]
Average of above 2 (Ξ_b lifetime)			$1.39^{+0.34}_{-0.28}$	

[a] The combined DELPHI result quoted in [77] is $1.14 \pm 0.08 \pm 0.04$ ps.
[b] The combined OPAL result quoted in [79] is $1.16 \pm 0.11 \pm 0.06$ ps.
[p] Preliminary.

3.2.7 Summary and comparison to theoretical predictions

Averages of lifetimes of specific b hadron species are collected below in Table 10.

As described in Sec. 3.2, Heavy Quark Effective Theory can be employed to explain the hierarchy of $\tau(B_c^+) \ll \tau(\Lambda_b^0) < \tau(B_s^0) \approx \tau(B^0) < \tau(B^+)$, and used to predict the ratios between lifetimes. A recent prediction of the ratio between the B^+ and B^0 lifetimes, is 1.06 ± 0.02 [26]. The ratio $\tau(\Lambda_b^0)/\tau(B^0)$ has particularly been the source of theoretical scrutiny since earlier calculations [80] predicted a value greater than 0.90, almost two sigma higher than the world average at the time. Recent calculations of this ratio that include higher order effects predict a ratio between the Λ_b^0 and B^0 lifetimes of 0.86 ± 0.05 [24] and reduces this difference. Ref. [24] presents probability density functions of its predictions with variation of theoretical inputs, and the indicated errors (and ranges in Table 11 below) are the RMS of the distributions. Measured lifetime ratios compared to predicted ranges are given in Table 11.

3.3 Neutral B-meson mixing

There are two neutral $B-\overline{B}$ systems, $B^0-\overline{B}^0$ and $B_s^0-\overline{B}_s^0$, which both exhibit the phenomenon of particle-antiparticle mixing. For each of these systems, there are two mass eigenstates which are linear combinations of the two flavour states, B or $\overline{B}$. We consider the case where a neutral B meson is produced and detected in a flavour state, through its decay to a flavour-specific

Table 10: Summary of lifetimes of different b hadron species.

b hadron species	Measured lifetime
B^+	1.653 ± 0.014 ps
B^0	1.534 ± 0.013 ps
B_s^0 ($\rightarrow$ flavor specific)	1.442 ± 0.066 ps
B_s^0 ($\rightarrow J/\psi\phi$)	1.404 ± 0.066 ps
B_c^+	0.45 ± 0.12 ps
Λ_b^0	1.232 ± 0.072 ps
Ξ_b mixture	$1.39^{+0.34}_{-0.28}$ ps
b-baryon mixture	1.210 ± 0.048 ps
b-hadron mixture	1.574 ± 0.008 ps

Table 11: Ratios of b-hadron lifetimes relative to the B^0 lifetime and theoretical ranges predicted by theory [24].

Lifetime ratio	Measured value	Predicted range
$\tau(B^+)/\tau(B^0)$	1.081 ± 0.015	1.04 – 1.08
$\tau(B_s^0)/\tau(B^0)^a$	0.939 ± 0.044	0.99 – 1.01
$\tau(\Lambda_b^0)/\tau(B^0)$	0.803 ± 0.047	0.81 – 0.91
$\tau(b\text{-baryon})/\tau(B^0)$	0.789 ± 0.032	0.81 – 0.91

[a] Using the $B_s^0 \rightarrow$ flavor specific lifetime for definiteness.

final state. There are four different time-dependent probabilities; if CPT is conserved (which will be assumed throughout), they can be written as

$$\left\{ \begin{array}{lcl} \mathcal{P}(B \rightarrow B) & = & \frac{e^{-\Gamma t}}{2}\left[\cosh\left(\frac{\Delta\Gamma}{2}t\right) + \cos(\Delta m t)\right] \\ \mathcal{P}(B \rightarrow \overline{B}) & = & \frac{e^{-\Gamma t}}{2}\left[\cosh\left(\frac{\Delta\Gamma}{2}t\right) - \cos(\Delta m t)\right] \left|\frac{q}{p}\right|^2 \\ \mathcal{P}(\overline{B} \rightarrow B) & = & \frac{e^{-\Gamma t}}{2}\left[\cosh\left(\frac{\Delta\Gamma}{2}t\right) - \cos(\Delta m t)\right] \left|\frac{p}{q}\right|^2 \\ \mathcal{P}(\overline{B} \rightarrow \overline{B}) & = & \frac{e^{-\Gamma t}}{2}\left[\cosh\left(\frac{\Delta\Gamma}{2}t\right) + \cos(\Delta m t)\right] \end{array} \right. , \quad (32)$$

where t is the proper time of the system (*i.e.* the time interval between the production and the decay in the rest frame of the B meson) and $\Gamma = 1/\tau(B)$ is the average decay width. At the B factories, only the proper-time difference Δt between the decays of the two neutral B mesons from the $\Upsilon(4S)$ can be determined, but, because the two B mesons evolve coherently (keeping opposite flavours as long as none of them has decayed), the above formulae remain valid if t is replaced with Δt and the production flavour is replaced by the flavour at the time of the decay of the accompanying B meson in a flavour specific state. As can be seen in the above expressions, the mixing probabilities depend on the following three observables: the mass difference Δm and the decay width difference $\Delta\Gamma$ between the two mass eigenstates, and the parameter $|q/p|^2$ which signals CP violation in the mixing if $|q/p|^2 \neq 1$.

In the following sections we review in turn the experimental knowledge on these three parameters, separately for the B^0 meson (Δm_d, $\Delta\Gamma_d$, $|q/p|_d$) and the B_s^0 meson (Δm_s, $\Delta\Gamma_s$,

$|q/p|_s$).

3.3.1 B^0 mixing parameters

CP violation parameter $|q/p|_d$

Evidence for *CP* violation in B^0 mixing has been searched for, both with flavor-specific and inclusive B^0 decays, in samples where the initial flavor state is tagged. In the case of semileptonic (or other flavor-specific) decays, where the final state tag is also available, the following asymmetry

$$\mathcal{A}_{\rm SL} = \frac{N(\overline{B}^0(t) \to \ell^+\nu_\ell X) - N(B^0(t) \to \ell^-\overline{\nu}_\ell X)}{N(\overline{B}^0(t) \to \ell^+\nu_\ell X) + N(B^0(t) \to \ell^-\overline{\nu}_\ell X)} = \frac{|p/q|_d^2 - |q/p|_d^2}{|p/q|_d^2 + |q/p|_d^2} \tag{33}$$

has been measured, either in time-integrated analyses at CLEO [81, 82, 83] and CDF [84], or in time-dependent analyses at OPAL [85], ALEPH [86], *BABAR* [87, 88] and Belle [89]. In the inclusive case, also investigated and published at ALEPH [86] and OPAL [90], no final state tag is used, and the asymmetry [91]

$$\frac{N(B^0(t) \to \text{all}) - N(\overline{B}^0(t) \to \text{all})}{N(B^0(t) \to \text{all}) + N(\overline{B}^0(t) \to \text{all})} \simeq \mathcal{A}_{\rm SL}\left[\frac{\Delta m_d}{2\Gamma_d}\sin(\Delta m_d\, t) - \sin^2\left(\frac{\Delta m_d\, t}{2}\right)\right] \tag{34}$$

must be measured as a function of the proper time to extract information on *CP* violation. In all cases asymmetries compatible with zero have been found, with a precision limited by the available statistics. A simple average of all published results for the B^0 meson [82, 83, 85, 86, 87, 88, 90] and of the preliminary Belle result [89] yields

$$\mathcal{A}_{\rm SL} = -0.0026 \pm 0.0067 \tag{35}$$

or, equivalently through Eq. (33),

$$|q/p|_d = 1.0013 \pm 0.0034\,. \tag{36}$$

This result[3], summarized in Table 12, is compatible with no *CP* violation in the mixing, an assumption we make for the rest of this section.

Mass and decay width differences Δm_d and $\Delta\Gamma_d$

Many time-dependent B^0–$\overline{B}^0$ oscillation analyses have been published by the ALEPH, *BABAR*, Belle, CDF, DELPHI, L3 and OPAL collaborations. The corresponding measurements of Δm_d are summarized in Tables 13 and 14, where only the most recent results are listed (*i.e.* measurements superseded by more recent ones have been omitted). Although a variety of different techniques have been used, the individual Δm_d results obtained at high-energy colliders have remarkably similar precision. Their average is compatible with the recent

[3]Early analyses and (perhaps hence) the PDG use the complex parameter $\epsilon_B = (p-q)/(p+q)$; if *CP* violation in the mixing in small, $\mathcal{A}_{\rm SL} \cong 4{\rm Re}(\epsilon_B)/(1+|\epsilon_B|^2)$ and our current world average is ${\rm Re}(\epsilon_B)/(1+|\epsilon_B|^2) = -0.0007 \pm 0.0017$.

Table 12: Measurements of *CP* violation in B^0 mixing and their average in terms of both $\mathcal{A}_{\rm SL}$ and $|q/p|_d$. The individual results are listed as quoted in the original publications, or converted[3] to an $\mathcal{A}_{\rm SL}$ value. When two errors are quoted, the first one is statistical and the second one systematic.

Exp. & Ref.	Method	Measured $\mathcal{A}_{\rm SL}$	Measured $\lvert q/p\rvert_d$
CLEO [82]	partial hadronic rec.	$+0.017 \pm 0.070 \pm 0.014$	
CLEO [83]	dileptons	$+0.013 \pm 0.050 \pm 0.005$	
CLEO [83]	average of above two	$+0.014 \pm 0.041 \pm 0.006$	
OPAL [85]	leptons	$+0.008 \pm 0.028 \pm 0.012$	
OPAL [90]	inclusive (Eq. (34))	$+0.005 \pm 0.055 \pm 0.013$	
ALEPH [86]	leptons	$-0.037 \pm 0.032 \pm 0.007$	
ALEPH [86]	inclusive (Eq. (34))	$+0.016 \pm 0.034 \pm 0.009$	
ALEPH [86]	average of above two	-0.013 ± 0.026 (tot)	
BABAR [88]	dileptons	$+0.005 \pm 0.012 \pm 0.014$	$0.998 \pm 0.006 \pm 0.007$
BABAR [87]	full hadronic rec.		$1.029 \pm 0.013 \pm 0.011$
Belle [89]	dileptons (prel.)	$-0.0013 \pm 0.0060 \pm 0.0056$	$1.0006 \pm 0.0030 \pm 0.0028$
	Average of all above	-0.0026 ± 0.0067 (tot)	1.0013 ± 0.0034 (tot)

and more precise measurements from the asymmetric B factories. The systematic uncertainties are not negligible; they are often dominated by sample composition, mistag probability, or b-hadron lifetime contributions. Before being combined, the measurements are adjusted on the basis of a common set of input values, including the averages of the b-hadron fractions and lifetimes given in this report (see Secs. 3.1 and 3.2). Some measurements are statistically correlated. Systematic correlations arise both from common physics sources (fractions, lifetimes, branching ratios of b hadrons), and from purely experimental or algorithmic effects (efficiency, resolution, flavour tagging, background description). Combining all published measurements listed in Table 13 and accounting for all identified correlations as described in [2] yields $\Delta m_d = 0.502 \pm 0.004 \pm 0.005$ ps^{-1}.

On the other hand, ARGUS and CLEO have published measurements of the time-integrated mixing probability χ_d [112, 81, 82], which average to $\chi_d = 0.182 \pm 0.015$. Following Ref. [82], the width difference $\Delta\Gamma_d$ could in principle be extracted from the measured value of $\Gamma_d = 1/\tau(B^0)$ and the above averages for Δm_d and χ_d (provided that $\Delta\Gamma_d$ has a negligible impact on the Δm_d analyses that have assumed $\Delta\Gamma_d = 0$), using the relation

$$\chi_d = \frac{x_d^2 + y_d^2}{2(x_d^2+1)} \quad \text{with} \quad x_d = \frac{\Delta m_d}{\Gamma_d} \quad \text{and} \quad y_d = \frac{\Delta\Gamma_d}{2\Gamma_d}\,. \tag{37}$$

However, direct time-dependent studies yield stronger constraints: DELPHI published the result $|\Delta\Gamma_d|/\Gamma_d < 18\%$ at 95% CL [94], while *BABAR* recently obtained $-8.4\% < \mathrm{sign}(\mathrm{Re}\lambda_{CP})\Delta\Gamma_d/\Gamma_d < 6.8\%$ at 90% CL [87].

Assuming $\Delta\Gamma_d = 0$ and using $1/\Gamma_d = \tau(B^0) = 1.534 \pm 0.013$ ps, the Δm_d and χ_d results are combined through Eq. (37) to yield the world average

$$\Delta m_d = 0.502 \pm 0.006 \text{ ps}^{-1}\,, \tag{38}$$

Table 13: Time-dependent measurements included in the Δm_d average. All these measurements have been adjusted to a common set of physics parameters before being combined. The CDF2 and D0 measurements are preliminary. The new *BABAR* [57] and Belle [58] measurements are not included here, but listed in Table 14.

Experiment and Ref.	Method rec.	Method tag	Published value of Δm_d in ps^{-1}	Adjusted value of Δm_d in ps^{-1}
ALEPH [92]	ℓ	$Q_{\rm jet}$	0.404±0.045±0.027	
ALEPH [92]	ℓ	ℓ	0.452±0.039±0.044	
ALEPH [92]	above two combined		0.422±0.032±0.026	0.441±0.032±0.021
ALEPH [92]	D^*	$\ell, Q_{\rm jet}$	0.482±0.044±0.024	0.482±0.044±0.024
DELPHI [93]	ℓ	$Q_{\rm jet}$	0.493±0.042±0.027	0.504±0.042±0.025
DELPHI [93]	$\pi^*\ell$	$Q_{\rm jet}$	0.499±0.053±0.015	0.501±0.053±0.015
DELPHI [93]	ℓ	ℓ	0.480±0.040±0.051	$0.487\pm0.040\ ^{+0.049}_{-0.048}$
DELPHI [93]	D^*	$Q_{\rm jet}$	0.523±0.072±0.043	0.517±0.072±0.043
DELPHI [94]	vtx	comb	0.531±0.025±0.007	0.530±0.025±0.006
L3 [95]	ℓ	ℓ	0.458±0.046±0.032	0.469±0.046±0.029
L3 [95]	ℓ	$Q_{\rm jet}$	0.427±0.044±0.044	0.436±0.044±0.042
L3 [95]	ℓ	ℓ(IP)	0.462±0.063±0.053	0.480±0.063±0.047
OPAL [98]	ℓ	ℓ	$0.430\pm0.043\ ^{+0.028}_{-0.030}$	$0.462\pm0.043\ ^{+0.018}_{-0.017}$
OPAL [97]	ℓ	$Q_{\rm jet}$	$0.444\pm0.029\ ^{+0.020}_{-0.017}$	$0.465\pm0.029\ ^{+0.015}_{-0.014}$
OPAL [96]	$D^*\ell$	$Q_{\rm jet}$	0.539±0.060±0.024	0.545±0.060±0.023
OPAL [96]	D^*	ℓ	$0.567\pm0.089\ ^{+0.029}_{-0.023}$	$0.571\pm0.089\ ^{+0.028}_{-0.022}$
OPAL [99]	$\pi^*\ell$	$Q_{\rm jet}$	0.497±0.024±0.025	0.496±0.024±0.025
CDF1 [100]	$D\ell$	SST	$0.471\ ^{+0.078}_{-0.068}\ ^{+0.033}_{-0.034}$	$0.471\ ^{+0.078}_{-0.068}\ ^{+0.033}_{-0.034}$
CDF1 [101]	μ	μ	0.503±0.064±0.071	0.514±0.064±0.070
CDF1 [102]	ℓ	$\ell, Q_{\rm jet}$	0.500±0.052±0.043	0.536±0.052±0.037
CDF1 [103]	$D^*\ell$	ℓ	$0.516\pm0.099\ ^{+0.029}_{-0.035}$	$0.523\pm0.099\ ^{+0.029}_{-0.035}$
CDF2 [104]	$D^{(*)}\ell$	SST,SMT,JQT	0.536±0.037±0.017	0.536±0.037±0.017
CDF2 [105]	B^0	SST	0.526±0.056±0.005	0.526±0.056±0.005
DØ [106]	$D^*\mu$	comb	0.456±0.034±0.025	0.456±0.034±0.025
BABAR [107]	B^0	ℓ, K, NN	0.516±0.016±0.010	0.518±0.016±0.008
BABAR [108]	ℓ	ℓ	0.493±0.012±0.009	0.489±0.012±0.007
BABAR [53]	$D^*\ell\nu$	ℓ, K, NN	0.492±0.017±0.014	0.490±0.017±0.013
Belle [109]	B^0	comb	0.528±0.017±0.011	0.529±0.017±0.011
Belle [110]	$D^*\ell\nu$	comb	0.494±0.012±0.015	0.496±0.012±0.014
Belle [111]	$D^*\pi$(part)	ℓ	0.509±0.017±0.020	0.511±0.017±0.019
Belle [7]	ℓ	ℓ	0.503±0.008±0.010	0.504±0.008±0.009
World average (all above measurements included):				0.502±0.004±0.005
– ALEPH, DELPHI, L3, OPAL and CDF1 only:				0.496±0.010±0.009
– Above measurements of *BABAR* and Belle only:				0.503±0.005±0.005

Table 14: Simultaneous measurements of Δm_d and $\tau(B^0)$, with the statistical correlations $\rho_{\rm stat}$ between them. The Belle analysis also measures $\tau(B^+)$ at the same time, but it is converted here into a two-dimensional measurement of Δm_d and $\tau(B^0)$, for an assumed value of $\tau(B^+)$. The first error on Δm_d and $\tau(B^0)$ is statistical and the second one systematic; the latter includes a contribution obtained from the variation of $\tau(B^+)$ or $\tau(B^+)/\tau(B^0)$ in the indicated range. Units are ps^{-1} for Δm_d and ps for the lifetimes. The second *BABAR* result is still preliminary.

Exp. & Ref.	Measured Δm_d	Measured $\tau(B^0)$	$\rho_{\rm stat}$	Assumed $\tau(B^+)$
BABAR [53]	$0.492 \pm 0.018 \pm 0.013$	$1.523 \pm 0.024 \pm 0.022$	-0.22	$(1.083 \pm 0.017)\tau(B^0)$
BABAR [57]	$0.523 \pm 0.004 \pm 0.007$	$1.501 \pm 0.008 \pm 0.030$	-0.012	1.671 ± 0.018
Belle [58]	$0.511 \pm 0.005 \pm 0.006$	$1.534 \pm 0.008 \pm 0.010$	-0.27	1.635 ± 0.011

or, equivalently,

$$x_d = 0.770 \pm 0.011 \quad \text{and} \quad \chi_d = 0.186 \pm 0.003\,. \tag{39}$$

Figure 4 compares the Δm_d values obtained by the different experiments.

The B^0 mixing averages given in Eqs. (38) and (39) and the b-hadron fractions of Table 2 have been obtained in a fully consistent way, taking into account the fact that the fractions are computed using the χ_d value of Eq. (39) and that many individual measurements of Δm_d at high energy depend on the assumed values for the b-hadron fractions. Furthermore, this set of averages is consistent with the lifetime averages of Sec. 3.2.

It should be noted that the above average of Δm_d, Table 13 and Figure 4 do not include two precise measurements that have been released for the Summer 2004 conferences by *BABAR* and Belle. The new *BABAR* analysis [57], based on partially reconstructed $B^0 \to D^*\ell\nu$ decays, extracts simultaneously Δm_d and $\tau(B^0)$ (similarly to the *BABAR* published result based on fully reconstructed $B^0 \to D^*\ell\nu$ decays [53] while the new Belle analysis [58] based on fully reconstructed hadronic B^0 decays and $B^0 \to D^*\ell\nu$ decays, extracts simultaneously Δm_d, $\tau(B^0)$ and $\tau(B^+)$.

The results of the three B-factory analyses extracting Δm_d and $\tau(B^0)$ at the same time are listed in Table 14. Performing a two-dimensional combination of these results needs a careful assessment of the statistical and systematic correlations between Δm_d and $\tau(B^0)$ in each analysis and between the measurements in the different analyses. This will be completed for a next version of this report.

3.3.2 B_s^0 mixing parameters

CP violation parameter $|q/p|_s$

No measurement or experimental limit exists on $|q/p|_s$, except in the form of a relatively weak constraint from CDF on a combination of $|q/p|_d$ and $|q/p|_s$, $f'_d\,\chi_d(1-|q/p|_d^2) + f'_s\,\chi_s(1-|q/p|_s^2) = 0.006 \pm 0.017$ [84], using inclusive semileptonic decays of b hadrons. The result is compatible with no CP violation in the mixing, an assumption made in all results described below.

Mass difference Δm_s

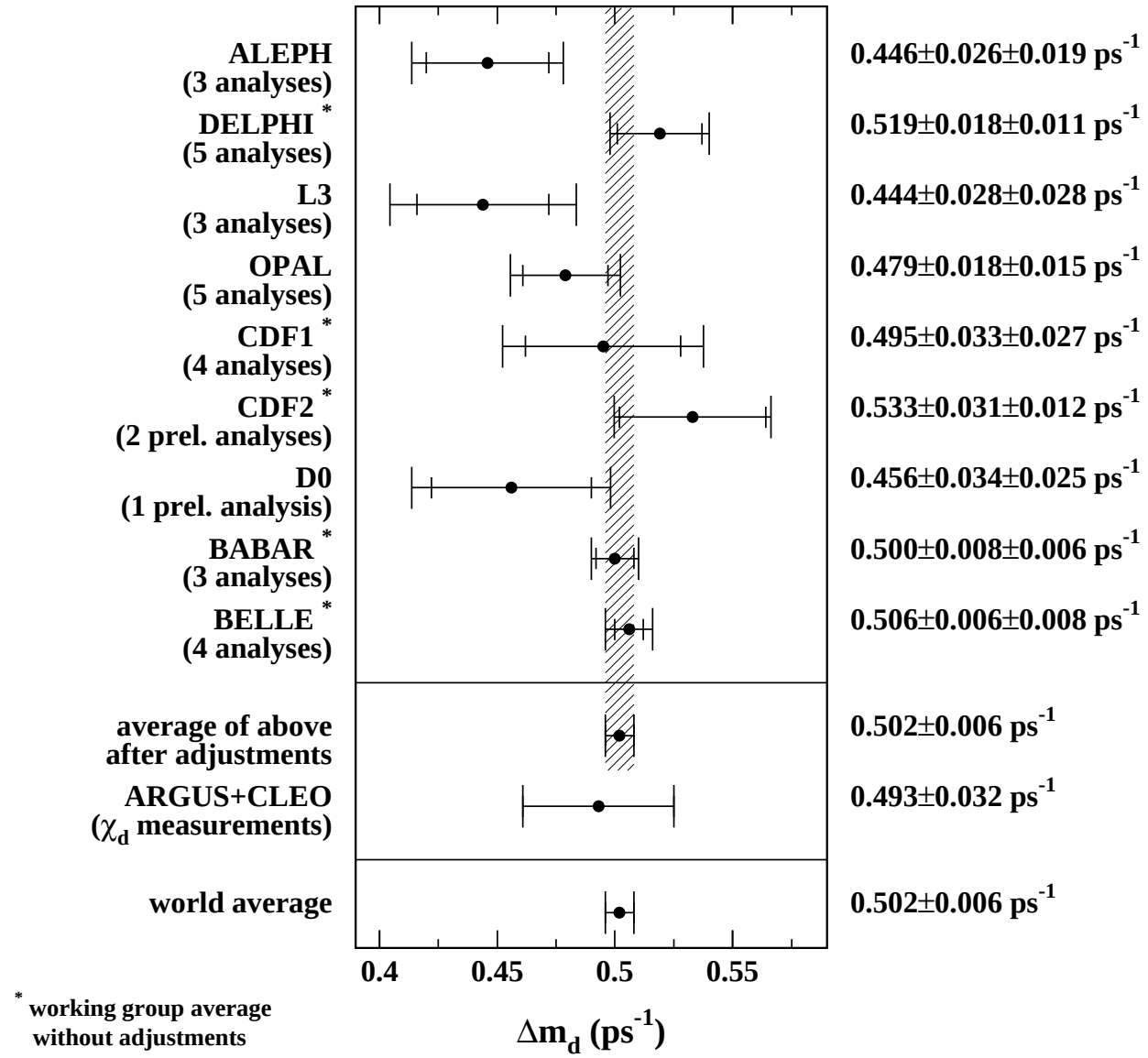

Figure 4: The B^0–$\overline{B}^0$ oscillation frequency Δm_d as measured by the different experiments. The averages quoted for ALEPH, L3 and OPAL are taken from the original publications, while the ones for DELPHI, CDF, *BABAR*, and Belle have been computed from the individual results listed in Table 13 without performing any adjustments. The time-integrated measurements of χ_d from the symmetric B factory experiments ARGUS and CLEO have been converted to a Δm_d value using $\tau(B^0) = 1.534 \pm 0.013$ ps. The two global averages have been obtained after adjustments of all the individual Δm_d results of Table 13 (see text).

The time-integrated measurements of $\overline{\chi}$ (see Sec. 3.1.2), when compared to our knowledge of χ_d and the b-hadron fractions, indicate that B_s^0 mixing is large, with a value of χ_s close to its maximal possible value of 1/2. However, the time dependence of this mixing (called B_s^0 oscillations) has not been observed yet, mainly because the period of these oscillations turns out to be so small that it can't be resolved with the proper-time resolutions achieved so far.

The statistical significance $\mathcal{S}$ of a B_s^0 oscillation signal can be approximated as [113]

$$\mathcal{S} \approx \sqrt{\frac{N}{2}}\, f_{\rm sig}\,(1-2w)\,\exp\left(-\frac{1}{2}\left(\frac{\Delta m_s}{\sigma_t}\right)^2\right), \tag{40}$$

where N and $f_{\rm sig}$ are the number of B_s^0 candidates and the fraction of B_s^0 signal in the selected sample, w is the total mistag probability, and σ_t is the resolution on proper time. As can be seen, the quantity $\mathcal{S}$ decreases very quickly as Δm_s increases: this dependence is controlled by σ_t, which is therefore the most critical parameter for Δm_s analyses. The method widely used for B_s^0 oscillation searches consists of measuring a B_s^0 oscillation amplitude $\mathcal{A}$ at several different test values of Δm_s, using a maximum likelihood fit based on the functions of Eq. (32) where the cosine terms have been multiplied by $\mathcal{A}$. One expects $\mathcal{A} = 1$ at the true value of Δm_s and to $\mathcal{A} = 0$ at a test value of Δm_s (far) below the true value. To a good approximation, the statistical uncertainty on $\mathcal{A}$ is Gaussian and equal to $1/\mathcal{S}$ [113].

Figures 5 and 6 show the amplitude spectra published by ALEPH [114], CDF [115], DELPHI [94, 116, 65, 117], OPAL [118, 119] and SLD [120, 121].[4] In each analysis, a particular value of Δm_s can be excluded at 95% CL if $\mathcal{A} + 1.645\,\sigma_{\mathcal{A}} < 1$, where $\sigma_{\mathcal{A}}$ is the total uncertainty on $\mathcal{A}$. Because of the proper time resolution, the quantity $\sigma_{\mathcal{A}}(\Delta m_s)$ is an increasing function of Δm_s (see Eq. (40) which merely models $1/\sigma_{\mathcal{A}}(\Delta m_s)$ since all results are limited by the available statistics). Therefore, if the true value of Δm_s were infinitely large, one expects to be able to exclude all values of Δm_s up to $\Delta m_s^{\rm sens}$, where $\Delta m_s^{\rm sens}$, called here the sensitivity of the analysis, is defined by $1.645\,\sigma_{\mathcal{A}}(\Delta m_s^{\rm sens}) = 1$. The most sensitive analyses appear to be the ones based on inclusive lepton samples at LEP, where reasonable statistics is available. Because of their better proper time resolution, the small data samples analyzed inclusively at SLD, as well as the few fully reconstructed B_s^0 decays at LEP, turn out to be also very useful to explore the high Δm_s region.

These oscillation searches can easily be combined by averaging the measured amplitudes $\mathcal{A}$ at each test value of Δm_s. The combined amplitude spectra for the individual experiments are displayed in Fig. 7, and the world average spectrum is displayed in Fig. 8. The individual results have been adjusted to common physics inputs, and all known correlations have been accounted for; in the case of the inclusive analyses, the sensitivities (*i.e.* the statistical uncertainties on $\mathcal{A}$), which depend directly through Eq. (40) on the assumed fraction $f_{\rm sig} \sim f_s$ of B_s^0 mesons in an unbiased sample of weakly-decaying b hadrons, have also been rescaled to a common average of $f_s = 0.104 \pm 0.015$. The combined sensitivity for 95% CL exclusion of Δm_s values is found to be 18.2 ps^{-1}. All values of Δm_s below 14.5 ps^{-1} are excluded at 95% CL, which we express as

$$\Delta m_s > 14.5 \text{ ps}^{-1} \text{ at } 95\% \text{ CL}\,. \tag{41}$$

[4] An unpublished analysis from SLD [122], based on an inclusive reconstruction from a lepton and a topologically reconstructed D meson, is not included in the plots or combined results quoted in this section. However, nothing is known to be wrong about this analysis, and including it would increase the combined Δm_s limit of Eq. (41) by less than 0.1 ps^{-1} and the combined sensitivity by 0.9 ps^{-1}.

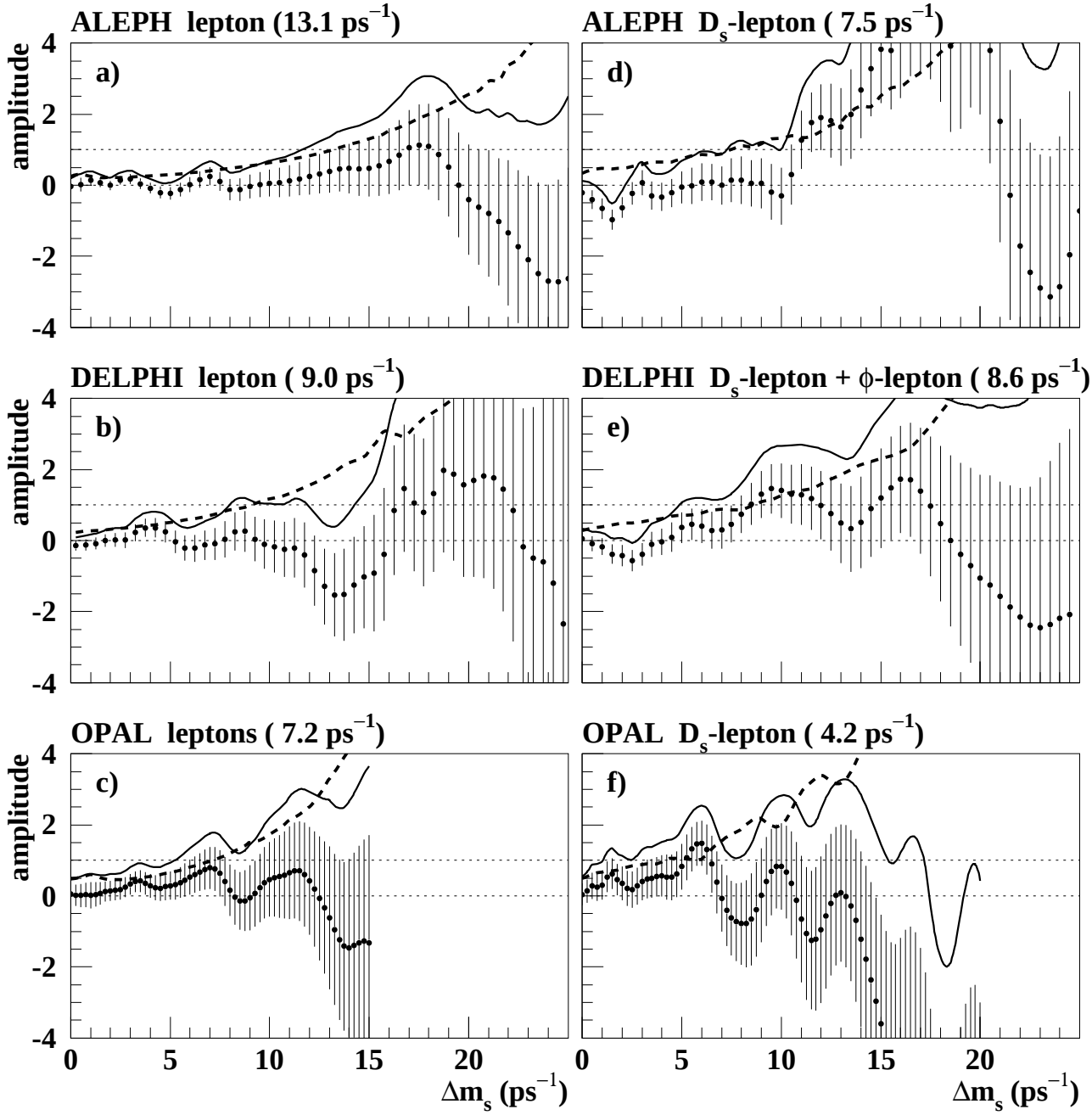

Figure 5: B_s^0-oscillation amplitude spectra, displayed separately for each B_s^0 oscillation analysis. The points and error bars represent the measurements of the amplitude $\mathcal{A}$ and their total uncertainties $\sigma_{\mathcal{A}}$, adjusted to a set of physics parameters common to all analyses (including $f_s = 0.104 \pm 0.015$). Values of Δm_s where the solid curve ($\mathcal{A} + 1.645\,\sigma_{\mathcal{A}}$) is below 1 are excluded at 95% CL. The dashed curve shows $1.645\,\sigma_{\mathcal{A}}$; the number in parenthesis indicates where this curve is equal to 1, and is a measure of the sensitivity of the analysis. a) ALEPH inclusive lepton [114], b) DELPHI inclusive lepton [117], c) OPAL inclusive lepton and dilepton [118], d) ALEPH D_s-ℓ [114], e) DELPHI D_s-ℓ [117] and ϕ-ℓ [116], f) OPAL D_s-ℓ [119] (continued on Fig. 6).

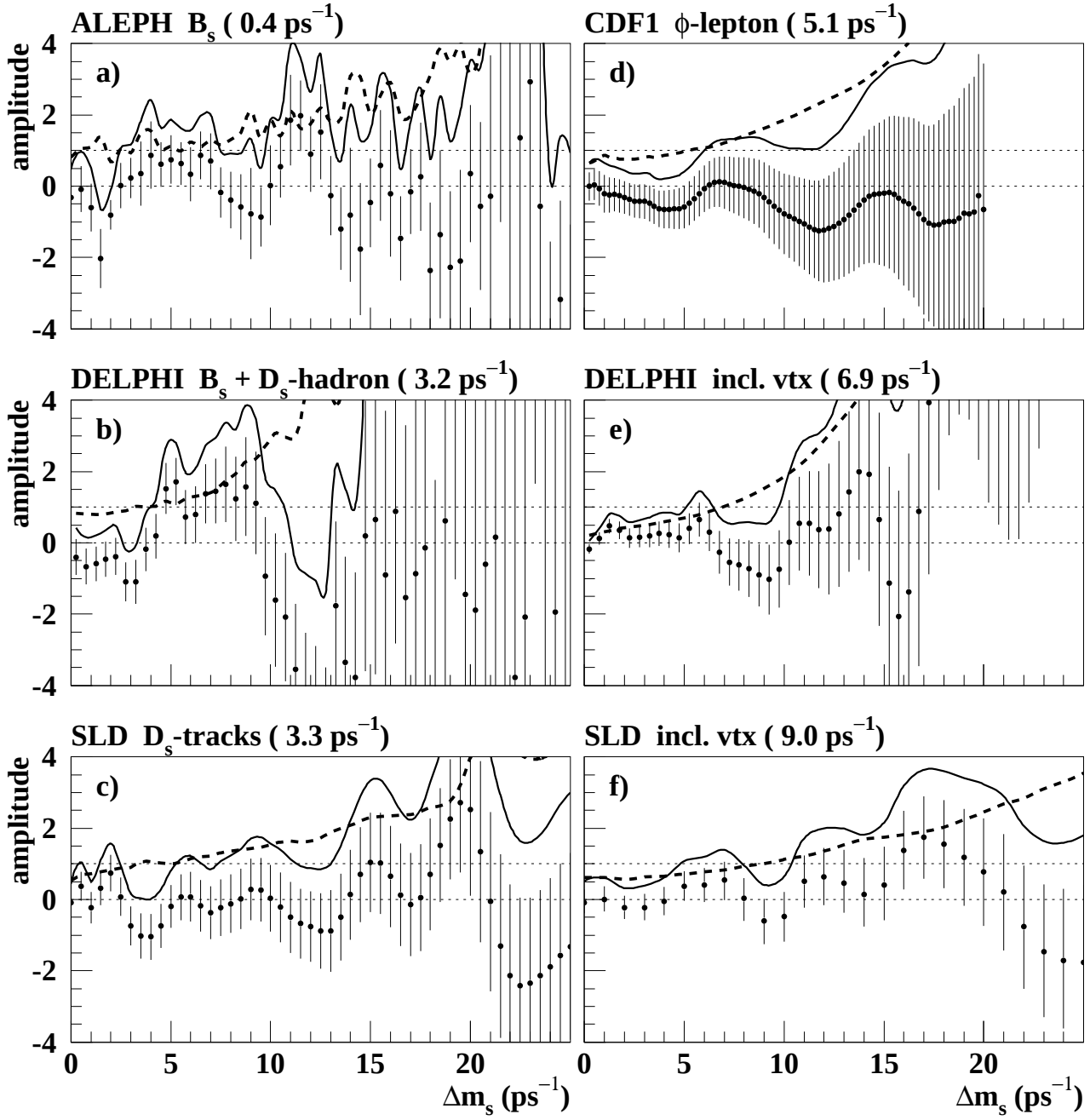

Figure 6: (continuation of Fig. 5) B_s^0-oscillation amplitude spectra, displayed separately for each B_s^0 oscillation analysis, in the same manner as in Fig. 5. a) ALEPH fully reconstructed B_s^0 [114], b) DELPHI fully reconstructed B_s^0 and D_s-hadron [65], c) SLD D_s +tracks [121], d) CDF ϕ-ℓ [115], e) DELPHI inclusive vertex [94], f) SLD inclusive vertex dipole [120].

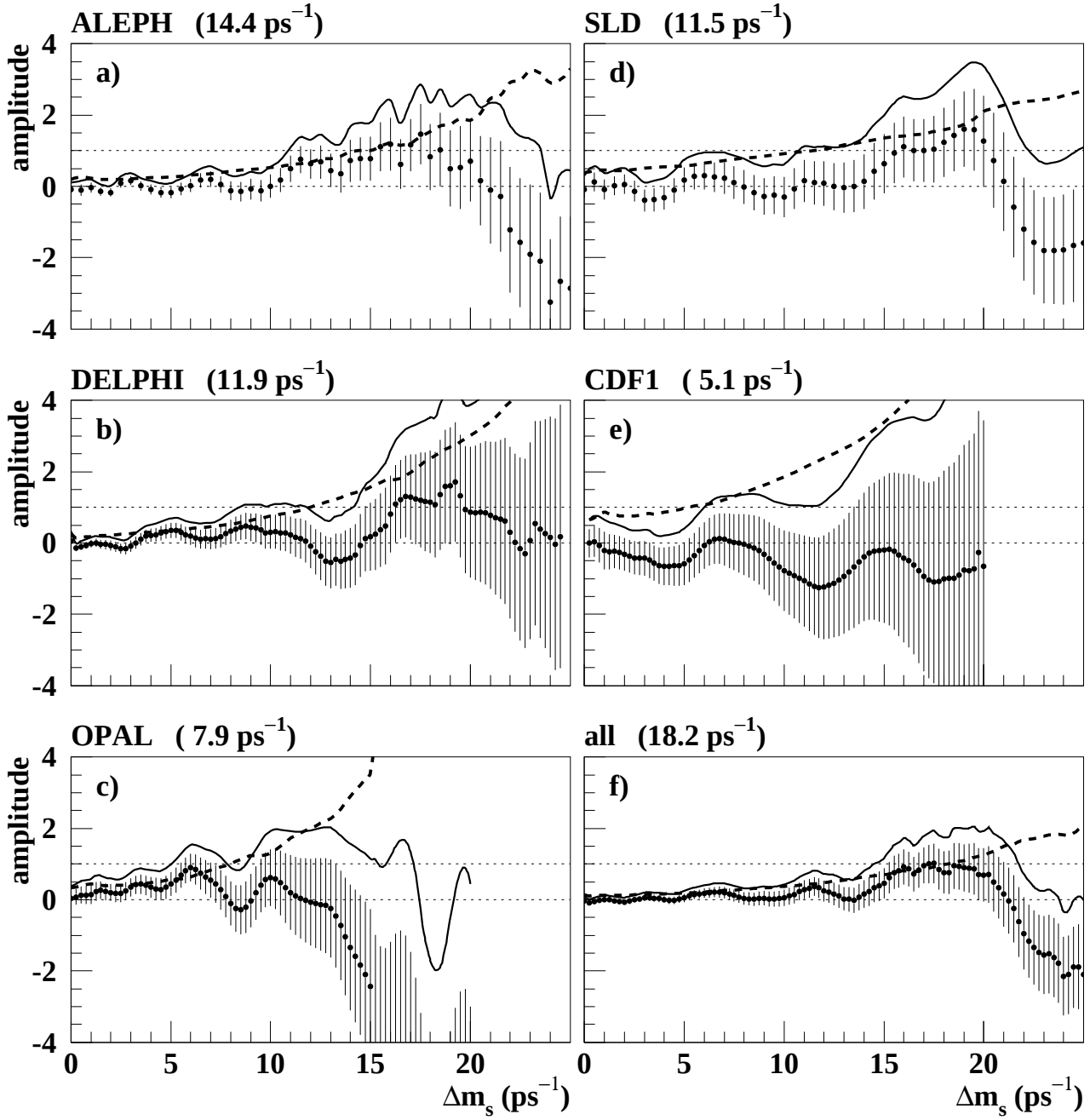

Figure 7: Combined B_s^0-oscillation amplitude spectra, displayed separately for each experiment, in the same manner as in Fig. 5. a) ALEPH [114], b) DELPHI [65, 116, 94, 117], c) OPAL[118, 119], d) SLD [121, 120], e) CDF [115], f) all experiments together.

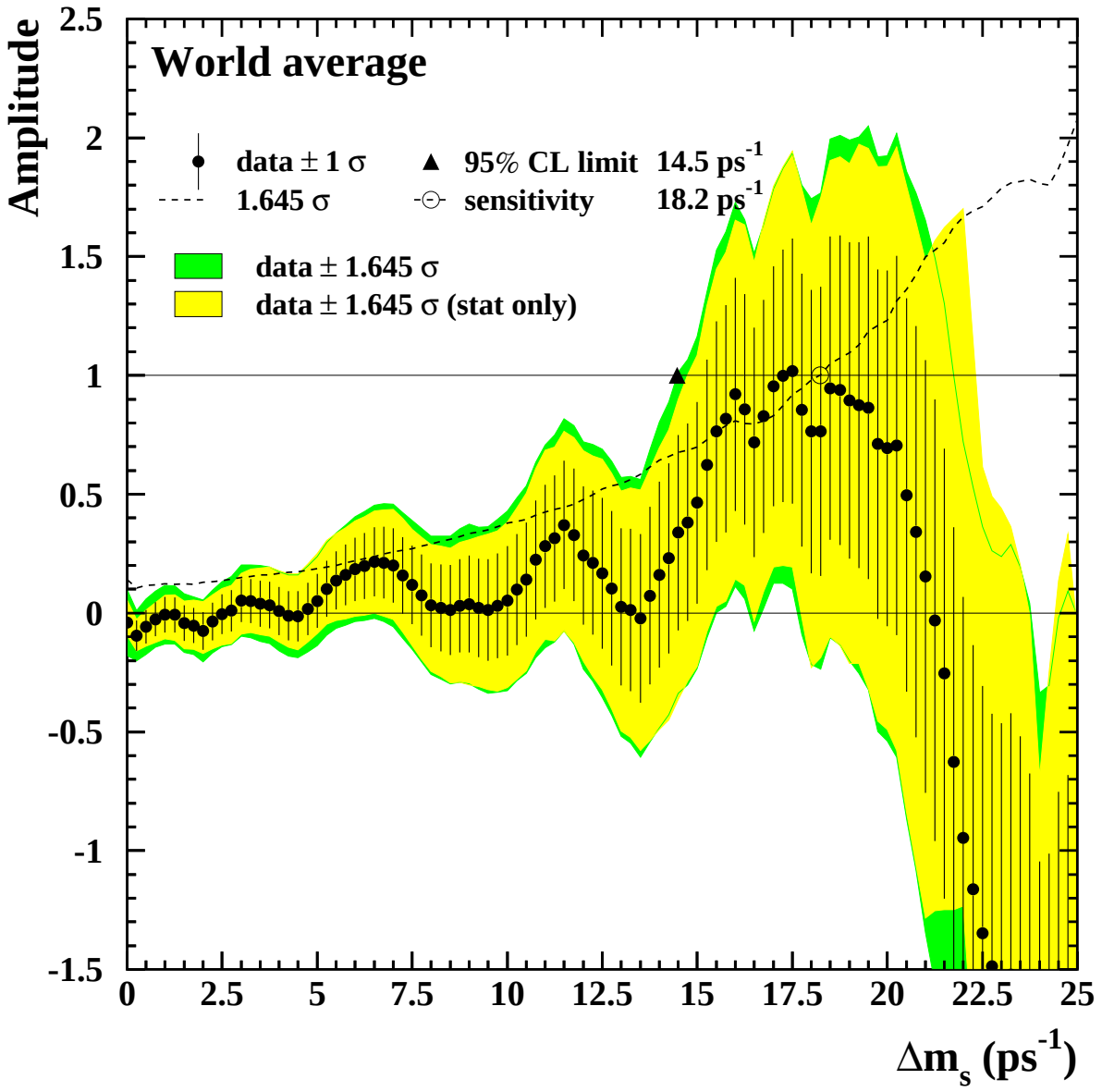

Figure 8: Combined measurements of the B_s^0 oscillation amplitude as a function of Δm_s, including all results published by Summer 2004 [120, 94, 116, 65, 114, 115, 117, 118, 119, 121]. The measurements are dominated by statistical uncertainties. Neighboring points are statistically correlated.

The values between 14.5 ps^{-1} and 21.7 ps^{-1} cannot be excluded, because the data is compatible with a signal in this region. However, no deviation from $\mathcal{A} = 0$ is seen in Fig. 8 that would indicate the observation of a signal.

It should be noted that most Δm_s analyses assume no decay-width difference in the B_s^0 system. Due to the presence of the cosh terms in Eq. (32), a non-zero value of $\Delta\Gamma_s$ would reduce the oscillation amplitude with a small time-dependent factor that would be very difficult to distinguish from time resolution effects.

Convoluting the average B_s^0 lifetime, 1.469 ± 0.059 ps, with the limit of Eq. (41) yields

$$x_s = \Delta m_s \, \tau(B_s^0) > 20.8 \text{ at } 95\% \text{ CL}\,. \tag{42}$$

Under the assumption $\Delta\Gamma_s = 0$, *i.e.* $y_s = \Delta\Gamma_s/(2\Gamma_s) = 0$ (and no *CP* violation in the mixing), this is equivalent to

$$\chi_s = \frac{x_s^2 + y_s^2}{2(x_s^2+1)} > 0.49885 \text{ at } 95\% \text{ CL}\,. \tag{43}$$

Decay width difference $\Delta\Gamma_s$

Information on $\Delta\Gamma_s$ can be obtained by studying the proper time distribution of untagged data samples enriched in B_s^0 mesons [123]. In the case of an inclusive B_s^0 selection [46] or a semileptonic B_s^0 decay selection [116, 61], both the short- and long-lived components are present, and the proper time distribution is a superposition of two exponentials with decay constants $\Gamma_s \pm \Delta\Gamma_s/2$. In principle, this provides sensitivity to both Γ_s and $(\Delta\Gamma_s/\Gamma_s)^2$. Ignoring $\Delta\Gamma_s$ and fitting for a single exponential leads to an estimate of Γ_s with a relative bias proportional to $(\Delta\Gamma_s/\Gamma_s)^2$. An alternative approach, which is directly sensitive to first order in $\Delta\Gamma_s/\Gamma_s$, is to determine the lifetime of B_s^0 candidates decaying to *CP* eigenstates; measurements exist for $B_s^0 \to J/\psi\phi$ [37, 56, 68] and $B_s^0 \to D_s^{(*)+} D_s^{(*)-}$ [124], which are mostly *CP*-even states [125]. However, a time-dependent angular analysis of $B_s^0 \to J/\psi\phi$ allows the simultaneous extraction of $\Delta\Gamma_s/\Gamma_s$ and the *CP*-even and *CP*-odd amplitudes [127]. An estimate of $\Delta\Gamma_s/\Gamma_s$ has also been obtained directly from a measurement of the $B_s^0 \to D_s^{(*)+} D_s^{(*)-}$ branching ratio [124], under the assumption that these decays account for all the *CP*-even final states (however, no systematic uncertainty due to this assumption is given, so the average quoted below will not include this estimate).

Present published data is not precise enough to efficiently constrain both Γ_s and $\Delta\Gamma_s/\Gamma_s$; since the B_s^0 and B^0 lifetimes are predicted to be equal within a percent [126, 24], an expectation compatible with the current experimental data (see Table 11), the constraint $\Gamma_s = \Gamma_d$ can also be used to improve the extraction of $\Delta\Gamma_s/\Gamma_s$. Applying the combination procedure of Ref. [2] on the published results [116, 61, 37, 124, 60, 63] yields

$$|\Delta\Gamma_s|/\Gamma_s < 0.54 \quad \text{at } 95\% \text{ CL} \tag{44}$$

without external constraint, or

$$|\Delta\Gamma_s|/\Gamma_s < 0.29 \quad \text{at } 95\% \text{ CL} \tag{45}$$

when constraining $1/\Gamma_s$ to the measured B^0 lifetime. This can be compared with the recent preliminary measurement of CDF [127] obtained from the time-dependent angular analysis of $B_s^0 \to J/\psi\phi$ decays:

$$\Delta\Gamma_s/\Gamma_s = 0.65^{+0.25}_{-0.33} \pm 0.01\,. \tag{46}$$

These results are not yet precise enough to test the Standard Model predictions.

4 Semileptonic B decays

The original charge of the "Semileptonic B decays" working group consisted in

- the determination of the best values of the inclusive and exclusive semileptonic B decay branching ratios from the combined data, both for Cabibbo-favored and Cabibbo-suppressed decays, fully taking into account correlations between the experiments;
- determining the best possible values of $F(1)|V_{cb}|$ from exclusive semileptonic B decays and of $|V_{cb}|$ from the inclusive semileptonic B decay rate;
- a detailed understanding of the correlated theoretical errors and the encouragement of a uniform and consistent error estimation among the active experiments.

Currently, this program is implemented to varying degrees. The work of the "LEP Heavy Flavor Steering Group" has resulted in averages for Cabibbo-favored exclusive and inclusive semileptonic decays (see, *e.g.*, Ref. [128]). Recently, the determination of $|V_{cb}|$ from inclusive decays has entered a new level precision with the inclusion of data on the moments of invariant mass and lepton energy distribution in semileptonic B decays. This approach is not yet implemented in HFAG.

In this edition of the HFAG updates, we present an average of inclusive determinations of $|V_{ub}|$. Work is in progress to achieve the same for exclusive decays and eventually for a combination of inclusive and exclusive results. See Ref. [129] for an alternative best estimate of $|V_{ub}|$.

In the following a detailed description of all parameters and published analyses (including preliminary results) relevant for the determination of the combined results is provided. The description is based on the information available on the web-page at

`http://www.slac.stanford.edu/xorg/hfag/semi/summer04/summer04.shtml`

In the combination of the published results, the central values and errors are rescaled to a common set of input parameters, summarized in Table 15 and provided in the file `common.param` (accessible from the web-page). All measurements with a dependency on any of these parameters are rescaled to the central values given in Table 15, and their error is recalculated based on the error provided in the column "Excursion". The detailed dependency for each measurement is contained in files (provided by the experiments) accessible from the web-page.

4.1 Exclusive Cabibbo-favored decays

Aspects of the phenomenology of exclusive Cabibbo-favored B decays and their use in the determination of $|V_{cb}|$ in the context of Heavy Quark Effective Theory (HQET) are described in many places, *e.g.*, in Ref. [128] and will not be repeated here.

Averages are provided for both the branching ratios $\mathcal{B}(\overline{B}^0 \to D^{*+}\ell^-\overline{\nu})$ plus $\mathcal{B}(\overline{B}^0 \to D^{+}\ell^-\overline{\nu})$ and the CKM matrix element $|V_{cb}|$ multiplied by the form factor at zero recoil of the decay $\overline{B}^0 \to D^{*+}\ell^-\overline{\nu}$ and $\overline{B}^0 \to D^{+}\ell^-\overline{\nu}$, respectively.

Table 15: Common input parameters for the combination of semileptonic B decays. Most of the parameters are taken from Ref. [3]. This table is encoded in the file `common.param`. The units are picoseconds for lifetimes and percentage for branching fractions.

Parameter	Assumed Value	Excursion	Description
rb	21.646	± 0.065	R_b
bdst	1.27	± 0.021	$\mathcal{B}(\overline{B} \to D^* \tau \overline{\nu})$
bdsd	1.62	± 0.040	$\mathcal{B}(\overline{B} \to D^* D)$
bdst2	0.65	± 0.013	$\mathcal{B}(b \to D^* \tau)$ (OPAL incl)
bdsd2	4.2	± 1.5	$\mathcal{B}(b \to D^* D)$ (OPAL incl)
bdsd3	0.87	$^{+0.23}_{-0.19}$	$\mathcal{B}(b \to D^* D)$ (DELPHI incl)
xe	0.702	± 0.008	B fragmentation: $\langle E_B \rangle / E_{\rm beam}$
bdsi	17.3	± 2.0	$\mathcal{B}(b \to D^{*+}$ incl)
cdsi	22.6	± 1.4	$\mathcal{B}(c \to D^{*+}$ incl)
tb0	1.534	± 0.013	$\tau(B^0)$
tbplus	1.653	± 0.014	$\tau(B^+)$
tbps	1.442	± 0.066	$\tau(B_s^0)$
fbd	39.8	± 1.0	B^0 fraction at $\sqrt{s} = m_{Z^0}$
fbs	10.5	± 1.5	B_s^0 fraction at $\sqrt{s} = m_{Z^0}$
fbar	9.9	± 1.7	Baryon fraction at $\sqrt{s} = m_{Z^0}$
dst	67.7	± 0.5	$\mathcal{B}(D^{*+} \to D^0 \pi^+)$
dkpp	9.20	± 0.6	$\mathcal{B}(D^+ \to K^- \pi^+ \pi^+)$
dkp	3.80	± 0.09	$\mathcal{B}(D^0 \to K^- \pi^+)$
dkpzp	13.0	± 0.8	$\mathcal{B}(D^0 \to K^- \pi^+ \pi^0)$
dkppp	7.46	± 0.31	$\mathcal{B}(D^0 \to K^- \pi^+ \pi^+ \pi^-)$
dkzpp	2.99	± 0.18	$\mathcal{B}(D^0 \to K^0 \pi^+ \pi^-)$
dkln	7.0	± 0.4	$\mathcal{B}(D^0 \to K^- \ell^+ \nu)$
dkk	4.3	± 0.2	$\mathcal{B}(D^0 \to K^- K^+)$
dkx	1.100	± 0.025	$K^- \pi^+ X$ rates
dkox	0.42	± 0.05	$\mathcal{B}(D^0 \to K^0 X)$
dnlx	6.87	± 0.28	$\mathcal{B}(D^0 \to X \ell \overline{\nu})$
dkpcl	61.2	± 2.9	$\mathcal{B}(D^{*0} \to D^0 \pi^0)$
dssR	0.64	± 0.11	$\mathcal{B}(b \to D^{**} \ell \overline{\nu}) \times \mathcal{B}(D^{**} \to D^{*+} X)$
fb0	49.4	± 0.8	$f^{00} = \mathcal{B}(\Upsilon(4S) \to B^0 \overline{B}^0)$
chid	0.186	± 0.004	χ_d, time-integrated probability for B^0 mixing
chi	0.092	± 0.002	$\chi = \chi_d \times (f^{00}/100)$

4.1.1 $\overline{B}^0 \to D^{*+} \ell^- \overline{\nu}$

The measurements included in the average, shown in Table 16 are scaled to a consistent set of input parameters and their errors. Therefore some of the (older) measurements are subject to considerable adjustments.

- In order to reduce the dependence on theoretical error estimates, the central values and errors for the form factors R_1 and R_2 are taken from the measurement by CLEO [130].

However, all experiments (except for the CLEO [135], the recent DELPHI [136] and the *BABAR* [137] measurements) quote in their abstracts $F(1)|V_{cb}|$ based on form factors (and their respective errors) from theory. Belle provides a second result evaluated with the CLEO form factors. All other experiments have recalculated $F(1)|V_{cb}|$ to rely on the CLEO form factors. In the future, a substantial improvement in the error associated with form factors is expected by including form factor measurements at the B factories.

- Updates in the branching fractions of D mesons and the production of D^{**} mesons in B decays have generally lead to increased rates for $\mathcal{B}(\overline{B}^0 \to D^{*+}\ell^-\overline{\nu})$.

- The average B^0 lifetime has changed considerably since the ALEPH measurement, especially with the much higher precision available at the B factories. This effect is less visible in the other measurements as they are more recent.

- The production of B^0 mesons at $\sqrt{s} = m_{Z^0}$ has a direct impact on all LEP measurements. Adjusting results on the $\Upsilon(4S)$ for the branching fraction of $\mathcal{B}(\Upsilon(4S) \to B^0\overline{B}^0) \equiv f^{00}$ yields an increase compared to the assumption of $f^{00} = 0.5$.

- Many input parameters are now known with a much increased precision—this decreases some of the systematic errors of the rescaled results with respect to the original publication.

The largest correlated errors are the fraction of B^0 mesons (fbd and fb0, respectively), the form factors $R_1(1)$ and $R_2(1)$ at zero recoil, B^0 meson lifetime, branching fractions of D mesons, and the details of D^{**} modeling.

At LEP, the measurements of $\overline{B}^0 \to D^{*+}\ell^-\overline{\nu}$ decays have been done both with "inclusive" analyses based on a partial reconstruction of the $\overline{B}^0 \to D^{*+}\ell^-\overline{\nu}$ decay and a full reconstruction of the exclusive decay. The average branching ratio $\mathcal{B}(\overline{B}^0 \to D^{*+}\ell^-\overline{\nu})$ is determined in a one-dimensional fit from the measurements provided in Table 16. The statistical correlation between two analyses from the same experiment (DELPHI and OPAL, respectively) is taken into account. Figure 9(a) illustrates the measurements and the resulting average. The $\chi^2/\text{dof} = 14.7/7$ is slightly above the level where the PDG starts to introduce scale factors. The measurement by CLEO provides the largest contribution to the χ^2.

The average for $F(1)|V_{cb}|$ is determined by the two-dimensional combination of the results provided in Table 17. This allows to fully incorporate the correlation between $F(1)|V_{cb}|$ and ρ^2. Figure 10(b) illustrates the average $F(1)|V_{cb}|$ and the measurements included in the average. Figure 10(a) provides a one-dimensional projection for illustrative purposes. The $\chi^2/\text{dof} = 27.5/14$ is below the level where the PDG starts to introduce scale factors. The measurement by CLEO provides the largest contribution to the χ^2.

For a determination of $|V_{cb}|$, the form factor at zero recoil $F(1)$ needs to be computed. A possible choice is $F(1) = 0.91 \pm 0.04_{\text{theo}}$ [138], resulting in

$$|V_{cb}| = (41.4 \pm 1.0_{\text{exp}} \pm 1.8_{\text{theo}}) \times 10^{-3}.$$

The value for $F(1)$ and its error is based on a comparison of estimates using OPE sum rules and with an HQET based lattice gauge calculation (see Ref. [138] for more details).

Table 16: Average branching ratio $\mathcal{B}(\overline{B}^0 \to D^{*+}\ell^-\overline{\nu})$ and individual results. See the description in the text for explanations why the published results are lower than the rescaled results.

Experiment	$\mathcal{B}(\overline{B}^0 \to D^{*+}\ell^-\overline{\nu})[\%]$ (rescaled)	$\mathcal{B}(\overline{B}^0 \to D^{*+}\ell^-\overline{\nu})[\%]$ (published)
ALEPH (excl) [131]	$5.78 \pm 0.26_{\rm stat} \pm 0.36_{\rm syst}$	$5.53 \pm 0.26_{\rm stat} \pm 0.52_{\rm syst}$
OPAL (excl) [132]	$5.51 \pm 0.19_{\rm stat} \pm 0.40_{\rm syst}$	$5.11 \pm 0.19_{\rm stat} \pm 0.49_{\rm syst}$
OPAL (incl) [132]	$6.20 \pm 0.27_{\rm stat} \pm 0.58_{\rm syst}$	$5.92 \pm 0.27_{\rm stat} \pm 0.68_{\rm syst}$
DELPHI (incl) [133]	$5.04 \pm 0.13_{\rm stat} \pm 0.36_{\rm syst}$	$4.70 \pm 0.13_{\rm stat}\ ^{+0.36}_{-0.31\ \rm syst}$
Belle (excl) [134]	$4.72 \pm 0.23_{\rm stat} \pm 0.42_{\rm syst}$	$4.60 \pm 0.23_{\rm stat} \pm 0.40_{\rm syst}$
CLEO (excl) [135]	$6.26 \pm 0.19_{\rm stat} \pm 0.39_{\rm syst}$	$6.09 \pm 0.19_{\rm stat} \pm 0.40_{\rm syst}$
DELPHI (excl) [136]	$5.80 \pm 0.22_{\rm stat} \pm 0.47_{\rm syst}$	$5.90 \pm 0.22_{\rm stat} \pm 0.50_{\rm syst}$
BABAR (excl) [137]	$4.85 \pm 0.07_{\rm stat} \pm 0.34_{\rm syst}$	$4.90 \pm 0.07_{\rm stat} \pm 0.36_{\rm syst}$
Average	$\mathbf{5.34 \pm 0.20}$	$\boldsymbol{\chi^2/\mathrm{dof} = 14.7/7}$

Table 17: Average of $F(1)|V_{cb}|$ determined in the decay $\overline{B}^0 \to D^{*+}\ell^-\overline{\nu}$ and individual results. The fit for the average has $\chi^2/\mathrm{dof} = 27.5/14$. The total correlation between the average $F(1)|V_{cb}|$ and ρ^2 is 0.57.

Experiment	$F(1)\lvert V_{cb}\rvert[10^{-3}]$ (rescaled) $F(1)\lvert V_{cb}\rvert[10^{-3}]$ (published)	ρ^2 (rescaled) ρ^2 (published)
ALEPH (excl) [131]	$33.7 \pm 2.1_{\rm stat} \pm 1.6_{\rm syst}$	$0.75 \pm 0.25_{\rm stat} \pm 0.37_{\rm syst}$
	$31.9 \pm 1.8_{\rm stat} \pm 1.9_{\rm syst}$	$0.37 \pm 0.26_{\rm stat} \pm 0.14_{\rm syst}$
OPAL (incl) [132]	$38.6 \pm 1.2_{\rm stat} \pm 2.4_{\rm syst}$	$1.25 \pm 0.14_{\rm stat} \pm 0.39_{\rm syst}$
	$37.5 \pm 1.2_{\rm stat} \pm 2.5_{\rm syst}$	$1.12 \pm 0.14_{\rm stat} \pm 0.29_{\rm syst}$
OPAL (excl) [132]	$39.3 \pm 1.6_{\rm stat} \pm 1.8_{\rm syst}$	$1.49 \pm 0.21_{\rm stat} \pm 0.26_{\rm syst}$
	$36.8 \pm 1.6_{\rm stat} \pm 2.0_{\rm syst}$	$1.31 \pm 0.21_{\rm stat} \pm 0.16_{\rm syst}$
DELPHI (incl) [133]	$37.0 \pm 1.4_{\rm stat} \pm 2.5_{\rm syst}$	$1.50 \pm 0.14_{\rm stat} \pm 0.37_{\rm syst}$
	$35.5 \pm 1.4_{\rm stat}\ ^{+2.3}_{-2.4\rm syst}$	$1.34 \pm 0.14_{\rm stat}\ ^{+0.24}_{-0.22\rm syst}$
Belle (excl) [134]	$36.5 \pm 1.9_{\rm stat} \pm 1.9_{\rm syst}$	$1.45 \pm 0.16_{\rm stat} \pm 0.20_{\rm syst}$
	$35.8 \pm 1.9_{\rm stat} \pm 1.9_{\rm syst}$	$1.45 \pm 0.16_{\rm stat} \pm 0.20_{\rm syst}$
CLEO (excl) [135]	$43.7 \pm 1.3_{\rm stat} \pm 1.8_{\rm syst}$	$1.61 \pm 0.09_{\rm stat} \pm 0.21_{\rm syst}$
	$43.1 \pm 1.3_{\rm stat} \pm 1.8_{\rm syst}$	$1.61 \pm 0.09_{\rm stat} \pm 0.21_{\rm syst}$
DELPHI (excl) [136]	$38.9 \pm 1.8_{\rm stat} \pm 2.1_{\rm syst}$	$1.32 \pm 0.15_{\rm stat} \pm 0.33_{\rm syst}$
	$39.2 \pm 1.8_{\rm stat} \pm 2.3_{\rm syst}$	$1.32 \pm 0.15_{\rm stat} \pm 0.33_{\rm syst}$
BABAR (excl) [137]	$35.4 \pm 0.3_{\rm stat} \pm 1.6_{\rm syst}$	$1.29 \pm 0.03_{\rm stat} \pm 0.27_{\rm syst}$
	$35.5 \pm 0.3_{\rm stat} \pm 1.6_{\rm syst}$	$1.29 \pm 0.03_{\rm stat} \pm 0.27_{\rm syst}$
Average	$\mathbf{37.7 \pm 0.9}$	$\mathbf{1.55 \pm 0.14}$

4.1.2 $\overline{B}^0 \to D^+\ell^-\overline{\nu}$

The average branching ratio $\mathcal{B}(\overline{B}^0 \to D^+\ell^-\overline{\nu})$ is determined by the combination of the results provided in Table 18. The error sources here are the same as discussed in Sec. 4.1.1, but

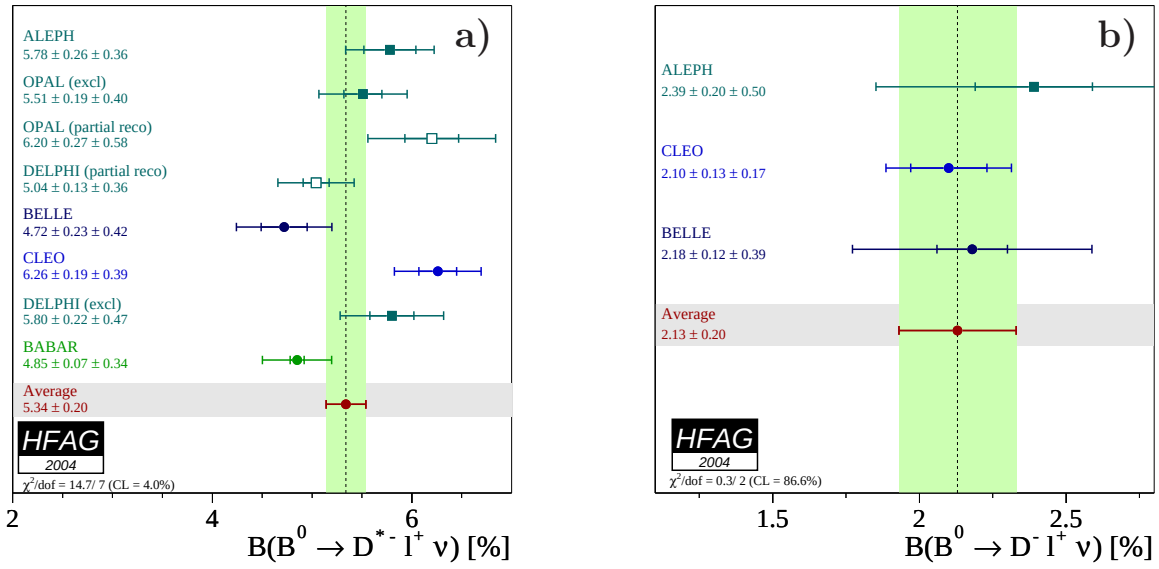

Figure 9: Average branching ratio of exclusive semileptonic B decays. (a) $\overline{B}^0 \to D^{*+}\ell^-\overline{\nu}$ and (b) $\overline{B}^0 \to D^+\ell^-\overline{\nu}$.

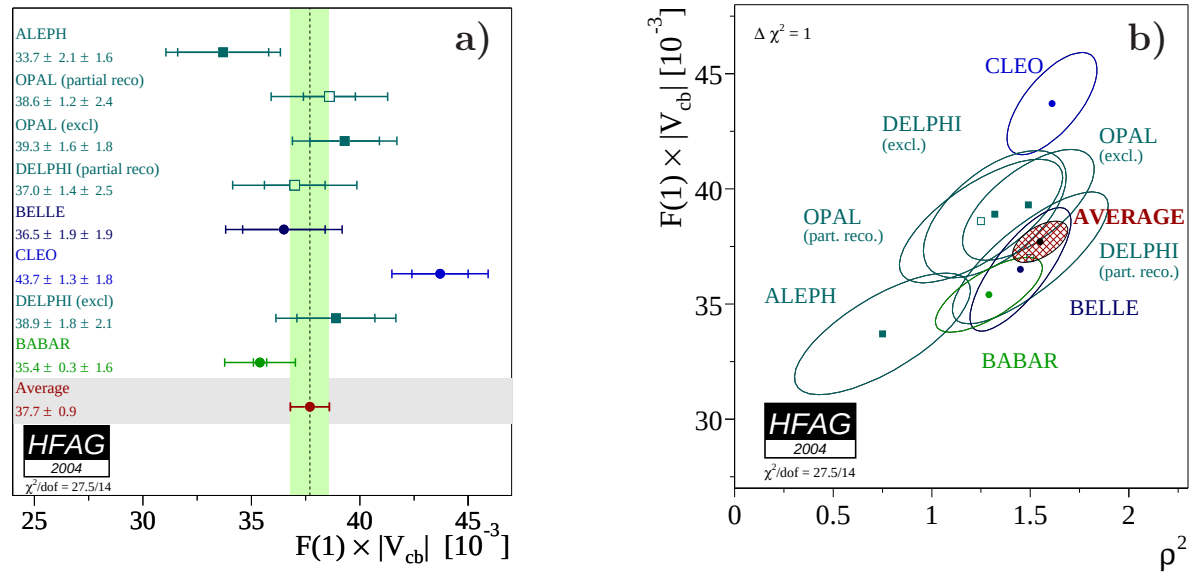

Figure 10: (a) Illustration of the average $F(1)|V_{cb}|$ and rescaled measurements of exclusive $\overline{B}^0 \to D^{*+}\ell^-\overline{\nu}$ decays determined in a two-dimensional fit. (b) Illustration of $F(1)|V_{cb}|$ vs. ρ^2. The error ellipses correspond to $\Delta\chi^2 = 1$.

generally at a higher level due to larger background levels, less stringent kinematic constraints, and larger kinematic suppression at the endpoint. Figure 9(b) illustrates the measurements and the resulting average.

Table 18: Average of the branching ratio $\mathcal{B}(\overline{B}^0 \to D^+\ell^-\overline{\nu})$ and individual results.

Experiment	$\mathcal{B}(\overline{B}^0 \to D^+\ell^-\overline{\nu})[\%]$ (rescaled)	$\mathcal{B}(\overline{B}^0 \to D^+\ell^-\overline{\nu})[\%]$ (published)
ALEPH [131]	$2.39 \pm 0.20_{\rm stat} \pm 0.50_{\rm syst}$	$2.35 \pm 0.20_{\rm stat} \pm 0.44_{\rm syst}$
CLEO [139]	$2.10 \pm 0.13_{\rm stat} \pm 0.17_{\rm syst}$	$2.20 \pm 0.16_{\rm stat} \pm 0.19_{\rm syst}$
Belle [140]	$2.18 \pm 0.12_{\rm stat} \pm 0.39_{\rm syst}$	$2.13 \pm 0.12_{\rm stat} \pm 0.39_{\rm syst}$
Average	$\mathbf{2.13 \pm 0.20}$	$\boldsymbol{\chi^2/\mathrm{dof} = 0.3/2}$

The average for $G(1)|V_{cb}|$ is determined by the two-dimensional combination of the results provided in Table 19. Figure 11(b) illustrates the average $F(1)|V_{cb}|$ and the measurements included in the average. Figure 11(a) provides a one-dimensional projection for illustrative purposes.

Table 19: Average of $G(1)|V_{cb}|$ determined in the decay $\overline{B}^0 \to D^+\ell^-\overline{\nu}$ and individual results. The fit for the average has $\chi^2/\mathrm{dof} = 0.3/4$.

Experiment	$G(1)\lvert V_{cb}\rvert[10^{-3}]$ (rescaled) $G(1)\lvert V_{cb}\rvert[10^{-3}]$ (published)	ρ^2 (rescaled) ρ^2 (published)
ALEPH [131]	$39.9 \pm 10.0_{\rm stat} \pm 6.4_{\rm syst}$	$1.01 \pm 0.98_{\rm stat} \pm 0.37_{\rm syst}$
	$31.1 \pm 9.9_{\rm stat} \pm 8.6_{\rm syst}$	$0.20 \pm 0.98_{\rm stat} \pm 0.50_{\rm syst}$
CLEO [139]	$44.9 \pm 5.8_{\rm stat} \pm 3.5_{\rm syst}$	$1.27 \pm 0.25_{\rm stat} \pm 0.14_{\rm syst}$
	$44.8 \pm 6.1_{\rm stat} \pm 3.7_{\rm syst}$	$1.30 \pm 0.27_{\rm stat} \pm 0.14_{\rm syst}$
Belle [140]	$41.6 \pm 4.4_{\rm stat} \pm 5.2_{\rm syst}$	$1.12 \pm 0.22_{\rm stat} \pm 0.14_{\rm syst}$
	$41.1 \pm 4.4_{\rm stat} \pm 5.1_{\rm syst}$	$1.12 \pm 0.22_{\rm stat} \pm 0.14_{\rm syst}$
Average	$\mathbf{42.1 \pm 3.7}$	$\mathbf{1.15 \pm 0.16}$

For a determination of $|V_{cb}|$, the form factor at zero recoil $G(1)$ needs to be computed. A possible choice is $G(1) = 1.04 \pm 0.06_{\rm theo}$ [138], resulting in

$$|V_{cb}| = (40.4 \pm 3.6_{\rm exp} \pm 2.3_{\rm theo}) \times 10^{-3}.$$

4.2 Inclusive Cabibbo-favored decays

Aspects of the theory and phenomenology of inclusive Cabibbo-favored B decays and their use in the determination of $|V_{cb}|$ in the context of the Heavy Quark Expansion (HQE), an Operator Product Expansion based on HQET, are described in many places (see, *e.g.*, Ref. [141] and references therein).

Averages are provided for the total semileptonic branching ratio $\mathcal{B}(\overline{B} \to X\ell\overline{\nu})$ and the partial semileptonic branching fraction $\mathcal{B}(\overline{B} \to X\ell\overline{\nu}; E_\ell > 0.6\,\mathrm{GeV})$.

The measurements of the total semileptonic branching ratio $\mathcal{B}(b \to X\ell\overline{\nu})$ at LEP (see, *e.g.*, Ref [3] or Ref. [142]) represent a different analysis class with a more explicit model dependence

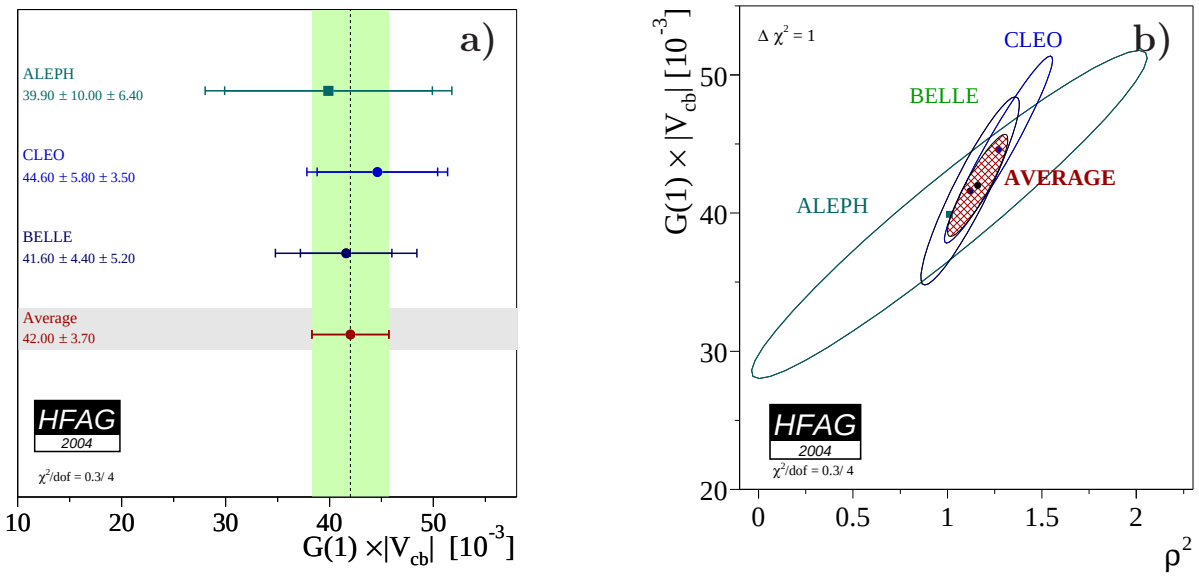

Figure 11: (a) Illustration of the average $G(1)|V_{cb}|$ and rescaled measurements of exclusive $\overline{B}^0 \to D^+\ell^-\overline{\nu}$ decays determined in a two-dimensional fit. (b) Illustration of $F(1)|V_{cb}|$ vs. ρ^2. The error ellipses correspond to $\Delta\chi^2 = 1$.

than the (lepton-)tagged analyses used at the $\Upsilon(4S)$. Therefore the LEP measurements are not used in the averages computed here.

4.2.1 Total semileptonic branching fraction

The average for the total branching ratio $\mathcal{B}(\overline{B} \to X\ell\overline{\nu})$ is determined by the combination of the results provided in Table 20. In this average, the extrapolation of the measured rate to the total decay rate is performed by each experiment, usually with a fit of several components to the experimental spectrum.

Table 20: Average of the total semileptonic branching fractions $\mathcal{B}(\overline{B} \to X\ell\overline{\nu})$ determined in tagged measurements on the $\Upsilon(4S)$.

Experiment	$\mathcal{B}_{tot}(\overline{B} \to X\ell\overline{\nu})[\%]$ (rescaled)	$\mathcal{B}_{tot}(\overline{B} \to X\ell\overline{\nu})[\%]$ (published)
ARGUS (ℓ-tag) [143]	$9.76 \pm 0.50 \pm 0.39$	$9.70 \pm 0.50 \pm 0.60$
BABAR (B_{reco}-tag) [144]	$10.40 \pm 0.50 \pm 0.46$	$10.40 \pm 0.50 \pm 0.46$
Belle (ℓ-tag) [145]	$10.97 \pm 0.12 \pm 0.49$	$10.90 \pm 0.12 \pm 0.49$
BABAR (e-tag) [146]	$10.92 \pm 0.18 \pm 0.29$	$10.87 \pm 0.18 \pm 0.30$
Belle (B_{reco}-tag) [147]	$11.19 \pm 0.20 \pm 0.31$	$11.19 \pm 0.20 \pm 0.31$
CLEO (ℓ-tag) [148]	$10.91 \pm 0.08 \pm 0.30$	$10.88 \pm 0.08 \pm 0.33$
Average	$\mathbf{10.90 \pm 0.23}$	$\boldsymbol{\chi^2/\mathrm{dof} = 5.0/5}$

It is possible to determine $|V_{cb}|$ from the total semileptonic branching fraction and the

lifetime of B mesons. However, this approach has limitations so that it is no longer applied. Recently, several groups have published global fits to the partial branching fraction plus the moments of the hadronic mass distribution and the lepton energy has been done by different groups [151, 152].

4.2.2 Partial semileptonic branching fraction

The average for the visible branching ratio $\mathcal{B}(\overline{B} \to X\ell\overline{\nu}; p_\ell > 0.6\,\mathrm{GeV}/c)$ is determined by the combination of the results provided in Table 21. For the determination of $|V_{cb}|$, the extrapolation to the full spectrum is not necessary, as the HQE allows the direct determination of $|V_{cb}|$ from a partial rate.

Table 21: Average of $\mathcal{B}(\overline{B} \to X\ell\overline{\nu}; p_\ell > 0.6\,\mathrm{GeV}/c)$ determined in (model-independent) lepton-tagged measurements on the $\Upsilon(4S)$.

Experiment	$\mathcal{B}_{vis}(\overline{B} \to X\ell\overline{\nu})[\%]$ (rescaled)	$\mathcal{B}_{vis}(\overline{B} \to X\ell\overline{\nu})[\%]$ (published)
Belle (ℓ-tag) [145]	$10.31 \pm 0.11 \pm 0.47$	$10.24 \pm 0.11 \pm 0.46$
BABAR (e-tag) [146]	$10.37 \pm 0.06 \pm 0.23$	$10.36 \pm 0.06 \pm 0.23$
CLEO (ℓ-tag) [148, 149]	$10.23 \pm 0.08 \pm 0.22$	$10.21 \pm 0.08 \pm 0.22$
Average	$\mathbf{10.29 \pm 0.18}$	$\boldsymbol{\chi^2/\mathrm{dof} = 0.22/2}$

4.2.3 Determination of $|V_{cb}|$

The determination of $|V_{cb}|$ directly from the visible branching fraction in combination with moments of the hadronic mass distribution and the lepton energy has been done by different groups [150, 151, 152]. It is foreseen to use a similar approach here as well in the future.

4.3 Exclusive Cabibbo-suppressed decays

Here we list results on exclusive determinations of $|V_{ub}|$. An average of (these) exclusive $b \to u\ell\overline{\nu}$ results is envisioned for the future. The measurements are separated into two classes: a first one averaging over the entire q^2 range (shown in Table 22), and a second class, where the decay rate is measured differentially in (few) bins of q^2 (shown in Table 23).

Table 22: Summary of exclusive determinations of $\mathcal{B}(\overline{B} \to X\ell\overline{\nu})$ and $|V_{ub}|$ using the entire q^2 range. The errors quoted on $|V_{ub}|$ correspond to statistical, experimental systematic and theoretical systematic, respectively.

Experiment	Mode	$\mathcal{B}[10^{-4}]$	$\lvert V_{ub}\rvert$ $[10^{-3}]$ (rescaled)
CLEO [153]	$B^0 \to \rho^-\ell^+\nu$	$2.69 \pm 0.41\ ^{+0.35}_{-0.40} \pm 0.50$	$3.24 \pm 0.25\ ^{+0.21}_{-0.24} \pm 0.58$
BABAR [154]	$B^0 \to \rho^-\ell^+\nu$	$3.29 \pm 0.42 \pm 0.47 \pm 0.60$	$3.59 \pm 0.23 \pm 0.26 \pm 0.66$
Belle [155]	$B^0 \to \omega\ell^+\nu$	$1.3 \pm 0.4 \pm 0.2 \pm 0.3$	$3.1 \pm 0.2 \pm 0.2 \pm 0.6$

Table 23: Summary of exclusive determinations of $\mathcal{B}(\overline{B} \to X\ell\overline{\nu})$ and $|V_{ub}|$ binned in q^2. The errors quoted on $|V_{ub}|$ correspond to statistical, experimental systematic, theoretical systematic, and signal form-factor shape, respectively.

Experiment	Mode	$\mathcal{B}[10^{-4}]$	$\lvert V_{ub}\rvert$ $[10^{-3}]$ (rescaled)
CLEO [156]	$B^0 \to \pi^-\ell^+\nu$	$1.33 \pm 0.18 \pm 0.11 \pm 0.01 \pm 0.07$	$2.88 \pm 0.55 \pm 0.30\ ^{+0.45}_{-0.35} \pm 0.18$
CLEO [156]	$B^0 \to \rho^-\ell^+\nu$	$2.17 \pm 0.34\ ^{+0.47}_{-0.54} \pm 0.41 \pm 0.01$	$3.34 \pm 0.32\ ^{+0.27}_{-0.36}\ ^{+0.50}_{-0.40}$
Belle [157]	$B^0 \to \pi^-\ell^+\nu$	$1.76 \pm 0.28\ \pm 0.20 \pm 0.03$	$3.90 \pm 0.71 \pm 0.23\ ^{+0.62}_{-0.48}$
Belle [157]	$B^0 \to \rho^-\ell^+\nu$	$2.54 \pm 0.78\ \pm 0.85 \pm 0.30$	
BABAR [158]	$B^0 \to \pi^-\ell^+\nu$	$1.46 \pm 0.27\ \pm 0.28$	

4.4 Inclusive Cabibbo-suppressed decays

A recent discussion of the theoretical issues and errors is provided, *e.g.*, in Refs. [159] and [160]. An independent estimate of the size of the theoretical uncertainties can be found in Ref. [129]. The following description is focusing on a technical description of the relevant details of the averaging procedure.

4.4.1 Determination of $|V_{ub}|$

Inclusive determinations of $|V_{ub}|$ based on charmless semileptonic B decays have been presented by all four LEP experiments [161] and, more recently, by the experiments at the $\Upsilon(4S)$. In all cases, the experimental approach is to measure the charmless semileptonic rate in a restricted region of phase space where the background from $B \to X_c\ell\overline{\nu}$ is suppressed. Theoretical input is used to extrapolate to the full rate and/or to determine $|V_{ub}|$. The determination of $|V_{ub}|$ from the full rate $\mathcal{B}(\overline{B} \to X_u\ell\overline{\nu})$ is accomplished with the following formula:

$$|V_{ub}| = 0.00424 \cdot \sqrt{\frac{\mathcal{B}(\overline{B} \to X_u\ell\overline{\nu})}{0.002}\frac{1.604\ \text{ps}}{\tau_B}} \times (1.000 \pm 0.028_{\text{pert}} \pm 0.039_{1/m_b^3}),$$

where τ_B is the average lifetime of B^0 and B^+ mesons and the theoretical error is based on Refs. [162, 163] using the moments measurements of the *BABAR* collaboration [151].

Here we combine results of the *BABAR*, Belle, and CLEO collaborations as they present measurements in well-defined phase-space regions and are based on the same theoretical description of the decay in terms of an OPE. Due to the large background from Cabibbo-favored $\overline{B} \to X_c\ell\overline{\nu}$ decays, the measurements are sensitive to $B \to X_u\ell\overline{\nu}$ decays only in restricted regions of phase-space. The convergence of the OPE is affected by these restrictions and complicate the extrapolation to the full rate and thus the determination of $|V_{ub}|$.

In the theoretical description, the motion of the b quark inside the B meson is described with a "shape function", usually in the two-parameter "exponential form". These parameters can be determined from a measurement of the photon energy spectrum in the rare decay $b \to s\gamma$. This decay has a smaller branching fraction than the decay $B \to X_u\ell\overline{\nu}$, which limits the precision possible in this approach. Recently, there has been theoretical interest to use moments measured in semileptonic $\overline{B} \to X_c\ell\overline{\nu}$ decays for the determination of the shape function parameters.

In the average $|V_{ub}|$ presented here, all measurements are scaled to a common set of the shape function parameters and their uncertainties. Both are taken from the photon energy spectrum in $B \to s\gamma$ decays as measured by the Belle collaboration [164]. The (large) errors of the shape function parameters are dominated by statistical uncertainties in the measurement of the photon energy spectrum.

For the average, the systematic error is divided into the categories shown in Table 24. In the averaging procedure, the errors belonging to a specific category are taken as 100% correlated between the different measurements. The numerical values of the errors for each measurement are given in a spreadsheet [165].

Table 24: Errors in the average of $|V_{ub}|$. The numerical values for all measurements can be found in a spreadsheet [165]. The entries in the "Name" column correspond to the names in the spreadsheet.

Name	Explanation
Uncorr	**Quadratic sum of statistical and experimental errors**
Statistical	Statistical
Exp	Experimental detector systematics (uncorrelated)
Corr	**Quadratic sum of correlated errors**
B2C(bg)	Modeling of $\overline{B} \to X_c \ell \overline{\nu}$ (Branching fractions, form factors, etc)
B2U(eff)	Modeling of $B \to X_u \ell \overline{\nu}$ (Branching fractions, ε_{vis}, $s\overline{s}$ popping, etc)
BF→Vub	Theoretical error $\Gamma \to |V_{ub}|$ (m_b, α_s)
fu(extrapol)	Extrapolation from visible range
Additional errors not provided by the experiments	
SSF	Subleading shape functions (power corrections)
WA	Weak annihilation
QHD	(Local) Quark-Hadron Duality

In Table 24, the largest and most critical uncertainties are the extrapolation "fu" and the additional errors not provided by the experiments:

- fu: This error estimates the uncertainty in the extrapolation from the observed phase-space to the full phase-space. For this, all measurements use the triple-differential calculation of Ref. [166]. The shape function is parametrized with the "exponential form". All measurements are rescaled to correspond to the shape function parameters determined from the photon energy spectrum measurement of Belle [164]. In previous update (Winter 2004), the data of CLEO [167] had been used for this purpose. The change substantially reduces the errors and leads to a shift in the central value. The extrapolation errors for each measurement are determined by the uncertainty of the shape function parameters [168], largely dominated by statistics. Recent theoretical work [169] may allow the extraction of the shape function parameters from the high-precision measurements of moments in semileptonic $\overline{B} \to X_c \ell \overline{\nu}$ decays.

- SSF: Uncertainties due to power corrections are summarized into the term labeled "subleading shape function" effects. They have been calculated for the endpoint measurements [170]; the errors of the corrections are used as estimate for the error (without

scaling the central values). These corrections strongly depend on the fraction of phase-space covered in a measurement. They are much larger for the CLEO and Belle endpoint analyses with the higher lepton energy threshold. We use the uncertainty for the case $E_\ell > 2.2$GeV as estimate for the m_X analysis of *BABAR*. This is roughly consistent with theoretical expectations [171]. For the (m_X, q^2) results, the error is expected to be significantly smaller; here we use half of the m_X error. The SSF errors are summarized in Table 25.

- WA: The error for weak annihilation estimates the uncertainty from parametrically enhanced nonperturbative effects predominantly expected at high-q^2. The estimates in Ref. [172] are used for the (m_X, q^2) analysis and scaled to the other phase-space regions as shown in Table 25. Because of the concentration at high-q^2, the effects of weak annihilation are diluted as more phase-space is covered.

- QHD: The error due to the violation of quark-hadron duality is estimated for the (m_X, q^2) analysis in Ref. [129]. It is found to be substantially smaller than the uncertainties from weak annihilation and power corrections. Therefore, we neglect it here.

Table 25: Scaling of theoretical errors in different regions of phase-space. The m_X analysis requires for the hadronic system in $B \to X_u \ell \overline{\nu}$ decays $m_X < 1.55\,\mathrm{GeV}/c^2$, the (m_X, q^2) analysis selects the phase-space $m_X < 1.7\,\mathrm{GeV}/c^2, q^2 > 8\,\mathrm{GeV}^2$.

Component	m_X	(m_X, q^2)	$E_\ell > 2.0$GeV	$E_\ell > 2.2$GeV	$E_\ell > 2.3$GeV
SSF	4%	2%	2%	4%	6%
WA	2%	4%	4%	6%	8%

The average of $|V_{ub}|$ is based on the measurements summarized in Table 26. The *BABAR* and Belle collaborations provided these central values. The average B meson lifetime used varies by less than 0.5% between the *BABAR* and Belle collaboration; no rescaling to a common lifetime value is applied because of its small effect. No re-evaluation of the endpoint results was available from the CLEO collaboration. Therefore their previous result was scaled with $(2.23/1.72)^{1/2}$, the ratio of branching fractions for $E_\ell > 2$GeV as determined with the Belle and CLEO $b \to s\gamma$ photon energy spectra, as tabulated in Ref. [176]. The relative extrapolation error in Ref. [176] is applied for the CLEO measurement. After this adjustment, the average $|V_{ub}|$ amounts to

$$|V_{ub}| = (4.70 \pm 0.44) \times 10^{-3}.$$

This error contains contributions from the perturbative expansion and the uncertainty of the b quark mass. The error of this average contains a relative contribution of 4.8% for the translation of $\Gamma(b \to u\ell\overline{\nu})$ to $|V_{ub}|$, which has been derived using the semileptonic moments measurements of the *BABAR* collaboration [151].

The current extrapolation error on $|V_{ub}|$ is based on the approach of Ref. [166] for the shape function effect, where the shape function parameter errors are based only on the photon energy spectrum. Recent reports [169, 180] studied the radiative corrections to the shape function and

the prescription of Ref. [166] must be modified. In particular Bosch *et al.* [169] showed that the sensitivity of the extrapolation to the shape function is reduced for the m_X and (m_X, q^2) analyses, but becomes larger for the endpoint analyses. Furthermore, it may become possible to substantially improve the precision of the shape function parameters (and hence reduce the extrapolation errors) when using the moments measurements in semileptonic B decays.

Table 26: Average of $|V_{ub}|$ determined in inclusive measurements on the $\Upsilon(4S)$. The errors quoted for the measurements correspond to uncorrelated and correlated, respectively. The correlated error of the measurements do not include the common and constant error of 2.8% $\oplus$ 3.9% from the full rate to $|V_{ub}|$; however, this error is included in the average $|V_{ub}|$.

Experiment	Method ([GeV$^{(2)}$])	$\lvert V_{ub}\rvert$ [10^{-3}] (rescaled)	$\lvert V_{ub}\rvert$ [10^{-3}] (published)
CLEO [173]	Endpoint, $p_\ell > 2.2$	$4.69 \pm 0.23 \pm 0.63$	$4.08 \pm 0.20 \pm 0.62$
Belle [174]	$(m_X < 1.70, q^2 > 8)$	$4.75 \pm 0.46 \pm 0.46$	$4.66 \pm 0.45 \pm 0.61$
Belle [175]	Endpoint, $p_\ell > 2.3$	$4.46 \pm 0.23 \pm 0.61$	$3.99 \pm 0.20 \pm 0.61$
BABAR [176]	Endpoint, $p_e > 2.0$	$4.40 \pm 0.15 \pm 0.44$	$4.40 \pm 0.15 \pm 0.44$
BABAR [177]	$m_X < 1.55$	$5.22 \pm 0.30 \pm 0.43$	$5.22 \pm 0.30 \pm 0.43$
BABAR [177]	$(m_X < 1.70, q^2 > 8)$	$5.18 \pm 0.52 \pm 0.42$	$5.18 \pm 0.52 \pm 0.42$
BABAR [178]	(E_ℓ, q^2)	$4.99 \pm 0.34 \pm 0.51$	$4.99 \pm 0.34 \pm 0.51$
Belle [179]	$(m_X < 1.70, q^2 > 8)$	$5.54 \pm 0.65 \pm 0.54$	$5.54 \pm 0.65 \pm 0.54$
Average		$\mathbf{4.70 \pm 0.44}$	$\boldsymbol{\chi^2/\mathrm{dof} = 6.7/7}$

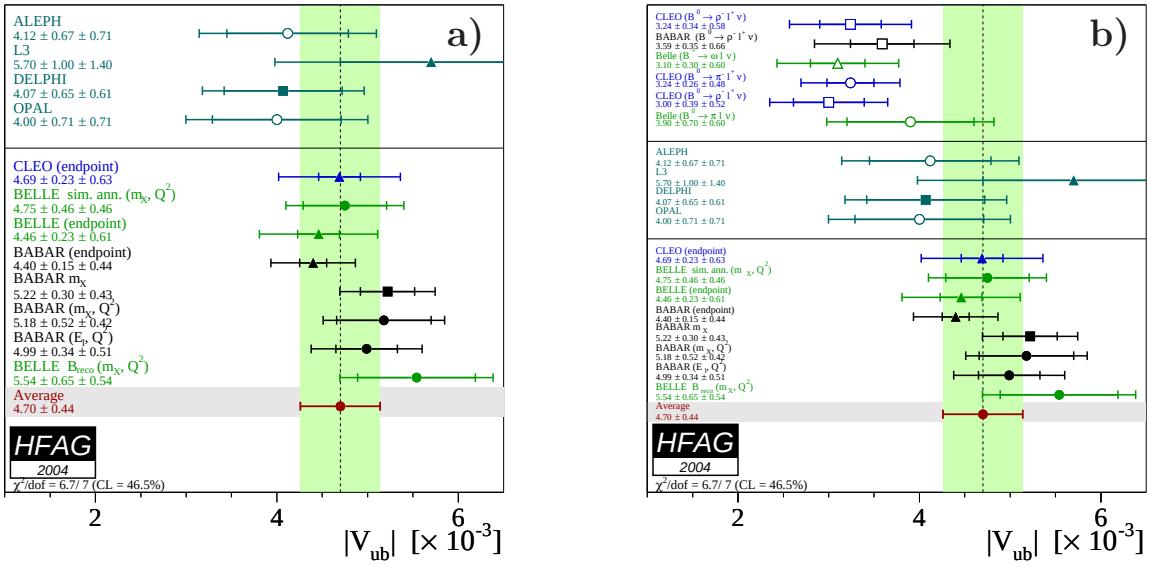

Figure 12: (a) Illustration of the average $|V_{ub}|$ from inclusive semileptonic B decays measured at the $\Upsilon(4S)$. The measurements from LEP [161] are shown only for illustration, they are not included in the average. (b) Illustration of additional exclusive $|V_{ub}|$ measurements together with the average $|V_{ub}|$ from inclusive semileptonic B decays measured at the $\Upsilon(4S)$.

4.4.2 Discussion

In the future, improvements to this average will be studied and implemented. The following is a starting point, not an exhaustive list, for possible improvements.

- The paper by de Fazio and Neubert [166] with a shape function parametrization provides a triple differential decay rate for $B \to X_u \ell \overline{\nu}$ decays that is used in all measurements over the entire phase-space. Recent theoretical work seems to indicate that it can be improved even at its nominal order ($1/m_B$ and α_s) [169, 180].
- Every experiment should provide the result in an unfolded rate so that theoretical improvements can be applied in the future. The idea is to separate the "unfoldings" of a rate or distribution from the "extrapolation" (the former is experimental, the latter theoretical).
- All three experiments have a "hybrid" MC model for signal decays. The differential spectra should be compared. Its applicability should be understood (probably good for unfolding, but questionable for extrapolation).
- There should be agreement on one specific recipe to evaluate the common errors. This can include items like
  - $\overline{B} \to X_c \ell \overline{\nu}$ modeling:
    - Variation of inclusive and exclusive branching fractions for B and D decays (full list and range)
    - Variation of form factors describing $\overline{B} \to X_c \ell \overline{\nu}$ decays
  - $B \to X_u \ell \overline{\nu}$ modeling and theoretical error
    - Variation of exclusive branching fraction (full list and range)
    - Comparison with inclusive-only signal model and comparison with exclusive-only signal model.
    - $s\overline{s}$ popping (if applicable in the analysis)
    - Central values of shape function parameters
    - Variation of shape function parameters (this is linked to recent theoretical work)

A close collaboration between the experiments will be necessary to obtain an even more consistent treatment of errors not only for the most critical ones (as shown here), but also for the remaining smaller errors.

5 Measurements related to Unitarity Triangle angles

The charge of the "$CP(t)$ and Unitarity Triangle angles" group is to provide averages of measurements related (mostly) to the angles of the Unitarity Triangle (UT). To date, most of the measurements that can be used to obtain model-independent information on the UT angles come from time-dependent CP asymmetry analyses. In cases where considerable theoretical input is required to extract the fundamental quantities, no attempt is made to do so at this stage. However, straightforward interpretations of the averages are given, where possible.

In Sec. 5.1 a brief introduction to the relevant phenomenology is given. In Sec. 5.2 an attempt is made to clarify the various different notations in use. In Sec. 5.3 the common inputs to which experimental results are rescaled in the averaging procedure are listed. We also briefly introduce the treatment of experimental errors. In the remainder of this section, the experimental results and their averages are given, divided into subsections based on the underlying quark-level decays.

5.1 Introduction

The Standard Model Cabibbo-Kobayashi-Maskawa (CKM) quark mixing matrix V must be unitary. A 3×3 unitary matrix has four free parameters,[5] and these are conventionally written by the product of three (complex) rotation matrices [181], where the rotations are characterized by the Euler angles θ_{12}, θ_{13} and θ_{23}, which are the mixing angles between the generations, and one overall phase δ,

$$V = \begin{pmatrix} V_{ud} & V_{us} & V_{ub} \\ V_{cd} & V_{cs} & V_{cb} \\ V_{td} & V_{ts} & V_{tb} \end{pmatrix} = \begin{pmatrix} c_{12}c_{13} & s_{12}c_{13} & s_{13}e^{-i\delta} \\ -s_{12}c_{23} - c_{12}s_{23}s_{13}e^{i\delta} & c_{12}c_{23} - s_{12}s_{23}s_{13}e^{i\delta} & s_{23}c_{13} \\ s_{12}s_{23} - c_{12}c_{23}s_{13}e^{i\delta} & -c_{12}s_{23} - s_{12}c_{23}s_{13}e^{i\delta} & c_{23}c_{13} \end{pmatrix} \quad (47)$$

where $c_{ij} = \cos\theta_{ij}$, $s_{ij} = \sin\theta_{ij}$ for $i < j = 1, 2, 3$.

Following the observation of a hierarchy between the different matrix elements, the Wolfenstein parameterization [182] is an expansion of V in terms of the four real parameters λ (the expansion parameter), A, ρ and η. Defining to all orders in λ [183]

$$\begin{aligned} s_{12} &\equiv \lambda, \\ s_{23} &\equiv A\lambda^2, \\ s_{13}e^{-i\delta} &\equiv A\lambda^3(\rho - i\eta), \end{aligned} \quad (48)$$

and inserting these into the representation of Eq. (47), unitarity of the CKM matrix is achieved to all orders. A Taylor expansion of V leads to the familiar approximation

$$V = \begin{pmatrix} 1 - \lambda^2/2 & \lambda & A\lambda^3(\rho - i\eta) \\ -\lambda & 1 - \lambda^2/2 & A\lambda^2 \\ A\lambda^3(1 - \rho - i\eta) & -A\lambda^2 & 1 \end{pmatrix} + \mathcal{O}\left(\lambda^4\right). \quad (49)$$

The non-zero imaginary part of the CKM matrix, which is the origin of *CP* violation in the Standard Model, is encapsulated in a non-zero value of η.

The unitarity relation $V^\dagger V = 1$ results in nine expressions which can be written $\sum_{i=u,c,t} V_{ij}^* V_{ik} = \delta_{jk}$, where δ_{jk} is the Kronecker symbol. Of the off-diagonal expressions ($j \neq k$), three can be trivially transformed into the other three (under $j \leftrightarrow k$), leaving six relations, in which three complex numbers sum to zero, which therefore can be expressed as triangles in the complex plane.

One of these,

$$V_{ud}V_{ub}^* + V_{cd}V_{cb}^* + V_{td}V_{tb}^* = 0, \quad (50)$$

is specifically related to B decays. The three terms in Eq. (50) are of the same order ($\mathcal{O}(\lambda^3)$), and this relation is commonly known as the Unitarity Triangle. For presentational purposes, it is convenient to rescale the triangle by $(V_{cd}V_{cb}^*)^{-1}$, as shown in Fig. 13.

[5] In the general case there are nine free parameters, but five of these are absorbed into unobservable quark phases.

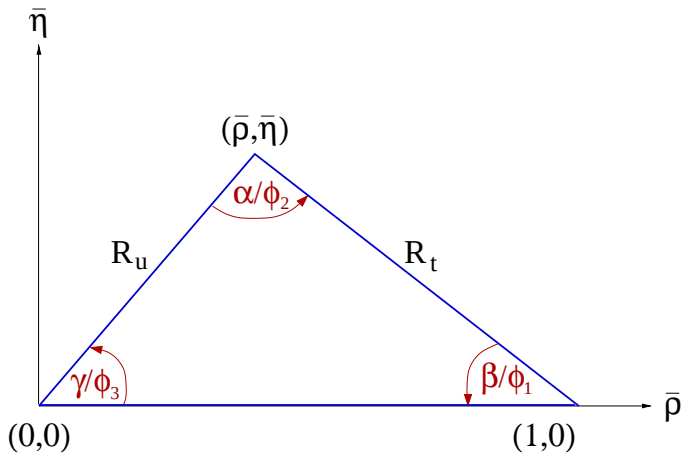

Figure 13: The Unitarity Triangle.

Two popular naming conventions for the UT angles exist in the literature:

$$\alpha \equiv \phi_2 = \arg\left[-\frac{V_{td}V_{tb}^*}{V_{ud}V_{ub}^*}\right], \quad \beta \equiv \phi_1 = \arg\left[-\frac{V_{cd}V_{cb}^*}{V_{td}V_{tb}^*}\right], \quad \gamma \equiv \phi_3 = \arg\left[-\frac{V_{ud}V_{ub}^*}{V_{cd}V_{cb}^*}\right].$$

In this document the (α, β, γ) set is used.

The apex of the Unitarity Triangle is given by the following definition [183]

$$\overline{\rho} + i\overline{\eta} \equiv -\frac{V_{ud}V_{ub}^*}{V_{cd}V_{cb}^*} = (\rho + i\eta)(1 - \frac{1}{2}\lambda^2) + \mathcal{O}(\lambda^4). \tag{51}$$

The sides R_u and R_t of the Unitarity Triangle (the third side being normalized to unity) are given by

$$R_u = \left|\frac{V_{ud}V_{ub}^*}{V_{cd}V_{cb}^*}\right| = \sqrt{\overline{\rho}^2 + \overline{\eta}^2}, \tag{52}$$

$$R_t = \left|\frac{V_{td}V_{tb}^*}{V_{cd}V_{cb}^*}\right| = \sqrt{(1-\overline{\rho})^2 + \overline{\eta}^2}. \tag{53}$$

5.2 Notations

Several different notations for *CP* violation parameters are commonly used. This section reviews those found in the experimental literature, in the hope of reducing the potential for confusion, and to define the frame that is used for the averages.

In some cases, when B mesons decay into multibody final states via broad resonances (ρ, K^*, *etc.*), the experiments ignore interference effects in the analyses. This is referred to as the quasi-two-body (Q2B) approximation in the following.

5.2.1 *CP* asymmetries

The *CP* asymmetry is defined as the difference between the rate involving a b quark and that involving a $\overline{b}$ quark, divided by the sum. For example, the partial rate (or charge) asymmetry

for a charged B decay would be given as

$$\mathcal{A}_f \equiv \frac{\Gamma(B^- \to f) - \Gamma(B^+ \to \overline{f})}{\Gamma(B^- \to f) + \Gamma(B^+ \to \overline{f})}. \tag{54}$$

5.2.2 Time-dependent *CP* asymmetries in decays to *CP* eigenstates

If the amplitudes for B^0 and $\overline{B}^0$ to decay to a final state f, which is a CP eigenstate with eigenvalue η_f, are given by A_f and $\overline{A}_f$, respectively, then the decay distributions for neutral B mesons, with known flavour at time $\Delta t = 0$, are given by

$$\Gamma_{\overline{B}^0 \to f}(\Delta t) = \frac{e^{-|\Delta t|/\tau(B^0)}}{4\tau(B^0)} \left[1 + \frac{2\,\mathrm{Im}(\lambda_f)}{1+|\lambda_f|^2} \sin(\Delta m \Delta t) - \frac{1-|\lambda_f|^2}{1+|\lambda_f|^2} \cos(\Delta m \Delta t) \right], \tag{55}$$

$$\Gamma_{B^0 \to f}(\Delta t) = \frac{e^{-|\Delta t|/\tau(B^0)}}{4\tau(B^0)} \left[1 - \frac{2\,\mathrm{Im}(\lambda_f)}{1+|\lambda_f|^2} \sin(\Delta m \Delta t) + \frac{1-|\lambda_f|^2}{1+|\lambda_f|^2} \cos(\Delta m \Delta t) \right]. \tag{56}$$

Here $\lambda_f = \frac{q}{p}\frac{\overline{A}_f}{A_f}$ contains terms related to B^0-$\overline{B}^0$ mixing and to the decay amplitude (the eigenstates of the effective Hamiltonian in the $B^0\overline{B}^0$ system are $|B_\pm\rangle = p\,|B^0\rangle \pm q\,|\overline{B}^0\rangle$). This formulation assumes CPT invariance, and neglects possible lifetime differences in the neutral B meson system. The time-dependent CP asymmetry, again defined as the difference between the rate involving a b quark and that involving a $\overline{b}$ quark, is then given by

$$\mathcal{A}_f(\Delta t) \equiv \frac{\Gamma_{\overline{B}^0 \to f}(\Delta t) - \Gamma_{B^0 \to f}(\Delta t)}{\Gamma_{\overline{B}^0 \to f}(\Delta t) + \Gamma_{B^0 \to f}(\Delta t)} = \frac{2\,\mathrm{Im}(\lambda_f)}{1+|\lambda_f|^2} \sin(\Delta m \Delta t) - \frac{1-|\lambda_f|^2}{1+|\lambda_f|^2} \cos(\Delta m \Delta t). \tag{57}$$

While the coefficient of the $\sin(\Delta m \Delta t)$ term in Eq. (57) is everywhere[6] denoted S_f:

$$S_f \equiv \frac{2\,\mathrm{Im}(\lambda_f)}{1+|\lambda_f|^2}, \tag{58}$$

different notations are in use for the coefficient of the $\cos(\Delta m \Delta t)$ term:

$$C_f \equiv -A_f \equiv \frac{1-|\lambda_f|^2}{1+|\lambda_f|^2}. \tag{59}$$

The C notation is used by the *BABAR* collaboration (see *e.g.* [192]), and also in this document. The A notation is used by the Belle collaboration (see *e.g.* [58]).

Neglecting effects due to CP violation in mixing (*i.e.*, taking $|q/p| = 1$), if the decay amplitude contains terms with a single weak phase then $|\lambda_f| = 1$ and one finds $S_f = -\eta_f \sin(\phi_{\rm mix} + \phi_{\rm dec})$, $C_f = 0$, where $\phi_{\rm mix} = \arg(q/p)$ and $\phi_{\rm dec} = \arg(\overline{A}_f/A_f)$. Note that $\phi_{\rm mix} \approx 2\beta$ in the Standard Model (in the usual phase convention). If amplitudes with different weak phases contribute to the decay, no clean interpretation of S_f is possible. If the decay amplitudes have in addition different CP conserving strong phases, then $|\lambda_f| \neq 1$ and no clean interpretation is possible. The coefficient of the cosine term becomes non-zero, indicating direct CP violation. The sign of A_f as defined above is consistent with that of $\mathcal{A}_f$ in Eq. (54).

[6] Occasionally one also finds Eq. (57) written as $\mathcal{A}_f(\Delta t) = \mathcal{A}_f^{\rm mix} \sin(\Delta m \Delta t) + \mathcal{A}_f^{\rm dir} \cos(\Delta m \Delta t)$, or similar.

5.2.3 Time-dependent *CP* asymmetries in decays to vector-vector final states

Consider B decays to states consisting of two vector particles, such as $J/\psi K^{*0}(\to K^0_S\pi^0)$, $D^{*+}D^{*-}$ and $\rho^+\rho^-$, which are eigenstates of charge conjugation but not of parity.[7] In fact, for such a system, there are three possible final states; in the helicity basis these can be written h_{-1}, h_0, h_{+1}. The h_0 state is an eigenstate of parity, and hence of *CP*; however, *CP* transforms $h_{+1} \leftrightarrow h_{-1}$ (up to an unobservable phase). In the transversity basis, these states are transformed into $h_\parallel = (h_{+1}+h_{-1})/2$ and $h_\perp = (h_{+1}-h_{-1})/2$. In this basis all three states are *CP* eigenstates, and $h_\perp$ has the opposite *CP* to the others.

The amplitudes to these states are usually given by $A_{0,\perp,\parallel}$ (here we use a normalization such that $|A_0|^2+|A_\perp|^2+|A_\parallel|^2=1$). Then the effective *CP* of the vector-vector state is known if $|A_\perp|^2$ is measured. An alternative strategy is to measure just the longitudinally polarized component, $|A_0|^2$ (sometimes denoted by $f_{\rm long}$), which allows a limit to be set on the effective *CP* since $|A_\perp|^2 \le |A_\perp|^2+|A_\parallel|^2 = 1-|A_0|^2$. The most complete treatment for neutral B decays to vector-vector final states is time-dependent angular analysis (also known as time-dependent transversity analysis). In such an analysis, the interference between the *CP* even and *CP* odd states provides additional sensitivity to the weak and strong phases involved.

5.2.4 Time-dependent *CP* asymmetries in decays to non-*CP* eigenstates

Consider a non-*CP* eigenstate f, and its conjugate $\overline{f}$. For neutral B decays to these final states, there are four amplitudes to consider: those for B^0 to decay to f and $\overline{f}$ (A_f and $A_{\overline{f}}$, respectively), and the equivalents for $\overline{B}^0$ ($\overline{A}_f$ and $\overline{A}_{\overline{f}}$). If *CP* is conserved in the decay, then $A_f = \overline{A}_{\overline{f}}$ and $A_{\overline{f}} = \overline{A}_f$.

The time-dependent decay distributions can be written in many different ways. Here, we follow Sec. 5.2.2 and define $\lambda_f = \frac{q}{p}\frac{\overline{A}_f}{A_f}$ and $\lambda_{\overline{f}} = \frac{q}{p}\frac{\overline{A}_{\overline{f}}}{A_{\overline{f}}}$. The time-dependent *CP* asymmetries then follow Eq. (57):

$$\mathcal{A}_f(\Delta t) \equiv \frac{\Gamma_{\overline{B}^0\to f}(\Delta t) - \Gamma_{B^0\to f}(\Delta t)}{\Gamma_{\overline{B}^0\to f}(\Delta t) + \Gamma_{B^0\to f}(\Delta t)} = S_f \sin(\Delta m\Delta t) - C_f\cos(\Delta m\Delta t), \quad (60)$$

$$\mathcal{A}_{\overline{f}}(\Delta t) \equiv \frac{\Gamma_{\overline{B}^0\to \overline{f}}(\Delta t) - \Gamma_{B^0\to \overline{f}}(\Delta t)}{\Gamma_{\overline{B}^0\to \overline{f}}(\Delta t) + \Gamma_{B^0\to \overline{f}}(\Delta t)} = S_{\overline{f}} \sin(\Delta m\Delta t) - C_{\overline{f}}\cos(\Delta m\Delta t), \quad (61)$$

with the definitions of the parameters C_f, S_f, $C_{\overline{f}}$ and $S_{\overline{f}}$, following Eqs. (58) and (59).

The time-dependent decay rates are given by

$$\Gamma_{\overline{B}^0\to f}(\Delta t) = \frac{e^{-|\Delta t|/\tau(B^0)}}{8\tau(B^0)}(1+\langle\mathcal{A}_{f\overline{f}}\rangle)\left\{1+S_f\sin(\Delta m\Delta t) - C_f\cos(\Delta m\Delta t)\right\}, \quad (62)$$

$$\Gamma_{B^0\to f}(\Delta t) = \frac{e^{-|\Delta t|/\tau(B^0)}}{8\tau(B^0)}(1+\langle\mathcal{A}_{f\overline{f}}\rangle)\left\{1-S_f\sin(\Delta m\Delta t) + C_f\cos(\Delta m\Delta t)\right\}, \quad (63)$$

$$\Gamma_{\overline{B}^0\to \overline{f}}(\Delta t) = \frac{e^{-|\Delta t|/\tau(B^0)}}{8\tau(B^0)}(1-\langle\mathcal{A}_{f\overline{f}}\rangle)\left\{1+S_{\overline{f}}\sin(\Delta m\Delta t) - C_{\overline{f}}\cos(\Delta m\Delta t)\right\}, \quad (64)$$

$$\Gamma_{B^0\to \overline{f}}(\Delta t) = \frac{e^{-|\Delta t|/\tau(B^0)}}{8\tau(B^0)}(1-\langle\mathcal{A}_{f\overline{f}}\rangle)\left\{1-S_{\overline{f}}\sin(\Delta m\Delta t) + C_{\overline{f}}\cos(\Delta m\Delta t)\right\}, \quad (65)$$

[7] This is not true of all vector-vector final states, *e.g.*, $D^{*\pm}\rho^\mp$ is clearly not an eigenstate of charge conjugation.

where the time-independent parameter $\langle \mathcal{A}_{f\overline{f}} \rangle$ represents an overall asymmetry in the production of the f and $\overline{f}$ final states,[8]

$$\langle \mathcal{A}_{f\overline{f}} \rangle = \frac{\left(|A_f|^2 + \left|\overline{A}_f\right|^2\right) - \left(\left|A_{\overline{f}}\right|^2 + \left|\overline{A}_{\overline{f}}\right|^2\right)}{\left(|A_f|^2 + \left|\overline{A}_f\right|^2\right) + \left(\left|A_{\overline{f}}\right|^2 + \left|\overline{A}_{\overline{f}}\right|^2\right)}. \tag{66}$$

Assuming $|q/p| = 1$, the parameters C_f and $C_{\overline{f}}$ can also be written in terms of the decay amplitudes as follows:

$$C_f = \frac{|A_f|^2 - \left|\overline{A}_f\right|^2}{|A_f|^2 + \left|\overline{A}_f\right|^2} \quad \text{and} \quad C_{\overline{f}} = \frac{\left|A_{\overline{f}}\right|^2 - \left|\overline{A}_{\overline{f}}\right|^2}{\left|A_{\overline{f}}\right|^2 + \left|\overline{A}_{\overline{f}}\right|^2}, \tag{67}$$

giving asymmetries in the decay amplitudes of B^0 and $\overline{B}^0$ to the final states f and $\overline{f}$ respectively. In this notation, the direct *CP* invariance conditions are $\langle \mathcal{A}_{f\overline{f}} \rangle = 0$ and $C_f = -C_{\overline{f}}$. Note that C_f and $C_{\overline{f}}$ are typically non-zero; *e.g.*, for a flavour-specific final state, $\overline{A}_f = A_{\overline{f}} = 0$ ($A_f = \overline{A}_{\overline{f}} = 0$), they take the values $C_f = -C_{\overline{f}} = 1$ ($C_f = -C_{\overline{f}} = -1$).

The coefficients of the sine terms contain information about the weak phase. In the case that each decay amplitude contains only a single weak phase (*i.e.*, no direct *CP* violation), these terms can be written

$$S_f = \frac{-2\,|A_f|\,\left|\overline{A}_f\right| \sin(\phi_{\rm mix} + \phi_{\rm dec} - \delta_f)}{|A_f|^2 + \left|\overline{A}_f\right|^2} \quad \text{and} \quad S_{\overline{f}} = \frac{-2\,\left|A_{\overline{f}}\right|\,\left|\overline{A}_{\overline{f}}\right| \sin(\phi_{\rm mix} + \phi_{\rm dec} + \delta_f)}{\left|A_{\overline{f}}\right|^2 + \left|\overline{A}_{\overline{f}}\right|^2}, \tag{68}$$

where δ_f is the strong phase difference between the decay amplitudes. If there is no *CP* violation, the condition $S_f = -S_{\overline{f}}$ holds. If amplitudes with different weak and strong phases contribute, no clean interpretation of S_f and $S_{\overline{f}}$ is possible.

Since two of the *CP* invariance conditions are $C_f = -C_{\overline{f}}$ and $S_f = -S_{\overline{f}}$, there is motivation for a rotation of the parameters:

$$S_{f\overline{f}} = \frac{S_f + S_{\overline{f}}}{2}, \quad \Delta S_{f\overline{f}} = \frac{S_f - S_{\overline{f}}}{2}, \quad C_{f\overline{f}} = \frac{C_f + C_{\overline{f}}}{2}, \quad \Delta C_{f\overline{f}} = \frac{C_f - C_{\overline{f}}}{2}. \tag{69}$$

With these parameters, the *CP* invariance conditions become $S_{f\overline{f}} = 0$ and $C_{f\overline{f}} = 0$. The parameter $\Delta C_{f\overline{f}}$ gives a measure of the "flavour-specificity" of the decay: $\Delta C_{f\overline{f}} = \pm 1$ corresponds to a completely flavour-specific decay, in which no interference between decays with and without mixing can occur, while $\Delta C_{f\overline{f}} = 0$ results in maximum sensitivity to mixing-induced *CP* violation. The parameter $\Delta S_{f\overline{f}}$ is related to the strong phase difference between the decay amplitudes of B^0 to f and to $\overline{f}$. We note that the observables of Eq. (69) exhibit experimental correlations (typically of $\sim 20\%$, depending on the tagging purity, and other effects) between $S_{f\overline{f}}$ and $\Delta S_{f\overline{f}}$, and between $C_{f\overline{f}}$ and $\Delta C_{f\overline{f}}$. On the other hand, the final state specific observables of Eq. (60) tend to have low correlations.

Alternatively, if we recall that the *CP* invariance conditions at the amplitude level are $A_f = \overline{A}_{\overline{f}}$ and $A_{\overline{f}} = \overline{A}_f$, we are led to consider the parameters [216]

$$\mathcal{A}_{f\overline{f}} = \frac{\left|\overline{A}_{\overline{f}}\right|^2 - |A_f|^2}{\left|\overline{A}_{\overline{f}}\right|^2 + |A_f|^2} \quad \text{and} \quad \mathcal{A}_{\overline{f}f} = \frac{\left|\overline{A}_f\right|^2 - \left|A_{\overline{f}}\right|^2}{\left|\overline{A}_f\right|^2 + \left|A_{\overline{f}}\right|^2}. \tag{70}$$

[8] This parameter is often denoted $\mathcal{A}_f$ (or $\mathcal{A}_{CP}$), but here we avoid this notation to prevent confusion with the time-dependent *CP* asymmetry.

These are sometimes considered more physically intuitive parameters since they characterize direct *CP* violation in decays with particular topologies. For example, in the case of $B^0 \to \rho^\pm\pi^\mp$ (choosing $f = \rho^+\pi^-$ and $\overline{f} = \rho^-\pi^+$), $\mathcal{A}_{f\overline{f}}$ (also denoted $\mathcal{A}_{\rho\pi}^{+-}$) parameterizes direct *CP* violation in decays in which the produced ρ meson does not contain the spectator quark, while $\mathcal{A}_{\overline{f}f}$ (also denoted $\mathcal{A}_{\rho\pi}^{-+}$) parameterizes direct *CP* violation in decays in which it does. Note that we have again followed the sign convention that the asymmetry is the difference between the rate involving a b quark and that involving a $\overline{b}$ quark, *cf.* Eq. (54). Of course, these parameters are not independent of the other sets of parameters given above, and can be written

$$\mathcal{A}_{f\overline{f}} = -\frac{\langle\mathcal{A}_{f\overline{f}}\rangle + C_{f\overline{f}} + \langle\mathcal{A}_{f\overline{f}}\rangle\Delta C_{f\overline{f}}}{1 + \Delta C_{f\overline{f}} + \langle\mathcal{A}_{f\overline{f}}\rangle C_{f\overline{f}}} \quad \text{and} \quad \mathcal{A}_{\overline{f}f} = \frac{-\langle\mathcal{A}_{f\overline{f}}\rangle + C_{f\overline{f}} + \langle\mathcal{A}_{f\overline{f}}\rangle\Delta C_{f\overline{f}}}{-1 + \Delta C_{f\overline{f}} + \langle\mathcal{A}_{f\overline{f}}\rangle C_{f\overline{f}}}. \tag{71}$$

They usually exhibit strong correlations.

We now consider the various notations which have been used in experimental studies of time-dependent *CP* asymmetries in decays to non-*CP* eigenstates.

$B^0 \to D^{*\pm}D^\mp$

The above set of parameters ($\langle\mathcal{A}_{f\overline{f}}\rangle$, C_f, S_f, $C_{\overline{f}}$, $S_{\overline{f}}$), has been used by both *BABAR* [212] and Belle [213] in the $D^{*\pm}D^\mp$ system ($f = D^{*+}D^-$, $\overline{f} = D^{*-}D^+$). However, slightly different names for the parameters are used: *BABAR* uses ($\mathcal{A}$, C_{+-}, S_{+-}, C_{-+}, S_{-+}); Belle uses ($\mathcal{A}$, C_+, S_+, C_-, S_-). In this document, we follow the notation used by *BABAR*.

$B^0 \to \rho^\pm\pi^\mp$

In the $\rho^\pm\pi^\mp$ system, the ($\langle\mathcal{A}_{f\overline{f}}\rangle$, $C_{f\overline{f}}$, $S_{f\overline{f}}$, $\Delta C_{f\overline{f}}$, $\Delta S_{f\overline{f}}$) set of parameters has been used originally by *BABAR* [221], and more recently by Belle [223], in the Q2B approximation; the exact names[9] used in this case are ($\mathcal{A}_{CP}^{\rho\pi}, C_{\rho\pi}, S_{\rho\pi}, \Delta C_{\rho\pi}, \Delta S_{\rho\pi}$), and these names are also used in this document.

Since $\rho^\pm\pi^\mp$ is reconstructed in the final state $\pi^+\pi^-\pi^0$, the interference between the ρ resonances can provide additional information about the phases. *BABAR* [222] has performed a time-dependent Dalitz plot analysis, from which the weak phase α is directly extracted. In such an analysis, the measured Q2B parameters are also naturally corrected for interference effects.

$B^0 \to D^\pm\pi^\mp, D^{*\pm}\pi^\mp, D^\pm\rho^\mp$

Time-dependent *CP* analyses have also been performed for the final states $D^\pm\pi^\mp$, $D^{*\pm}\pi^\mp$ and $D^\pm\rho^\mp$. In these theoretically clean cases, no penguin contributions are possible, so there is no direct *CP* violation. Furthermore, due to the smallness of the ratio of the magnitudes of the suppressed ($b \to u$) and favoured ($b \to c$) amplitudes (denoted R_f), to a very good approximation, $C_f = -C_{\overline{f}} = 1$ (using $f = D^{(*)-}h^+$, $\overline{f} = D^{(*)+}h^-$ $h = \pi, \rho$), and the coefficients of the sine terms are given by

$$S_f = -2R_f \sin(\phi_{\rm mix} + \phi_{\rm dec} - \delta_f) \quad \text{and} \quad S_{\overline{f}} = -2R_f \sin(\phi_{\rm mix} + \phi_{\rm dec} + \delta_f). \tag{72}$$

Thus weak phase information can be cleanly obtained from measurements of S_f and $S_{\overline{f}}$, although external information on at least one of R_f or δ_f is necessary. (Note that $\phi_{\rm mix} + \phi_{\rm dec} = 2\beta + \gamma$ for all the decay modes in question, while R_f and δ_f depend on the decay mode.)

[9] *BABAR* has used the notations $A_{CP}^{\rho\pi}$ [221] and $\mathcal{A}_{\rho\pi}$ [222] in place of $\mathcal{A}_{CP}^{\rho\pi}$.

Table 27: Conversion between the various notations used for *CP* violation parameters in the $D^{\pm}\pi^{\mp}$, $D^{*\pm}\pi^{\mp}$ and $D^{\pm}\rho^{\mp}$ systems. The b_i terms used by *BABAR* have been neglected.

	BABAR	Belle partial rec.	Belle full rec.
$S_{D^+\pi^-}$	$-S_- = -(a + c_i)$	N/A	$2R_{D\pi}\sin(2\phi_1 + \phi_3 + \delta_{D\pi})$
$S_{D^-\pi^+}$	$-S_+ = -(a - c_i)$	N/A	$2R_{D\pi}\sin(2\phi_1 + \phi_3 - \delta_{D\pi})$
$S_{D^{*+}\pi^-}$	$-S_- = -(a + c_i)$	S^+	$-2R_{D^*\pi}\sin(2\phi_1 + \phi_3 + \delta_{D^*\pi})$
$S_{D^{*-}\pi^+}$	$-S_+ = -(a - c_i)$	S^-	$-2R_{D^*\pi}\sin(2\phi_1 + \phi_3 - \delta_{D^*\pi})$
$S_{D^+\rho^-}$	$-S_- = -(a + c_i)$	N/A	N/A
$S_{D^-\rho^+}$	$-S_+ = -(a - c_i)$	N/A	N/A

Again, different notations have been used in the literature. *BABAR* [229, 231] defines the time-dependent probability function by

$$f^{\pm}(\eta, \Delta t) = \frac{e^{-|\Delta t|/\tau}}{4\tau}\left[1 \mp S_\zeta \sin(\Delta m \Delta t) \mp \eta C_\zeta \cos(\Delta m \Delta t)\right], \tag{73}$$

where the upper (lower) sign corresponds to the tagging meson being a B^0 ($\overline{B}^0$). [Note here that a tagging B^0 ($\overline{B}^0$) corresponds to $-S_\xi$ ($+S_\xi$).] The parameters η and ζ take the values $+1$ and $+$ (-1 and $-$) when the final state is, *e.g.*, $D^-\pi^+$ ($D^+\pi^-$). However, in the fit, the substitutions $C_\zeta = 1$ and $S_\zeta = a \mp \eta b_i - \eta c_i$ are made. [Note that, neglecting b terms, $S_+ = a - c$ and $S_- = a + c$, so that $a = (S_+ + S_-)/2$, $c = (S_- - S_+)/2$, in analogy to the parameters of Eq. (69).] The subscript i denotes the tagging category. These are motivated by the possibility of *CP* violation on the tag side [233], which is absent for semileptonic B decays (mostly lepton tags). The parameter a is not affected by tag side *CP* violation.

The parameters used by Belle in the analysis using partially reconstructed B decays [232], are similar to the S_ζ parameters defined above. However, in the Belle convention, a tagging B^0 corresponds to a + sign in front of the sine coefficient; furthermore the correspondence between the super/subscript and the final state is opposite, so that $S_\pm$ (*BABAR*) $= -S^\mp$ (Belle). In this analysis, only lepton tags are used, so there is no effect from tag side *CP* violation. In the Belle analysis using fully reconstructed B decays [230], this effect is measured and taken into account using $D^* l\nu$ decays; in neither Belle analysis are the a, b and c parameters used. In the latter case, the measured parameters are $2R_{D^{(*)}\pi}\sin(2\phi_1 + \phi_3 \pm \delta_{D^{(*)}\pi})$; the definition is such that $S^\pm$ (Belle) $= -2R_{D^*\pi}\sin(2\phi_1 + \phi_3 \pm \delta_{D^*\pi})$. However, the definition includes an angular momentum factor $(-1)^L$ [234], and so for the results in the $D\pi$ system, there is an additional factor of -1 in the conversion.

Explicitly, the conversion then reads as given in Table 27, where we have neglected the b_i terms used by *BABAR*. For the averages in this document, we use the a and c parameters, and give the explicit translations used in Table 28. It is to be fervently hoped that the experiments will converge on a common notation in future.

Time-dependent asymmetries in radiative B decays

As a special case of decays to non-*CP* eigenstates, let us consider radiative B decays. Here, the emitted photon has a distinct helicity, which is in principle observable, but in practice is

Table 28: Translations used to convert the parameters measured by Belle to the parameters used for averaging in this document. The angular momentum factor L is -1 for $D^*\pi$ and $+1$ for $D\pi$.

	$D^*\pi$ partial rec.	$D^{(*)}\pi$ full rec.
a	$-(S^+ + S^-)$	$\frac{1}{2}(-1)^{L+1}\left(2R_{D^{(*)}\pi}\sin(2\phi_1+\phi_3+\delta_{D^{(*)}\pi}) + 2R_{D^{(*)}\pi}\sin(2\phi_1+\phi_3-\delta_{D^{(*)}\pi})\right)$
c	$-(S^+ - S^-)$	$\frac{1}{2}(-1)^{L+1}\left(2R_{D^{(*)}\pi}\sin(2\phi_1+\phi_3+\delta_{D^{(*)}\pi}) - 2R_{D^{(*)}\pi}\sin(2\phi_1+\phi_3-\delta_{D^{(*)}\pi})\right)$

not usually measured. Thus the measured time-dependent decay rates are given by [184, 185]

$$\begin{aligned}
\Gamma_{\overline{B}^0\to X\gamma}(\Delta t) &= \Gamma_{\overline{B}^0\to X\gamma_L}(\Delta t) + \Gamma_{\overline{B}^0\to X\gamma_R}(\Delta t) \qquad (74)\\
&= \frac{e^{-|\Delta t|/\tau(B^0)}}{4\tau(B^0)}\left\{1 + (S_L+S_R)\sin(\Delta m\Delta t) - (C_L+C_R)\cos(\Delta m\Delta t)\right\},\\
\Gamma_{B^0\to X\gamma}(\Delta t) &= \Gamma_{B^0\to X\gamma_L}(\Delta t) + \Gamma_{B^0\to X\gamma_R}(\Delta t) \qquad (75)\\
&= \frac{e^{-|\Delta t|/\tau(B^0)}}{8\tau(B^0)}\left\{1 - (S_L+S_R)\sin(\Delta m\Delta t) + (C_L+C_R)\cos(\Delta m\Delta t)\right\},
\end{aligned}$$

where in place of the subscripts f and $\overline{f}$ we have used L and R to indicate the photon helicity. In order for interference between decays with and without B^0-$\overline{B}^0$ mixing to occur, the X system must not be flavour-specific, *e.g.*, in case of $B^0 \to K^{*0}\gamma$, the final state must be $K^0_S\pi^0\gamma$. The sign of the sine term depends on the C eigenvalue of the X system. The photons from $b \to q\gamma$ ($\overline{b} \to \overline{q}\gamma$) are predominantly left (right) polarized, with corrections of order of m_q/m_b, thus interference effects are suppressed. The predicted smallness of the S terms in the Standard Model results in sensitivity to new physics contributions.

5.2.5 Asymmetries in $B \to D^{(*)}K^{(*)}$ decays

CP asymmetries in $B \to D^{(*)}K^{(*)}$ decays are sensitive to γ. The neutral $D^{(*)}$ meson produced is an admixture of $D^{(*)0}$ (produced by a $b \to c$ transition) and $\overline{D}^{(*)0}$ (produced by a colour-suppressed $b \to u$ transition) states. If the final state is chosen so that both $D^{(*)0}$ and $\overline{D}^{(*)0}$ can contribute, the two amplitudes interfere, and the resulting observables are sensitive to γ, the relative weak phase between the two B decay amplitudes. Various methods have been proposed to exploit this interference, including those where the neutral D meson is reconstructed as a *CP* eigenstate (GLW) [186], in a suppressed final state (ADS) [187], or in a self-conjugate three-body final state, such as $K^0_S\pi^+\pi^-$ (Dalitz) [188].

Consider the case of $B^\mp \to DK^\mp$, with D decaying to a final state f, which is accessible to both D^0 and $\overline{D}^0$. We can write the decay rates for B^- and B^+ ($\Gamma_\mp$), the charge averaged rate ($\Gamma = (\Gamma_- + \Gamma_+)/2$) and the charge asymmetry ($\mathcal{A} = (\Gamma_- - \Gamma_+)/(\Gamma_- + \Gamma_+)$, see Eq. (54)) as

$$\begin{aligned}
\Gamma_\mp &\propto r_B^2 + r_D^2 + 2r_Br_D\cos(\delta_B + \delta_D \mp \gamma), \qquad (76)\\
\Gamma &\propto r_B^2 + r_D^2 + 2r_Br_D\cos(\delta_B+\delta_D)\cos(\gamma), \qquad (77)\\
\mathcal{A} &= \frac{2r_Br_D\sin(\delta_B+\delta_D)\sin(\gamma)}{r_B^2 + r_D^2 + 2r_Br_D\cos(\delta_B+\delta_D)\cos(\gamma)}, \qquad (78)
\end{aligned}$$

where the ratio of B decay amplitudes[10] is usually defined to be less than one,

$$r_B = \frac{\left|A\left(B^- \to \overline{D}^0 K^-\right)\right|}{\left|A\left(B^- \to D^0 K^-\right)\right|}, \tag{79}$$

and the ratio of D decay amplitudes is correspondingly defined by

$$r_D = \frac{\left|A\left(D^0 \to f\right)\right|}{\left|A\left(\overline{D}^0 \to f\right)\right|}. \tag{80}$$

The strong phase differences between the B and D decay amplitudes are given by δ_B and δ_D, respectively. The values of r_D and δ_D depend on the final state f: for the GLW analysis, $r_D = 1$ and δ_D is trivial (either zero or π), in the Dalitz plot analysis r_D and δ_D vary across the Dalitz plot, and depend on the D decay model used, for the ADS analysis, the values of r_D and δ_D are not trivial.

In the GLW analysis, the measured quantities are the partial rate asymmetry, and the charge averaged rate, which are measured both for *CP* even and *CP* odd D decays. For the latter, it is experimentally convenient to measure a double ratio,

$$R_{CP} = \frac{\Gamma\left(B^- \to D_{CP} K^-\right) / \Gamma\left(B^- \to D^0 K^-\right)}{\Gamma\left(B^- \to D_{CP} \pi^-\right) / \Gamma\left(B^- \to D^0 \pi^-\right)} \tag{81}$$

that is normalized both to the rate for the favoured $D^0 \to K^-\pi^+$ decay, and to the equivalent quantities for $B^- \to D\pi^-$ decays (charge conjugate modes are implicitly included in Eq. (81)). In this way the constant of proportionality drops out of Eq. (77).

For the ADS analysis, using a suppressed $D \to f$ decay, the measured quantities are again the partial rate asymmetry, and the charge averaged rate. In this case it is sufficient to measure the rate in a single ratio (normalized to the favoured $D \to \overline{f}$ decay) since detection systematics cancel naturally. In the ADS analysis, there are an additional two unknowns (r_D and δ_D) compared to the GLW case. However, the value of r_D can be measured using decays of D mesons of known flavour.

The relations between the measured quantities and the underlying parameters are summarized in Table 29. Note carefully that the hadronic factors r_B and δ_B are different, in general, for each B decay mode. In the Dalitz plot analysis, once a model is assumed for the D decay, which gives the values of r_D and δ_D across the Dalitz plot, the values of (γ, r_B, δ_B) can be directly extracted from a simultaneous fit to the B^- and B^+ data.

5.3 Common inputs and error treatment

The common inputs used for rescaling are listed in Table 30. The B^0 lifetime ($\tau(B^0)$) and mixing parameter (Δm_d) averages are provided by the HFAG Lifetimes and Oscillations subgroup (Sec. 3). The fraction of the perpendicularly polarized component ($|A_\perp|^2$) in $B \to J/\psi K^*(892)$ decays, which determines the *CP* composition, is averaged from results by *BABAR* [190] and Belle [191].

[10]Note that here we use the notation r_B to denote the ratio of B decay amplitudes, whereas in Sec. 5.2.4 we used, *e.g.*, $R_{D\pi}$, for a rather similar quantity. The reason is that here we need to be concerned also with D decay amplitudes, and so it is convenient to use the subscript to denote the decaying particle. Hopefully, using r in place of R will help reduce potential confusion.

Table 29: Summary of relations between measured and physical parameters in GLW and ADS analyses of $B \to D^{(*)}K^{(*)}$.

GLW analysis	
$R_{CP\pm}$	$1 + r_B^2 \pm 2r_B \cos(\delta_B)\cos(\gamma)$
$A_{CP\pm}$	$\pm 2r_B \sin(\delta_B)\sin(\gamma)\,/R_{CP\pm}$
ADS analysis	
R_{ADS}	$r_B^2 + r_D^2 + 2r_B r_D \cos(\delta_B + \delta_D)\cos(\gamma)$
A_{ADS}	$2r_B r_D \sin(\delta_B + \delta_D)\sin(\gamma)\,/R_{ADS}$

Table 30: Common inputs used in calculating the averages.

$\tau(B^0)$ (ps)	1.536 ± 0.014
Δm_d (ps^{-1})	0.502 ± 0.007
$\lvert A_\perp \rvert^2 (J/\psi K^*)$	0.211 ± 0.011

At present, we only rescale to a common set of input parameters for modes with reasonably small statistical errors ($b \to c\bar{c}s$ and $b \to q\bar{q}s$ transitions). Correlated systematic errors are taken into account in these modes as well. For all other modes, the effect of such a procedure is currently negligible.

As explained in Sec. 1, we do not apply a rescaling factor on the error of an average that has $\chi^2/\mathrm{dof} > 1$ (unlike the procedure currently used by the PDG [3]). We provide a confidence level of the fit so that one can know the consistency of the measurements included in the average, and attach comments in case some care needs to be taken in the interpretation. Note that, in general, results obtained from data samples with low statistics will exhibit some non-Gaussian behaviour. For measurements where one error is given, it represents the total error, where statistical and systematic uncertainties have been added in quadrature. If two errors are given, the first is statistical and the second systematic. If more than two errors are given, the origin of the third will be explained in the text.

Averages are computed by maximizing a log-likelihood function $\mathcal{L}$ assuming Gaussian statistical and systematic errors. When observables are correlated (*e.g.*, sine and cosine coefficients in time-dependent *CP* asymmetries), a combined minimization is performed, taking into account the correlations. Asymmetric errors are treated by defining an asymmetric log-likelihood function: $\mathcal{L}_i = (x - x_i)^2/(2\sigma_i^2)$, where $\sigma_i = \sigma_{i,+}$ ($\sigma_i = \sigma_{i,-}$) if $x > x_i$ ($x < x_i$), and where x_i is the ith measurement of the observable x that is averaged. This example assumes no correlations between observables. The correlated case is a straightforward extension to this.

5.4 Time-dependent *CP* asymmetries in $b \to c\bar{c}s$ transitions

In the Standard Model, the time-dependent parameters for $b \to c\bar{c}s$ transitions are predicted to be: $S_{b\to c\bar{c}s} = -\eta \sin(2\beta)$, $C_{b\to c\bar{c}s} = 0$ to very good accuracy. The averages for $S_{b\to c\bar{c}s}$ and $C_{b\to c\bar{c}s}$ are provided in Table 31. The averages for $S_{b\to c\bar{c}s}$ are shown in Fig. 15; averages for $C_{b\to c\bar{c}s}$ are included in Fig. 19.

Both *BABAR* and Belle use the $\eta = -1$ modes $J/\psi K^0_S$, $\psi(2S)K^0_S$, $\chi_{c1}K^0_S$ and $\eta_c K^0_S$, as well

Table 31: $S_{b\to c\bar{c}s}$ and $C_{b\to c\bar{c}s}$.

Experiment		$-\eta S_{b\to c\bar{c}s}$	$C_{b\to c\bar{c}s}$
BABAR	[192]	$0.722 \pm 0.040 \pm 0.023$	$0.051 \pm 0.033 \pm 0.014$
Belle	[58]	$0.728 \pm 0.056 \pm 0.023$	$-0.007 \pm 0.041 \pm 0.033$
B factory average		0.725 ± 0.037	0.031 ± 0.029
Confidence level		0.91	0.30
ALEPH	[193]	$0.84\,^{+0.82}_{-1.04} \pm 0.16$	
OPAL	[194]	$3.2\,^{+1.8}_{-2.0} \pm 0.5$	
CDF	[195]	$0.79\,^{+0.41}_{-0.44}$	
Average		0.726 ± 0.037	0.031 ± 0.029

Table 32: Averages from $B^0 \to J/\psi K^{*0}$ transversity analyses.

Experiment		$\sin(2\beta)$	$\cos(2\beta)$
BABAR	[190]	$-0.10 \pm 0.57 \pm 0.14$	$3.32\,^{+0.76}_{-0.96} \pm 0.27$
Belle	[191]	$0.30 \pm 0.32 \pm 0.02$	$0.31 \pm 0.91 \pm 0.11$
Average		0.21 ± 0.28	1.69 ± 0.67

as $J/\psi\, K^0_L$, which has $\eta = +1$ and $J/\psi\, K^{*0}(892)$, which is found to have η close to $+1$ based on the measurement of $|A_\perp|$ (see Sec. 5.3). ALEPH, OPAL and CDF use only the $J/\psi\, K^0_S$ final state.

These results give a precise constraint on the $(\overline{\rho}, \overline{\eta})$ plane, in remarkable agreement with other constraints from *CP* conserving quantities, and with *CP* violation in the kaon system, in the form of the parameter ϵ_K. Such comparisons have been performed by various phenomenological groups, such as CKMfitter [196] and UTFit [197]. Figure 14 displays the constraints obtained from these two groups.

5.5 Time-dependent transversity analysis of $B^0 \to J/\psi K^{*0}$

B meson decays to the vector-vector final state $J/\psi K^{*0}$ are also mediated by the $b \to c\bar{c}s$ transition. When a final state which is not flavour-specific ($K^{*0} \to K^0_S\pi^0$) is used, a time-dependent transversity analysis can be performed allowing sensitivity to both $\sin(2\beta)$ and $\cos(2\beta)$. Such analyses have been performed by both B factory experiments. In principle, the strong phases between the transversity amplitudes are not uniquely determined by such an analysis, leading to a discrete ambiguity in the sign of $\cos(2\beta)$. The *BABAR* [190] collaboration resolves this ambiguity using the known variation [198] of the P-wave phase (fast) relative to the S-wave phase (slow) with the invariant mass of the $K\pi$ system in the vicinity of the $K^*(892)$ resonance. The result is in agreement with the prediction from s quark helicity conservation, and corresponds to Solution II defined by Suzuki [199]. We use this phase convention for the averages given in Table 32.

While the statistical errors are large, and exhibit non-Gaussian behaviour, $\cos(2\beta) > 0$ is preferred by the experimental data in $J/\psi K^*$.

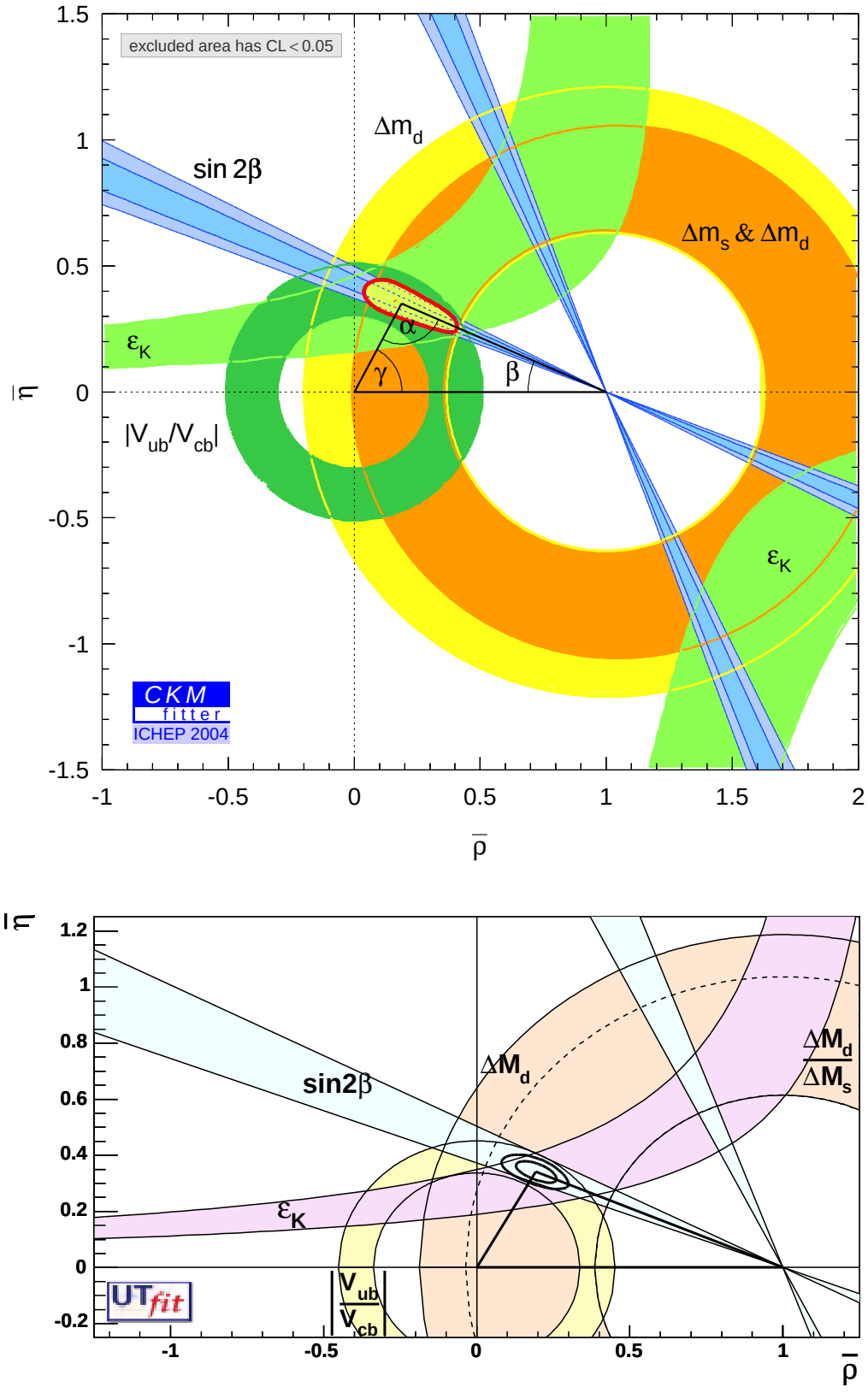

Figure 14: Standard Model constraints on the $(\overline{\rho}, \overline{\eta})$ plane, from (top) [196] and (bottom) [197].

5.6 Time-dependent *CP* asymmetries in $b \to q\overline{q}s$ transitions

The flavour changing neutral current $b \to s$ penguin can be mediated by any up-type quark in the loop, and hence the amplitude can be written as

$$\begin{aligned} A_{b\to s} &= F_u V_{ub}V_{us}^* + F_c V_{cb}V_{cs}^* + F_t V_{tb}V_{ts}^* \\ &= (F_u - F_c)V_{ub}V_{us}^* + (F_t - F_c)V_{tb}V_{ts}^* \\ &= \mathcal{O}(\lambda^4) + \mathcal{O}(\lambda^2) \end{aligned} \tag{82}$$

using the unitarity of the CKM matrix. Therefore, in the Standard Model, this amplitude is dominated by $V_{tb}V_{ts}^*$, and to within a few degrees ($\delta\beta \lesssim 2^\circ$ for $\beta \simeq 23.3^\circ$) the time-dependent parameters can be written[11] $S_{b\to q\overline{q}s} \approx -\eta \sin(2\beta)$, $C_{b\to q\overline{q}s} \approx 0$, assuming $b \to s$ penguin contributions only ($q = u, d, s$).

Due to the large virtual mass scales occurring in the penguin loops, additional diagrams from physics beyond the Standard Model, with heavy particles in the loops, may contribute. In general, these contributions will affect the values of $S_{b\to q\overline{q}s}$ and $C_{b\to q\overline{q}s}$. A discrepancy between the values of $S_{b\to c\overline{c}s}$ and $S_{b\to q\overline{q}s}$ can therefore provide a clean indication of new physics.

However, there is an additional consideration to take into account. The above argument assumes only the $b \to s$ penguin contributes to the $b \to q\overline{q}s$ transition. For $q = s$ this is a good assumption, which neglects only rescattering effects. However, for $q = u$ there is a colour-suppressed $b \to u$ tree diagram (of order $\mathcal{O}(\lambda^4)$), which has a different weak (and possibly strong) phase. In the case $q = d$, any light neutral meson that is formed from $d\overline{d}$ also has a $u\overline{u}$ component, and so again there is "tree pollution". The B^0 decays to $\pi^0 K_S^0$ and ωK_S^0 belong to this category. The mesons f_0 and η' are expected to have predominant $s\overline{s}$ parts, which reduces the possible tree pollution. If the inclusive decay $B^0 \to K^+K^-K^0$ (excluding ϕK^0) is dominated by a non-resonant three-body transition, an OZI-rule suppressed tree-level diagram can occur through insertion of an $s\overline{s}$ pair. The corresponding penguin-type transition proceeds via insertion of a $u\overline{u}$ pair, which is expected to be favored over the $s\overline{s}$ insertion by fragmentation models. Neglecting rescattering, the final state $K^0\overline{K}^0K^0$ has no tree pollution.

The averages for $S_{b\to q\overline{q}s}$ and $C_{b\to q\overline{q}s}$ can be found in Table 33. The averages for $S_{b\to q\overline{q}s}$ are shown in Fig. 15; averages for $C_{b\to q\overline{q}s}$ are included in Fig. 19. Results from both *BABAR* and Belle are averaged for the modes ϕK^0 (both ϕK_S^0 and ϕK_L^0 are used), $\eta' K_S^0$, $K^+K^-K_S^0$, $f_0 K_S^0$ and $\pi^0 K_S^0$. In addition, results from Belle are taken for the modes ωK_S^0 and $K_S^0K_S^0K_S^0$. Of these modes, ϕK_S^0, $\eta' K_S^0$, $\pi^0 K_S^0$ and ωK_S^0 have *CP* eigenvalue $\eta = -1$, while ϕK_L^0, $f_0 K_S^0$ and $K_S^0K_S^0K_S^0$ have $\eta = +1$.

The final state $K^+K^-K_S^0$ (contributions from ϕK_S^0 are implicitly excluded) is not a *CP* eigenstate. However, the *CP* composition can be determined using either an isospin argument (used by Belle to determine a *CP* even fraction of $1.03 \pm 0.15 \pm 0.05$ [200]) or a moments analysis (used by *BABAR* who finds a *CP* even fraction of $0.89 \pm 0.08 \pm 0.06$ [206]). The uncertainty in the *CP* even fraction leads to an asymmetric error on $S_{b\to q\overline{q}s}$, which is taken to be correlated among the experiments. To combine, we rescale the results to the average *CP* even fraction of 0.93 ± 0.09.

If we treat the combined error as a Gaussian quantity, we note that the average of $-\eta S_{b\to q\overline{q}s}$ of all $b \to q\overline{q}s$ dominated modes (0.41 ± 0.07) is more than 5σ from zero, and hence *CP* violation

[11] The presence of a small ($\mathcal{O}(\lambda^2)$) weak phase in the dominant amplitude of the s penguin decays introduces a phase shift given by $S_{b\to q\overline{q}s} = -\eta \sin(2\beta) \cdot (1 + \Delta)$. Using the CKMfitter results for the Wolfenstein parameters [216], one finds: $\Delta \simeq 0.033$, which corresponds to a shift of 2β of $+2.1$ degrees. Nonperturbative contributions can alter this result.

Table 33: $S_{b\to q\overline{q}s}$ and $C_{b\to q\overline{q}s}$.

Experiment		$-\eta S_{b\to q\overline{q}s}$	$C_{b\to q\overline{q}s}$
		ϕK^0	
BABAR	[201]	$0.50 \pm 0.25\,^{+0.07}_{-0.04}$	$0.00 \pm 0.23 \pm 0.05$
Belle	[202]	$0.06 \pm 0.33 \pm 0.09$	$-0.08 \pm 0.22 \pm 0.09$
Average		0.34 ± 0.20	-0.04 ± 0.17
Confidence level		0.30	0.81
		$\eta' K^0_S$	
BABAR	[203]	$0.27 \pm 0.14 \pm 0.03$	$-0.21 \pm 0.10 \pm 0.03$
Belle	[202]	$0.65 \pm 0.18 \pm 0.04$	$0.19 \pm 0.11 \pm 0.05$
Average		0.41 ± 0.11	-0.04 ± 0.08
Confidence level		0.10	0.01 (2.5σ)
		$f_0 K^0_S$	
BABAR	[204]	$0.95\,^{+0.23}_{-0.32} \pm 0.10$	$-0.24 \pm 0.31 \pm 0.15$
Belle	[202]	$-0.47 \pm 0.41 \pm 0.08$	$0.39 \pm 0.27 \pm 0.08$
Average		0.39 ± 0.26	0.14 ± 0.22
Confidence level		0.008 (2.7σ)	0.16 (1.4σ)
		$\pi^0 K^0_S$	
BABAR	[205]	$0.35\,^{+0.30}_{-0.33} \pm 0.04$	$0.06 \pm 0.18 \pm 0.06$
Belle	[202]	$0.30 \pm 0.59 \pm 0.11$	$0.12 \pm 0.20 \pm 0.07$
Average		$0.34\,^{+0.27}_{-0.29}$	0.09 ± 0.14
Confidence level		0.94	0.83
		ωK^0_S	
Belle	[202]	$0.75 \pm 0.64\,^{+0.13}_{-0.16}$	$-0.26 \pm 0.48 \pm 0.15$
		$K^+K^-K^0_S$	
BABAR	[206]	$0.55 \pm 0.22 \pm 0.04 \pm 0.11$	$0.10 \pm 0.14 \pm 0.06$
Belle	[202]	$0.49 \pm 0.18 \pm 0.04\,^{+0.17}_{-0.00}$	$0.08 \pm 0.12 \pm 0.07$
Average		0.53 ± 0.17	0.09 ± 0.10
Confidence level		0.72	0.92
		$K^0_S K^0_S K^0_S$	
Belle	[207]	$-1.26 \pm 0.68 \pm 0.18$	$0.54 \pm 0.34 \pm 0.08$
Average of all $b \to q\overline{q}s$		0.41 ± 0.07	0.03 ± 0.05
Confidence level		0.10 (1.7σ)	0.32
Average including $b \to c\overline{c}s$		0.665 ± 0.033	0.031 ± 0.025
Confidence level		1.2×10^{-4} (3.1σ)	0.40

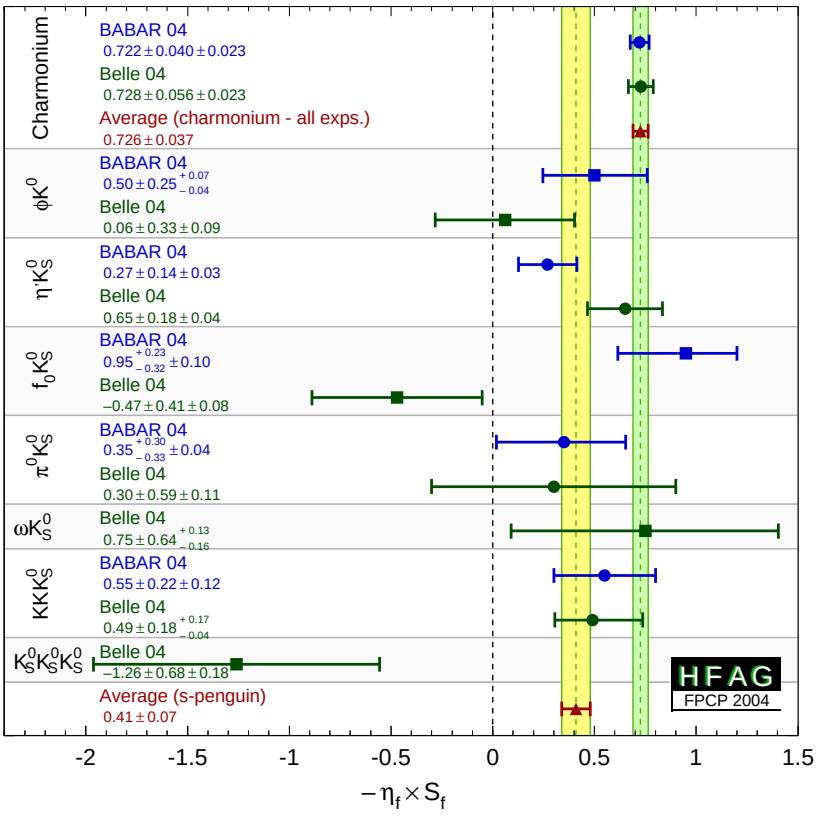

Figure 15: $S_{b\to c\bar{c}s}$ and $S_{b\to q\bar{q}s}$.

in $b \to q\bar{q}s$ transitions is established. Furthermore, the averages of $-\eta S_{b\to q\bar{q}s}$ for the modes $\eta' K^0_S$ and $K^+K^-K^0_S$ are more than 3σ from zero.

Neglecting theory errors due to suppressed contributions with different weak phases, the difference between $S_{b\to c\bar{c}s}$ and $S_{b\to q\bar{q}s}$ can be calculated. We find the confidence level (CL) of the joint $S_{b\to c\bar{c}s}$ and $S_{b\to q\bar{q}s}$ average to be 0.00012, which corresponds to a 3.8σ discrepancy. To give an idea of the theoretical uncertainties involved, Fig. 16 shows coarse estimates of the theoretical errors associated with the non-charmonium modes. These crude estimates are obtained from dimensional arguments only, based on the CKM suppression of the V_{ub} penguin, and on the naive contribution from tree diagrams. Including these estimates according to the procedure defined in Ref. [216] improves the CL of the joint average to about 3σ.

5.7 Time-dependent *CP* asymmetries in $b \to c\bar{c}d$ transitions

The transition $b \to c\bar{c}d$ can occur via either a $b \to c$ tree or a $b \to d$ penguin amplitude. Similarly to Eq. (82), the amplitude for the $b \to d$ penguin can be written

$$\begin{aligned} A_{b\to d} &= F_u V_{ub}V^*_{ud} + F_c V_{cb}V^*_{cd} + F_t V_{tb}V^*_{td} \\ &= (F_u - F_c)V_{ub}V^*_{ud} \;+\; (F_t - F_c)V_{tb}V^*_{td} \\ &= \mathcal{O}(\lambda^3) \;+\; \mathcal{O}(\lambda^3). \end{aligned} \tag{83}$$

From this it can be seen that the $b \to d$ penguin amplitude does not have a dominant weak phase.

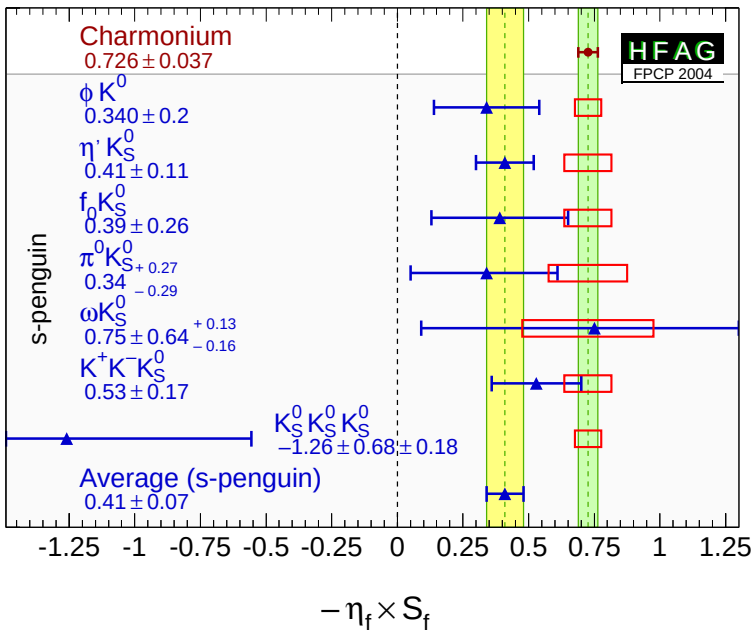

Figure 16: Averages for $S_{b\to q\overline{q}s}$ compared to $S_{b\to c\overline{c}s}$, with coarse dimensional estimates of associated theoretical uncertainties indicated by the open boxes.

In the above, we have followed Eq. (82) by eliminating the F_c term using unitarity. However, we could equally well write

$$\begin{aligned} A_{b\to d} &= (F_u - F_t)V_{ub}V_{ud}^* + (F_c - F_t)V_{cb}V_{cd}^*, \\ &= (F_c - F_u)V_{cb}V_{cd}^* + (F_t - F_u)V_{tb}V_{td}^*. \end{aligned} \tag{84}$$

Since the $b \to c\overline{c}d$ tree amplitude has the weak phase of $V_{cb}V_{cd}^*$, either of the above expressions allow the penguin to be decomposed into parts with weak phases the same and different to the tree amplitude (the relative weak phase can be chosen to be either β or γ). However, if the tree amplitude dominates, there is little sensitivity to any phase other than that from B^0-$\overline{B}^0$ mixing.

The $b \to c\overline{c}d$ transitions can be investigated with studies of various different final states. Results are available from both *BABAR* and Belle using the final states $J/\psi\pi^0$, $D^{*+}D^{*-}$ and $D^{*\pm}D^{\mp}$; the averages of these results are given in Table 34. The results using the *CP* eigenstate ($\eta = +1$) $J/\psi\pi^0$ are shown in Fig. 17. The vector-vector mode $D^{*+}D^{*-}$ is found to be dominated by the *CP* even longitudinally polarized component; *BABAR* measures a *CP* odd fraction of $0.063 \pm 0.055 \pm 0.009$ [210] while Belle measures a *CP* odd fraction of $0.19 \pm 0.08 \pm 0.01$ [211] (here we do not average these fractions and rescale the inputs, however the average is almost independent of the treatment). For the non-*CP* eigenstate mode $D^{*\pm}D^{\mp}$ *BABAR* uses fully reconstructed events while Belle combines both fully and partially reconstructed samples.

In the absence of the penguin contribution, the time-dependent parameters would be given by $S_{b\to c\overline{c}d} = -\eta\sin(2\beta)$, $C_{b\to c\overline{c}d} = 0$, $S_{+-} = \sin(2\beta + \delta)$, $S_{-+} = \sin(2\beta - \delta)$, $C_{+-} = -C_{-+}$ and $A_{+-} = 0$, where δ is the strong phase difference between the $D^{*+}D^-$ and $D^{*-}D^+$ decay amplitudes. In the presence of the penguin contribution, there is no clean interpretation in terms of CKM parameters, however direct *CP* violation may be observed as any of $C_{b\to c\overline{c}d} \neq 0$, $C_{+-} \neq -C_{-+}$ or $A_{+-} \neq 0$.

Table 34: Averages for $b \to c\bar{c}d$ modes.

Experiment		$S_{b\to c\bar{c}d}$	$C_{b\to c\bar{c}d}$
		$J/\psi\,\pi^0$	
BABAR	[208]	$0.05 \pm 0.49 \pm 0.16$	$0.38 \pm 0.41 \pm 0.09$
Belle	[209]	$-0.72 \pm 0.42 \pm 0.09$	$0.01 \pm 0.29 \pm 0.03$
Average		-0.40 ± 0.33	0.12 ± 0.24
Confidence level		combined average: 0.36	
		$D^{*+}D^{*-}$	
BABAR	[210]	$0.06 \pm 0.37 \pm 0.13$	$0.28 \pm 0.23 \pm 0.02$
Belle	[211]	$-0.75 \pm 0.56 \pm 0.12$	$0.26 \pm 0.26 \pm 0.04$
Average		-0.20 ± 0.32	0.28 ± 0.17
Confidence level		combined average: 0.49	

Experiment	S_{+-}	C_{+-}	S_{-+}	C_{-+}	A
			$D^{*\pm}D^{\mp}$		
BABAR [212]	$-0.82 \pm 0.75 \pm 0.14$	$-0.47 \pm 0.40 \pm 0.12$	$-0.24 \pm 0.69 \pm 0.12$	$-0.22 \pm 0.37 \pm 0.10$	$-0.03 \pm 0.11 \pm 0.05$
Belle [213]	$-0.55 \pm 0.39 \pm 0.12$	$-0.37 \pm 0.22 \pm 0.06$	$-0.96 \pm 0.43 \pm 0.12$	$0.23 \pm 0.25 \pm 0.06$	$0.07 \pm 0.08 \pm 0.04$
Average	-0.61 ± 0.36	-0.39 ± 0.20	-0.75 ± 0.38	0.09 ± 0.21	0.03 ± 0.07

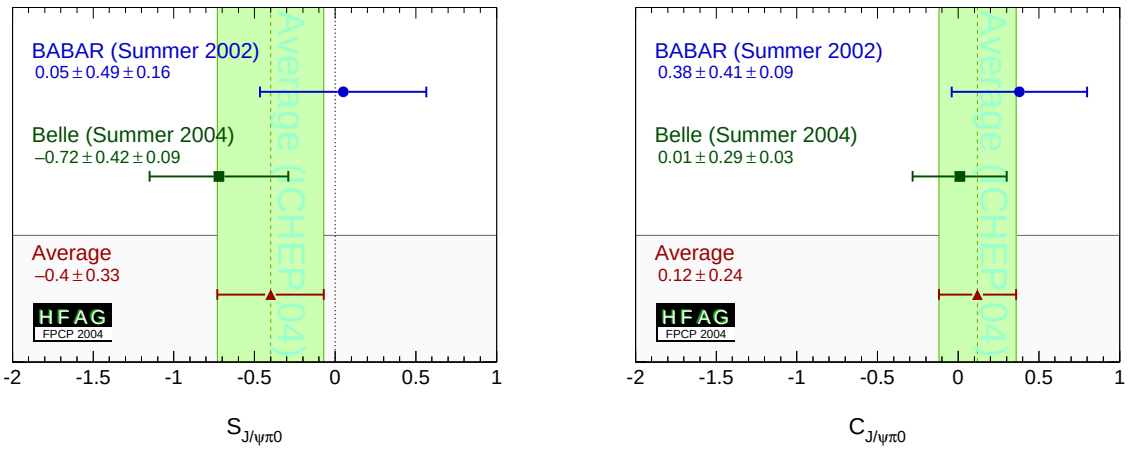

Figure 17: Averages of (left) $S_{b\to c\bar{c}d}$ and (right) $C_{b\to c\bar{c}d}$ for the mode $B^0 \to J/\psi\pi^0$.

The averages for the $b \to c\bar{c}d$ modes are shown in Fig. 18. Comparisons of the results for the $b \to c\bar{c}d$ modes to the $b \to c\bar{c}s$ and $b \to q\bar{q}s$ modes, can be seen in Fig. 19.

5.8 Time-dependent asymmetries in $b \to s\gamma$ transitions

The radiative decays $b \to s\gamma$ produce photons which are highly polarized in the Standard Model. The decays $B^0 \to F\gamma$ and $\overline{B}^0 \to F\gamma$ produce photons with opposite helicities, and since the polarization is, in principle, observable, these final states cannot interfere. The finite mass of the s quark introduces small corrections, to the limit of maximum polarization, but any large mixing induced CP violation would be a signal for new physics. Since a single weak phase dominates the $b \to s\gamma$ transition in the Standard Model, the cosine term is also expected

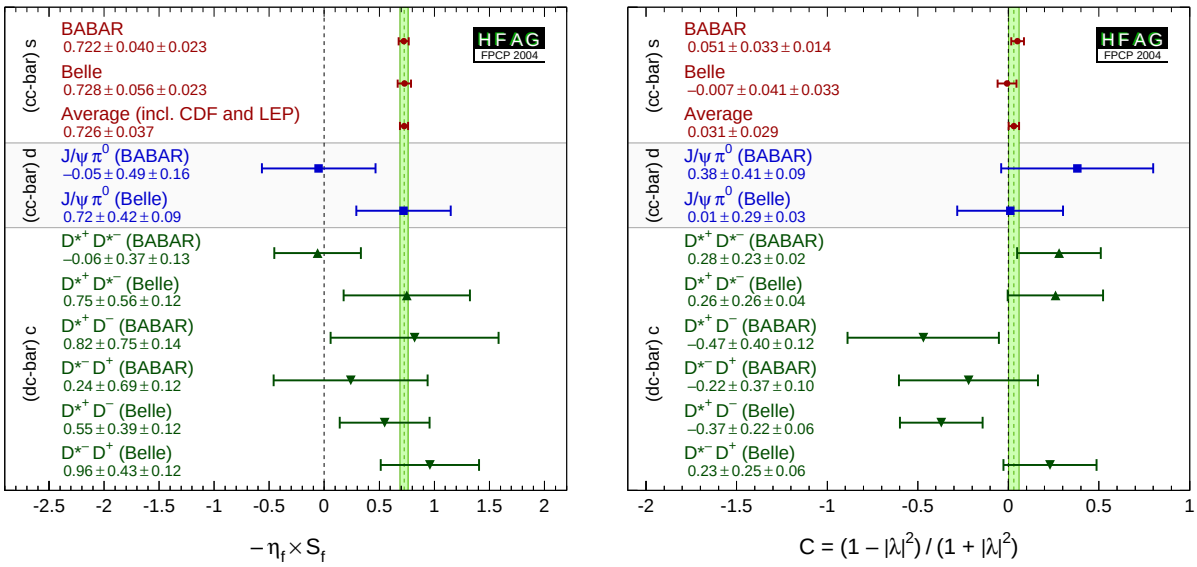

Figure 18: Averages of (left) $S_{b\to c\bar{c}d}$ and (right) $C_{b\to c\bar{c}d}$, compared to $S_{b\to c\bar{c}s}$ and $C_{b\to c\bar{c}s}$, respectively.

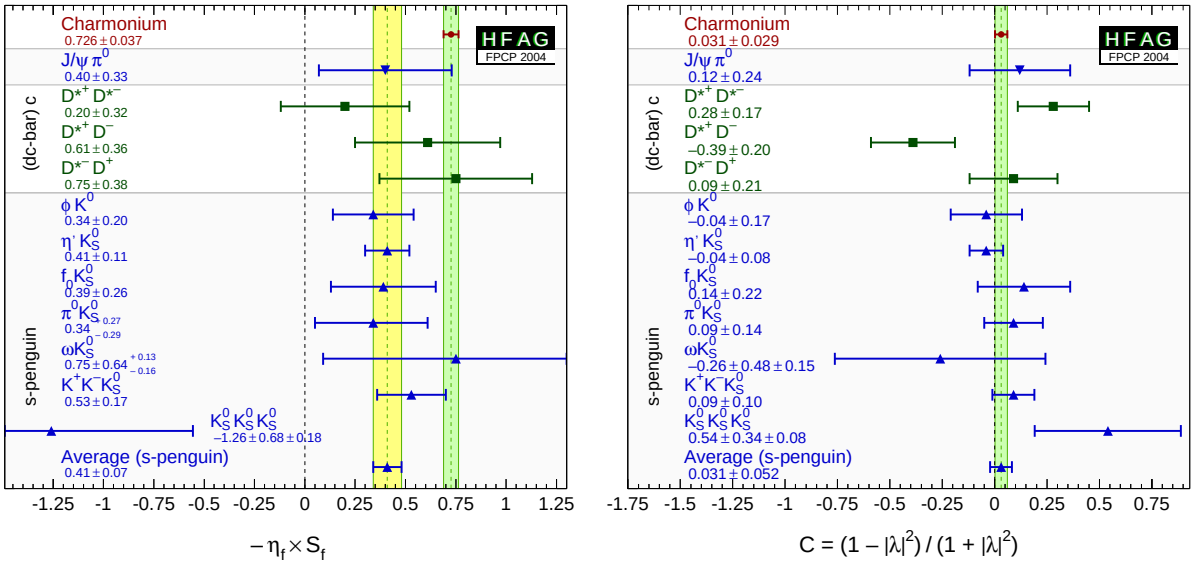

Figure 19: Comparisons of the averages of (left) $S_{b\to c\bar{c}s}$, $S_{b\to c\bar{c}d}$ and $S_{b\to q\bar{q}s}$, and (right) $C_{b\to c\bar{c}s}$, $C_{b\to c\bar{c}d}$ and $C_{b\to q\bar{q}s}$.

Table 35: Averages for $b \to s\gamma$ modes.

Experiment		$S_{b\to s\gamma}$	$C_{b\to s\gamma}$
		$K^0_S\pi^0\gamma$	
BABAR	[214]	$0.25 \pm 0.63 \pm 0.14$	$-0.57 \pm 0.32 \pm 0.09$
Belle	[215]	$-0.58\,^{+0.46}_{-0.38} \pm 0.11$	$0.03 \pm 0.34 \pm 0.11$
Average		-0.29 ± 0.38	-0.32 ± 0.24
Confidence level		combined average: 0.31 (1.0σ)	

to be small.

The *BABAR* collaboration has studied time-dependent asymmetries in $b \to s\gamma$ transitions using the decay $B^0 \to K^*\gamma$, with $K^* \to K^0_S\pi^0$. The Belle collaboration also uses the decay $B^0 \to K^0_S\pi^0\gamma$, but do not restrict themselves to the K^* mass region [185] (the invariant mass range 0.60 GeV/c^2 < $M_{K^0_S\pi^0}$ < 1.80 GeV/c^2 is used). These results, and their averages, are given in Table 35.

5.9 Time-dependent *CP* asymmetries in $b \to u\overline{u}d$ transitions

The $b \to u\overline{u}d$ transition can be mediated by either a $b \to u$ tree amplitude or a $b \to d$ penguin amplitude. These transitions can be investigated using the time dependence of B^0 decays to final states containing light mesons. Results are available from both *BABAR* and Belle for the *CP* eigenstate ($\eta = +1$) $\pi^+\pi^-$ final state. *BABAR* has also performed an analysis on the vector-vector final state $\rho^+\rho^-$, which they find to be dominated by the *CP* even longitudinally polarized component (they measure $f_{\rm long} = 0.99 \pm 0.03\,^{+0.04}_{-0.03}$ [220]).

For the non-*CP* eigenstate $\rho^\pm\pi^\mp$, Belle has performed a quasi-two-body analysis, while *BABAR* performs a time-dependent Dalitz plot (DP) analysis of the $\pi^+\pi^-\pi^0$ final state [217]; such an analysis allows direct measurements of the phases. These results, and averages, are listed in Table 36. The averages for $\pi^+\pi^-$ are shown in Fig. 20.

If the penguin contribution is negligible, the time-dependent parameters for $B^0 \to \pi^+\pi^-$ and $B^0 \to \rho^+\rho^-$ are given by $S_{b\to u\overline{u}d} = \eta\sin(2\alpha)$ and $C_{b\to u\overline{u}d} = 0$. With the notation described in Sec. 5.2 (Eq. (69)), the time-dependent parameters for $B^0 \to \rho^\pm\pi^\mp$ are, neglecting penguin contributions, given by $S_{\rho\pi} = \sqrt{1-(\frac{\Delta C}{2})^2}\sin(2\alpha)\cos(\delta)$, $\Delta S_{\rho\pi} = \sqrt{1-(\frac{\Delta C}{2})^2}\cos(2\alpha)\sin(\delta)$ and $C_{\rho\pi} = \mathcal{A}^{\rho\pi}_{CP} = 0$, where $\delta = \arg(A_{-+}A^*_{+-})$ is the strong phase difference between the $\rho^-\pi^+$ and $\rho^+\pi^-$ decay amplitudes. In the presence of the penguin contribution, there is no straightforward interpretation of $B^0 \to \rho^\pm\pi^\mp$ in terms of CKM parameters. However direct *CP* violation may arise, resulting in either or both of $C_{\rho\pi} \neq 0$ and $\mathcal{A}^{\rho\pi}_{CP} \neq 0$. Equivalently, direct *CP* violation may be seen by either of the decay-type-specific observables $\mathcal{A}^{+-}_{\rho\pi}$ and $\mathcal{A}^{-+}_{\rho\pi}$, defined in Eq. (70), deviating from zero. Results and averages for these parameters are also given in Table 36. They exhibit a linear correlation coefficient of +0.59. The significance of observing direct *CP* violation computed from the difference of the χ^2 obtained in the nominal average, compared to setting $C_{\rho\pi} = \mathcal{A}^{\rho\pi}_{CP} = 0$ is found to be 3.4σ in this mode. The confidence level contours of $\mathcal{A}^{+-}_{\rho\pi}$ versus $\mathcal{A}^{-+}_{\rho\pi}$ are shown in Fig. 21.

Some difference is seen between the *BABAR* and Belle measurements in the $\pi^+\pi^-$ system. The confidence level of the average is 0.0014, which corresponds to a 3.2σ discrepancy. Since

Table 36: Averages for $b \to u\overline{u}d$ modes.

Experiment		$S_{b\to u\overline{u}d}$	$C_{b\to u\overline{u}d}$
		$\pi^+\pi^-$	
BABAR	[218]	$-0.30 \pm 0.17 \pm 0.03$	$-0.09 \pm 0.15 \pm 0.04$
Belle	[219]	$-1.00 \pm 0.21 \pm 0.07$	$-0.58 \pm 0.15 \pm 0.07$
Average		-0.61 ± 0.14	-0.37 ± 0.11
Confidence level		combined average: 1.4×10^{-3} (3.2σ)	
		$\rho^+\rho^-$	
BABAR	[220]	$-0.19 \pm 0.33 \pm 0.11$	$-0.23 \pm 0.24 \pm 0.14$

		$\rho^\pm\pi^\mp$ Q2B/DP analysis				
Experiment		$S_{\rho\pi}$	$C_{\rho\pi}$	$\Delta S_{\rho\pi}$	$\Delta C_{\rho\pi}$	$\mathcal{A}_{CP}^{\rho\pi}$
BABAR	[222]	$-0.10 \pm 0.14 \pm 0.04$	$0.34 \pm 0.11 \pm 0.05$	$0.22 \pm 0.15 \pm 0.03$	$0.15 \pm 0.11 \pm 0.03$	$-0.088 \pm 0.049 \pm 0.013$
Belle	[223]	$-0.28 \pm 0.23^{+0.10}_{-0.08}$	$0.25 \pm 0.17^{+0.02}_{-0.06}$	$-0.30 \pm 0.24 \pm 0.09$	$0.38 \pm 0.18^{+0.02}_{-0.04}$	$-0.16 \pm 0.10 \pm 0.02$
Average		-0.13 ± 0.13	0.31 ± 0.10	0.09 ± 0.13	0.22 ± 0.10	-0.102 ± 0.045

		$\mathcal{A}_{\rho\pi}^{+-}$	$\mathcal{A}_{\rho\pi}^{-+}$
BABAR	[222]	$0.25 \pm 0.17^{+0.02}_{-0.06}$	$-0.47^{+0.14}_{-0.15} \pm 0.06$
Belle	[223]	$-0.02 \pm 0.16^{+0.05}_{-0.02}$	$-0.53 \pm 0.29^{+0.09}_{-0.04}$
Average		-0.15 ± 0.09	$-0.47^{+0.13}_{-0.14}$

		$\rho^\pm\pi^\mp$ DP analysis	
Experiment		α (°)	δ_{+-} (°)
BABAR	[222]	$113^{+27}_{-17} \pm 6$	$-67^{+28}_{-31} \pm 7$

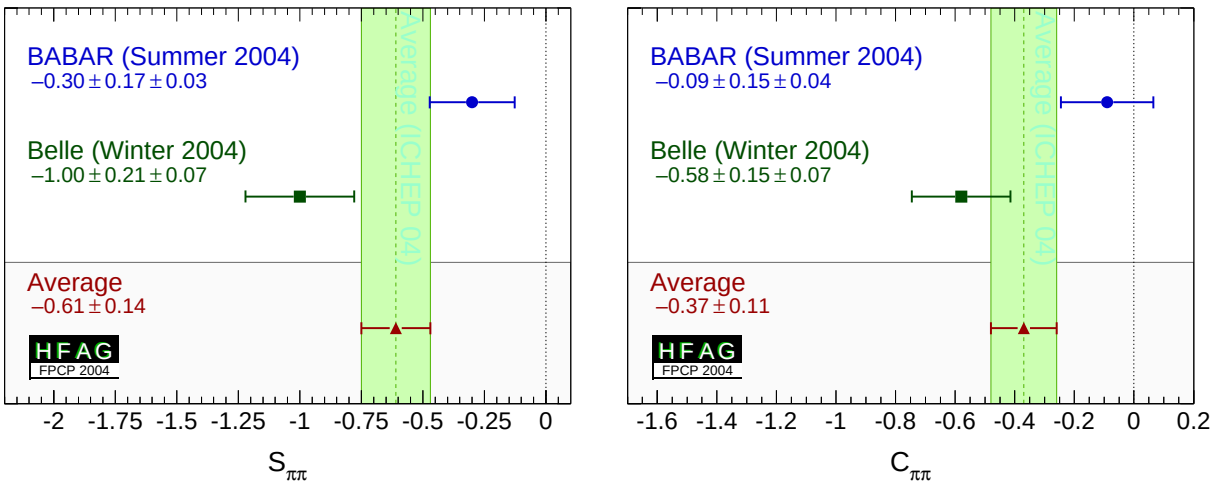

Figure 20: Averages of (left) $S_{b\to u\overline{u}d}$ and (right) $C_{b\to u\overline{u}d}$ for the mode $B^0 \to \pi^+\pi^-$.

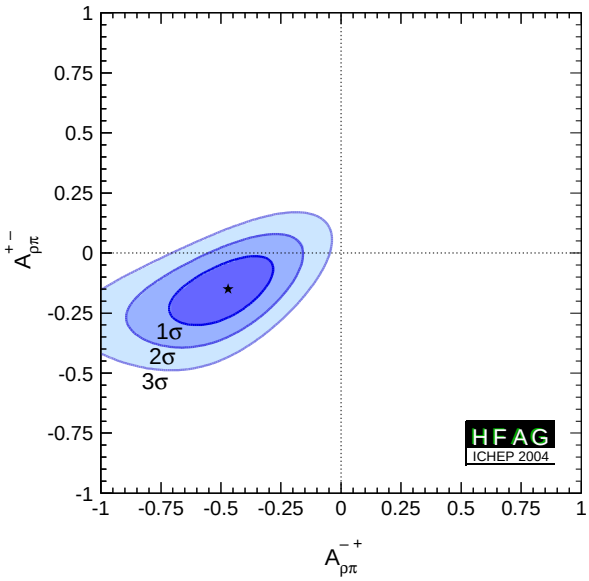

Figure 21: Direct *CP* violation in $B^0 \to \rho^\pm\pi^\mp$. The no-*CP* violation hypothesis is excluded at the 3.4σ level.

there is no evidence of systematic problems in either analysis, we do not rescale the errors of the averages.

The precision of the measured *CP* violation parameters in $b \to u\overline{u}d$ transitions allows constraints to be set on the UT angle α. In addition to the value of α from the *BABAR* time-dependent DP analysis, given in Table 36, constraints have been obtained with various methods:

- In the Belle analysis of $B^0 \to \pi^+\pi^-$ [219], constraints on the time-dependent *CP* violation parameters are used to obtain $90^\circ < \alpha < 146^\circ$ (95.5% CL) following the method proposed by Gronau and Rosner [224]. This result includes an assumption on the relative size of tree and penguin amplitudes.

- Using the measured time-dependent *CP* violation parameters in longitudinally polarized $B^0 \to \rho^+\rho^-$ decays [220], in combination with the upper limit for the $B^0 \to \rho^0\rho^0$ branching fraction [225], and the measurement of the branching fraction and longitudinal polarization of $B^+ \to \rho^+\rho^0$ [226, 227], *BABAR* performs an isospin analysis [228] and obtains $\alpha = (96 \pm 10 \pm 4 \pm 11)^\circ$, where the third error is due to the unknown penguin contribution.

- The CKMfitter group [196] uses the measurements from Belle and *BABAR* given in Table 36, with other branching fractions and *CP* asymmetries in $B \to \pi\pi$, $\rho\pi$ and $\rho\rho$ modes, to perform isospin analyses for each system. They then combine the results to obtain $\alpha = (100^{+\ 9}_{-10})^\circ$.

Note that each method suffers from ambiguities in the solutions. All the above measurements correspond to the choice that is in agreement with the global CKM fit.

At present we make no attempt to provide an HFAG average for α. More details on procedures to calculate a best fit value for α can be found in Refs. [196, 197].

Table 37: Averages for $b \to c\overline{u}d/u\overline{c}d$ modes.

Experiment		a	c
		$D^{*\pm}\pi^{\mp}$	
BABAR (full rec.)	[229]	$-0.049 \pm 0.031 \pm 0.020$	$0.044 \pm 0.054 \pm 0.033$
Belle (full rec.)	[230]	$0.060 \pm 0.040 \pm 0.019$	$0.049 \pm 0.040 \pm 0.019$
BABAR (partial rec.)	[231]	$-0.041 \pm 0.016 \pm 0.010$	$-0.015 \pm 0.036 \pm 0.019$
Belle (partial rec.)	[232]	$-0.031 \pm 0.028 \pm 0.018$	$-0.004 \pm 0.028 \pm 0.018$
Average		-0.030 ± 0.014	0.010 ± 0.021
Confidence level		0.19	0.66
		$D^{\pm}\pi^{\mp}$	
BABAR (full rec.)	[229]	$-0.032 \pm 0.031 \pm 0.020$	$-0.059 \pm 0.055 \pm 0.033$
Belle (full rec.)	[230]	$-0.062 \pm 0.037 \pm 0.018$	$-0.025 \pm 0.037 \pm 0.018$
Average		-0.045 ± 0.027	-0.035 ± 0.035
Confidence level		0.59	0.66
		$D^{\pm}\rho^{\mp}$	
BABAR (full rec.)	[229]	$-0.005 \pm 0.044 \pm 0.021$	$-0.147 \pm 0.074 \pm 0.035$

5.10 Time-dependent *CP* asymmetries in $b \to c\overline{u}d/u\overline{c}d$ transitions

Non-*CP* eigenstates such as $D^{\pm}\pi^{\mp}$, $D^{*\pm}\pi^{\mp}$ and $D^{\pm}\rho^{\mp}$ can be produced in decays of B^0 mesons either via Cabibbo favoured ($b \to c$) or doubly Cabibbo suppressed ($b \to u$) tree amplitudes. Since no penguin contribution is possible, these modes are theoretically clean. The ratio of the magnitudes of the suppressed and favoured amplitudes, R, is sufficiently small (predicted to be about 0.02), that terms of $\mathcal{O}(R^2)$ can be neglected, and the sine terms give sensitivity to the combination of UT angles $2\beta + \gamma$.

As described in Sec. 5.2.4, the averages are given in terms of parameters a and c. *CP* violation would appear as $a \neq 0$. Results are available from both *BABAR* and Belle in the modes $D^{\pm}\pi^{\mp}$ and $D^{*\pm}\pi^{\mp}$; for the latter mode both experiments have used both full and partial reconstruction techniques. Results are also available from *BABAR* using $D^{\pm}\rho^{\mp}$. These results, and their averages, are listed in Table 37, and are shown in Fig. 22.

5.11 Rates and asymmetries in $B^{\mp} \to D^{(*)}K^{(*)\mp}$ decays

As explained in Sec. 5.2.5, rates and asymmetries in $B^{\mp} \to D^{(*)}K^{(*)\mp}$ decays are sensitive to γ. Various methods using different $D^{(*)}$ final states exist.

Results are available from both *BABAR* and Belle on GLW analyses in the decay modes $B^{\mp} \to DK^{\mp}$, $B^{\mp} \to D^*K^{\mp}$ and $B^{\mp} \to DK^{*\mp}$. Both experiments use the *CP* even D decay final states K^+K^- and $\pi^+\pi^-$ in all three modes; both experiments also use only the $D^* \to D\pi^0$ decay, which gives $CP(D^*) = CP(D)$. For *CP* odd D decay final states, Belle uses $K^0_S\pi^0$, $K^0_S\eta$ and $K^0_S\phi$ in all three analyses, and also use $K^0_S\omega$ in $DK^{\mp}$ and $D^*K^{\mp}$ analyses. *BABAR* uses $K^0_S\pi^0$ only for $DK^{\mp}$ analysis; for $DK^{*\mp}$ analysis they also use $K^0_S\phi$ and $K^0_S\omega$ (and assign an asymmetric systematic error due to *CP* even pollution in these *CP* odd channels [237]). The results and averages are given in Table 38.

For ADS analysis, both *BABAR* and Belle have studied the mode $B^{\mp} \to DK^{\mp}$, and *BABAR*

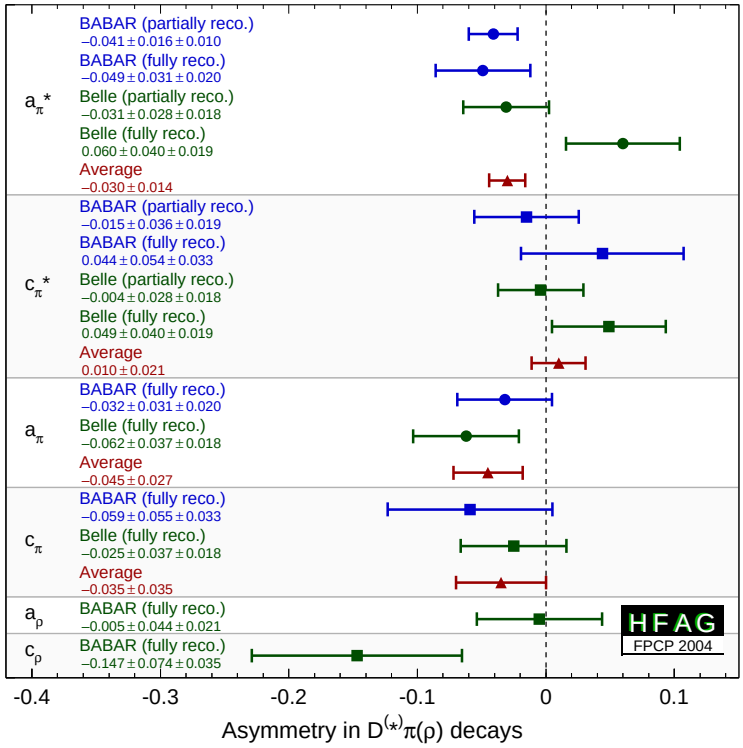

Figure 22: Averages for $b \to c\overline{u}d/u\overline{c}d$ modes.

Table 38: Averages from GLW analyses of $b \to c\overline{u}d/u\overline{c}d$ modes.

Experiment	A_{CP+}	A_{CP-}	R_{CP+}	R_{CP-}
		$D_{CP}K^-$		
BABAR [235]	$0.40 \pm 0.15 \pm 0.08$	$0.21 \pm 0.17 \pm 0.07$	$0.87 \pm 0.14 \pm 0.06$	$0.80 \pm 0.14 \pm 0.08$
Belle [236]	$0.07 \pm 0.14 \pm 0.06$	$-0.11 \pm 0.14 \pm 0.05$	$0.98 \pm 0.18 \pm 0.10$	$1.29 \pm 0.16 \pm 0.08$
Average	0.22 ± 0.11	0.02 ± 0.12	0.91 ± 0.12	1.02 ± 0.12
		$D^*_{CP}K^-$		
BABAR [237]	$-0.02 \pm 0.24 \pm 0.05$		$1.09 \pm 0.26\,^{+0.10}_{-0.08}$	
Belle [236]	$-0.27 \pm 0.25 \pm 0.04$	$0.26 \pm 0.26 \pm 0.03$	$1.43 \pm 0.28 \pm 0.06$	$0.94 \pm 0.28 \pm 0.06$
Average	-0.14 ± 0.18	0.26 ± 0.26	1.25 ± 0.20	0.94 ± 0.29
		$D_{CP}K^{*-}$		
BABAR [238]	$-0.09 \pm 0.20 \pm 0.06$	$-0.33 \pm 0.34 \pm 0.10\,^{+0.00}_{-0.06}$	$1.77 \pm 0.37 \pm 0.12$	$0.76 \pm 0.29 \pm 0.06\,^{+0.04}_{-0.14}$
Belle [239]	$-0.02 \pm 0.33 \pm 0.07$	$0.19 \pm 0.50 \pm 0.04$		
Average	-0.07 ± 0.18	-0.16 ± 0.29		

Table 39: Averages from ADS analyses of $b \to c\overline{u}d/u\overline{c}d$ modes.

Experiment		A_{ADS}	R_{ADS}
		DK^-, $D \to K^+\pi^-$	
BABAR	[240]		$0.013\,^{+0.011}_{-0.009}$
Belle	[241]	$0.49\,^{+0.53}_{-0.46} \pm 0.06$	$0.028\,^{+0.015}_{-0.014} \pm 0.010$
Average		$0.49\,^{+0.53}_{-0.46}$	0.017 ± 0.009
		D^*K^-, $D^* \to D\pi^0$, $D \to K^+\pi^-$	
BABAR	[240]		$-0.001\,^{+0.010}_{-0.006}$
		D^*K^-, $D^* \to D\gamma$, $D \to K^+\pi^-$	
BABAR	[240]		$0.011\,^{+0.019}_{-0.013}$

Table 40: Averages from Dalitz plot analyses of $b \to c\overline{u}d/u\overline{c}d$ modes.

Experiment		γ (°)	δ_B (°)	r_B
			DK^-, $D \to K^0_S\pi^+\pi^-$	
BABAR	[242]	$70 \pm 44 \pm 10 \pm 10$	$114 \pm 41 \pm 8 \pm 10$	< 0.19 @ 90% CL
Belle	[243]	$64 \pm 19 \pm 13 \pm 11$	$157 \pm 19 \pm 11 \pm 21$	$0.21 \pm 0.08 \pm 0.03 \pm 0.04$
Average			IN PREPARATION	
			D^*K^-, $D^* \to D\pi^0$ or $D\gamma$, $D \to K^0_S\pi^+\pi^-$	
BABAR	[242]	$73 \pm 35 \pm 8 \pm 10$	$303 \pm 34 \pm 14 \pm 10$	$0.16\,^{+0.07}_{-0.08} \pm 0.04 \pm 0.02$
Belle	[243]	$75 \pm 57 \pm 11 \pm 11$	$321 \pm 57 \pm 11 \pm 21$	$0.12\,^{+0.16}_{-0.11} \pm 0.02 \pm 0.04$
Average			IN PREPARATION	
			DK^- and D^*K^- combined	
BABAR	[242]	$70 \pm 26 \pm 10 \pm 10$		
Belle	[243]	$68\,^{+14}_{-15} \pm 13 \pm 11$		
Average			IN PREPARATION	

has also analyzed the $B^\mp \to D^*K^\mp$ mode ($D^* \to D\pi^0$ and $D^* \to D\gamma$ are studied separately). In all cases the suppressed decay $D \to K^+\pi^-$ has been used. The results and averages are given in Table 39. Note that although no clear signals for these modes have yet been seen, the central values are given in Table 39. In $B^- \to D^*K^-$ decays there is an effective shift of π in the strong phase difference between the cases that the D^* is reconstructed as $D\pi^0$ and $D\gamma$ [189]. As a consequence, the different D^* decay modes are treated separately.

For the Dalitz plot analysis, both *BABAR* and Belle have studied the mode $B^\mp \to DK^\mp$. Both have also studied the mode $B^\mp \to D^*K^\mp$; Belle has used only $D^* \to D\pi^0$, while *BABAR* has used both D^* decay modes and taken the effective shift in the strong phase difference into account. In all cases the decay $D \to K^0_S\pi^+\pi^-$ has been used. The results are given in Table 40. Since the measured values of r_B are positive definite, and since the error on γ depends on the value of r_B, some statistical treatment is necessary to correct for bias. Belle has used a frequentist treatment, while *BABAR* used a Bayesian approach. At present, we make no attempt to average the results.

6 Averages of charmless B-decay branching fractions and their asymmetries

The aim of this section is to provide the branching fractions and the partial rate asymmetries (A_{CP}) of rare B decays. The asymmetry is defined as $A_{CP} = \frac{N_{\overline{B}} - N_B}{N_{\overline{B}} + N_B}$, where $N_{\overline{B}}$ and N_B are number of $\overline{B}^0/B^-$ and B^0/B^+, respectively. Four different B decay categories are considered: charmless mesonic, baryonic, radiative and leptonic. Rare mesonic decays with charm are not in our scope but results of charmful baryonic decays are included. Measurements supported with written documents are accepted in our the averages; written documents could be journal papers, conference contributed papers, preprints or conference proceedings. Results from A_{CP} measurements obtained from time dependent analyses are listed and described in Sec. 5.

So far all branching fractions assume equal production of charged and neutral B pairs. The best measurements to date show that this is still a good approximation (see Sec. 3.1.1). For branching fractions, we provide either averages or the most stringent 90% confidence level upper limits. If one or more experiments have measurements with $>4\sigma$ for a decay channel, all available central values for that channel are used in the averaging. We also give central values and errors for cases where the significance of the average value is at least 3σ, even if no single measurement is above 4σ. For A_{CP} we provide averages in all cases.

Our averaging is performed by maximizing the likelihood,

$$\mathcal{L} = \prod_i \mathcal{P}_i(x), \tag{85}$$

where $\mathcal{P}_i$ is the probability density function (PDF) of the ith measurement, and x is the branching fraction or A_{CP}. The PDF is modeled by an asymmetric Gaussian function with the measured central value as its mean and the quadratic sum of the statistical and systematic errors as the standard deviations. The experimental uncertainties are considered to be uncorrelated with each other when the averaging is performed. No error scaling is applied when the fit χ^2 is greater than 1 since we believe that tends to overestimate the errors except in cases of extreme disagreement (we have no such cases).

At present, we have measurements of 230 B decay modes and asymmetry measurements for 35 of these decays. These results are reported in 112 separate papers. Because the number of references is so large, we do not include them with the tables shown here but the full set of references is available quickly from active gifs at the ICHEP04 link on the rare web page: `http://www.slac.stanford.edu/xorg/hfag/rare/index.html`

6.1 Mesonic charmless decays

Table 41: B^+ branching fractions (in units of 10^{-6}). Upper limits are at 90% CL. Values in red (blue) are new published (preliminary) result since PDG2004 [as of August 25th, 2004].

RPP#	Mode	PDG2004 Avg.	BABAR	Belle	CLEO	CDF	New Avg.
117	$K^0\pi^+$	18.8 ± 2.1	$26.0 \pm 1.3 \pm 1.0$	$22.0 \pm 1.9 \pm 1.1$	$18.8^{+3.7+2.1}_{-3.3-1.8}$		24.1 ± 1.3
118	$K^+\pi^0$	12.9 ± 1.2	$12.0 \pm 0.7 \pm 0.6$	$12.0 \pm 1.3^{+1.3}_{-0.9}$	$12.9^{+2.4+1.2}_{-2.2-1.1}$		12.1 ± 0.8
119	$\eta' K^+$	78 ± 5	$76.9 \pm 3.5 \pm 4.4$	$78 \pm 6 \pm 9$	$80^{+10}_{-9} \pm 7$		$77.6^{+4.6}_{-4.5}$
120	$\eta' K^{*+}$	< 35	< 14	< 90	< 35		< 14
121	ηK^+	< 6.9	$3.4 \pm 0.8 \pm 0.2$	$2.1 \pm 0.6 \pm 0.2$	$2.2^{+2.8}_{-2.2}$		2.6 ± 0.5
122	ηK^{*+}	26^{+10}_{-9}	$25.6 \pm 4.0 \pm 2.4$	$22.8^{+3.7}_{-3.5} \pm 2.2$	$26.4^{+9.6}_{-8.2} \pm 3.3$		$24.3^{+3.0}_{-2.9}$
–	$a_0^0(980)K^+$ †	New	< 2.5				< 2.5
–	$a_0^+(980)K^0$ †	New	< 3.9				< 3.9
123	ωK^+	$9.2^{+2.8}_{-2.5}$	$4.8 \pm 0.8 \pm 0.4$	$6.5^{+1.3}_{-1.2} \pm 0.6$	$3.2^{+2.4}_{-1.9} \pm 0.8$		5.1 ± 0.7
124	ωK^{*+}	< 87	< 7.4		< 87		< 7.4
125	$K^{*0}\pi^+$	19^{+6}_{-8}	$10.5 \pm 2.0 \pm 1.4$	$9.83 \pm 0.90^{+1.06}_{-1.24}$	$7.6^{+3.5}_{-3.0} \pm 1.6$		$9.76^{+1.16}_{-1.22}$
126	$K^{*+}\pi^0$	< 31			< 31		< 31
127	$K^+\pi^+\pi^-$	57 ± 4	$61.4 \pm 2.4 \pm 4.5$	$46.6 \pm 2.1 \pm 4.3$			53.5 ± 3.5
128	$K^+\pi^+\pi^-(NR)$	< 28	$4.9 \pm 0.6 \pm 1.4$		< 28		4.9 ± 1.5
129	$K^+ f_0(980)$ †	seen	$9.2 \pm 1.5 \pm 0.8$	$7.55 \pm 1.24^{+1.63}_{-1.18}$			$8.49^{+1.35}_{-1.26}$
130	$K^+\rho^0$	< 12	$5.2 \pm 1.2 \pm 0.7$	$4.78 \pm 0.75^{+1.01}_{-0.97}$	$8.4^{+4.0}_{-3.4} \pm 1.8$		$5.15^{+0.91}_{-0.89}$
–	$f_2(1270)K^+$ †	New		< 1.3			< 1.3
–	$f_2'(1525)K^+$ †	New		< 2.1			< 2.1
–	$K_0^*(1430)^0\pi^+$ †	New	$32.3 \pm 1.9 \pm 2.5$				32.3 ± 3.1
131	$K_2^*(1430)^0\pi^+$†	< 680		< 2.3			< 2.3
–	$K^*(1680)^0\pi^+$ †	New		< 3.1			< 3.1
132	$K^-\pi^+\pi^+$	< 1.8	< 1.8	< 4.5			< 1.8
135	$K^0\pi^+\pi^0$	< 66			< 66		< 66
136	$K^0\rho^+$	< 48			< 48		< 48
–	$K^{*0}\rho^+$	New	$17.0 \pm 2.9^{+2.0}_{-2.8}$	$6.6 \pm 2.2 \pm 0.8$			9.2 ± 2.0
138	$K^{*+}\rho^0$	11 ± 4	$10.6^{+3.0}_{-2.6} \pm 2.4$		< 74		$10.6^{+3.8}_{-3.5}$
139	$K^{*+}\overline{K^{*0}}$	< 71			< 71		< 71
142	$K^+\overline{K^0}$	< 2.0	< 2.4	< 3.3	< 3.3		< 2.4
143	$K^+\overline{K^0}\pi^0$	< 24			< 24		< 24
144	$K^+K_SK_S$	13.4 ± 2.4	$10.7 \pm 1.2 \pm 1.0$	$13.4 \pm 1.9 \pm 1.5$			11.5 ± 1.3
145	$K_SK_S\pi^+$	< 3.2		< 3.2			< 3.2
146	$K^+K^-\pi^+$	< 6.3	< 6.3	< 13			< 6.3
148	$K^+K^+\pi^-$	< 1.3	< 1.3	< 2.4			< 1.3
150	$\overline{K^{*0}}K^+$	< 5.3			< 5.3		< 5.3
152	$K^+K^-K^+$	30.8 ± 2.1	$29.6 \pm 2.1 \pm 1.6$	$30.6 \pm 1.2 \pm 2.3$			30.1 ± 1.9
153	ϕK^+	9.3 ± 1.0	$10.0^{+0.9}_{-0.8} \pm 0.5$	$9.60 \pm 0.92^{+1.05}_{-0.84}$	$5.5^{+2.1}_{-1.8} \pm 0.6$	$7.2 \pm 1.3 \pm 0.7$	$8.97^{+0.65}_{-0.63}$
–	a_2K^+†	New		< 1.1			< 1.1
–	$\phi(1680)K^+$†	New		< 1.1			< 1.1
156	ϕK^{*+}	9.6 ± 3.0	$12.7^{+2.2}_{-2.0} \pm 1.1$	$6.7^{+2.1+0.7}_{-1.9-1.0}$	$10.6^{+6.4+1.8}_{-4.9-1.6}$		9.7 ± 1.5
159	$\phi\phi K^+$ §	$2.6^{+1.1}_{-0.9}$		$2.6^{+1.1}_{-0.9} \pm 0.3$			$2.6^{+1.1}_{-0.9}$
173	$\pi^+\pi^0$	$5.6^{+0.9}_{-1.1}$	$5.8 \pm 0.6 \pm 0.4$	$5.0 \pm 1.2 \pm 0.5$	$4.6^{+1.8+0.6}_{-1.6-0.7}$		5.5 ± 0.6
174	$\pi^+\pi^-\pi^+$	11 ± 4	$16.2 \pm 2.1 \pm 1.3$				16.2 ± 2.5
175	$\rho^0\pi^+$	8.6 ± 2.0	$9.4 \pm 1.3 \pm 1.0$	$8.0^{+2.3}_{-2.0} \pm 0.7$	$10.4^{+3.3}_{-3.4} \pm 2.1$		9.1 ± 1.3
–	$\rho^0(1450)\pi^+$	New	$2.2 \pm 0.5 \pm 0.3$				2.2 ± 0.6
176	$\pi^+ f_0(980)$ †	< 140					< 140
177	$f_2(1270)\pi^+$	< 240	$2.3 \pm 0.4 \pm 0.3$				2.3 ± 0.5
180	$\rho^+\pi^0$	< 43	$10.9 \pm 1.9 \pm 1.9$	$13.2 \pm 2.3^{+1.4}_{-1.9}$	< 43		12.0 ± 2.0
182	$\rho^+\rho^0$	26 ± 6	$22.5^{+5.7}_{-5.4} \pm 5.8$	$31.7 \pm 7.1^{+3.8}_{-6.7}$			$26.4^{+6.1}_{-6.4}$
185	$\omega\pi^+$	$6.4^{+1.8}_{-1.6}$	$5.5 \pm 0.9 \pm 0.5$	$5.7^{+1.4}_{-1.3} \pm 0.6$	$11.3^{+3.3}_{-2.9} \pm 1.4$		5.9 ± 0.8
186	$\omega\rho^+$	< 61	$12.6^{+3.7}_{-3.3} \pm 1.6$		< 61		$12.6^{+4.1}_{-3.8}$
187	$\eta\pi^+$	< 5.7	$5.3 \pm 1.0 \pm 0.3$	$4.8 \pm 0.7 \pm 0.3$	$1.2^{+2.8}_{-1.2}$		4.8 ± 0.6
188	$\eta'\pi^+$	< 7	$4.2 \pm 1.0 \pm 0.5$	< 7	$1.0^{+5.8}_{-1.0}$		4.2 ± 1.1
189	$\eta'\rho^+$	< 33	< 22		< 33		< 22
190	$\eta\rho^+$	< 15	$8.6 \pm 2.2 \pm 1.1$	$8.5^{+2.6}_{-2.4} \pm 1.0$	$4.8^{+5.2}_{-3.8}$		$8.6^{+1.9}_{-1.8}$
–	$a_0^0(980)\pi^+$ †	New	< 5.8				< 5.8
191	$\phi\pi^+$	< 0.41	< 0.41		< 5		< 0.41
192	$\phi\rho^+$	< 16			< 16		< 16

†Product BF - daughter BF taken to be 100%; §$M_{\phi\phi} < 2.85$ GeV/c^2

Table 42: B^0 branching fractions (in units of 10^{-6}). Upper limits are at 90% CL. Values in red (blue) are new published (preliminary) result since PDG2004 [as of August 25th, 2004].

RPP#	Mode	PDG2004 Avg.	BABAR	Belle	CLEO	CDF	New Avg.
123	$K^+\pi^-$	18.5 ± 1.1	$17.9 \pm 0.9 \pm 0.7$	$18.5 \pm 1.0 \pm 0.7$	$18.0^{+2.3+1.2}_{-2.1-0.9}$		18.2 ± 0.8
124	$K^0\pi^0$	$9.5^{+2.1}_{-1.9}$	$11.4 \pm 0.9 \pm 0.6$	$11.7 \pm 2.3^{+1.2}_{-1.3}$	$12.8^{+4.0+1.7}_{-3.3-1.4}$		11.5 ± 1.0
125	$\eta' K^0$	63 ± 7	$60.6 \pm 5.6 \pm 4.6$	$68 \pm 10^{+9}_{-8}$	$89^{+18}_{-16} \pm 9$		$65.2^{+6.0}_{-5.9}$
126	$\eta' K^{*0}$	< 24	< 7.6	< 20	< 24		< 7.6
127	ηK^{*0}	14^{+6}_{-5}	$18.6 \pm 2.3 \pm 1.2$	$19.8^{+2.1}_{-2.0} \pm 1.4$	$13.8^{+5.5}_{-4.6} \pm 1.6$		18.7 ± 1.7
128	ηK^0	< 9.3	$2.5 \pm 0.8 \pm 0.1$	$0.3^{+0.9}_{-0.7} \pm 0.1$	$0.0^{+3.2}_{-0.0}$		1.5 ± 0.6
–	$\eta K^+\pi^-$	New		$33.4^{+3.5+2.1}_{-3.3-1.9}$			$33.4^{+4.1}_{-3.8}$
–	$a_0^-(980)K^+$ †	New	< 2.1	< 2.9			< 2.1
–	$a_0^0(980)K^0$ †	New	< 7.8				< 7.8
129	ωK^0	< 13	$5.9^{+1.6}_{-1.3} \pm 0.5$	$4.0^{+1.9}_{-1.6} \pm 0.5$	$10.0^{+5.4}_{-4.2} \pm 1.4$		$5.5^{+1.2}_{-1.1}$
131	ωK^{*0}	< 23	< 6.0		< 23		< 6.0
132	K^+K^-	< 0.6	< 0.6	< 0.7	< 0.8		< 0.6
133	$K^0\overline{K^0}$	< 3.3	$1.19^{+0.40}_{-0.35} \pm 0.13$	< 1.5	< 3.3		$1.19^{+0.42}_{-0.37}$
134	$K_SK_SK_S$	$4.2^{+1.8}_{-1.5}$	$6.5 \pm 0.8 \pm 0.8$	$4.2^{+1.6}_{-1.3} \pm 0.8$			5.8 ± 1.0
135	$K^+\pi^-\pi^0$	< 40	$34.9 \pm 2.1 \pm 3.9$	$36.6^{+4.2}_{-4.1} \pm 3.0$	< 40		$35.6^{+3.4}_{-3.3}$
136	$K^+\rho^-$	7.3 ± 1.8	$8.6 \pm 1.4 \pm 1.0$	$15.1^{+3.4+2.4}_{-3.3-2.6}$	$16^{+8}_{-6} \pm 3$		$9.9^{+1.6}_{-1.5}$
–	$K^+\rho(1450)^-$ †	New	< 3.2				< 3.2
–	$K^+\rho(1700)^-$ †	New	< 1.7				< 1.7
137	$K^0\pi^+\pi^-$	47 ± 7	$43.7 \pm 3.8 \pm 3.4$	$45.4 \pm 5.2 \pm 5.9$	$50^{+10}_{-9} \pm 7$		44.9 ± 4.0
–	$K^+\pi^-\pi^0(NR)$	New	< 4.6	< 9.4			< 4.6
–	$K_0^*(1430)^+\pi^-$ †	New	$11.2 \pm 1.5 \pm 3.5$				11.2 ± 3.8
–	$K_0^*(1430)^0\pi^0$ †	New	$7.9 \pm 1.5 \pm 2.7$				7.9 ± 3.1
138	$K^0\rho^0$	< 39	$5.1 \pm 1.0 \pm 1.2$	< 12.4	< 39		5.1 ± 1.6
139	$K^0 f_0(980)$ †	< 36	$6.0 \pm 0.9 \pm 1.3$	< 14			6.0 ± 1.6
140	$K^{*+}\pi^-$	16^{+6}_{-5}	$11.9 \pm 1.7 \pm 1.1$	$14.8^{+4.6+2.8}_{-4.4-1.3}$	$16^{+6}_{-5} \pm 2$		$12.7^{+1.8}_{-1.7}$
141	$K^{*0}\pi^0$	< 3.6	$3.0 \pm 0.9 \pm 0.5$	$0.4^{+1.9}_{-1.7} \pm 0.1$	$0.0^{+1.3+0.5}_{-0.0-0.0}$		1.7 ± 0.8
142	$K_2^*(1430)^+\pi^-$	< 18	< 13.2				< 13.2
–	$K_2^*(1430)^0\pi^0$	New	< 3.6				< 3.6
–	$K^*(1680)^+\pi^-$	New	< 19.4				< 19.4
–	$K^*(1680)^0\pi^0$	New	< 5.0				< 5.0
143	$K^+\overline{K^0}\pi^-$	< 21		< 18	< 21		< 18
144	$K^+K^-\pi^0$	< 19			< 19		< 19
145	$K^+K^-K^0$	28 ± 5	$23.8 \pm 2.0 \pm 1.6$	$28.3 \pm 3.3 \pm 4.0$			24.7 ± 2.3
146	ϕK^0	$8.6^{+1.3}_{-1.1}$	$8.4^{+1.5}_{-1.3} \pm 0.5$	$9.0^{+2.2}_{-1.8} \pm 0.7$	$5.4^{+3.7}_{-2.7} \pm 0.7$		$8.3^{+1.2}_{-1.0}$
149	$K^{*0}\rho^0$	< 34		< 2.6	< 34		< 2.6
–	$K^{*+}\rho^-$	New	< 24				< 24
154	ϕK^{*0}	10.7 ± 1.1	$9.2 \pm 0.9 \pm 0.5$	$10.0^{+1.6+0.7}_{-1.5-0.8}$	$11.5^{+4.5+1.8}_{-3.7-1.7}$		9.5 ± 0.9
155	$K^{*0}\overline{K^{*0}}$	< 22			< 22		< 22
157	$K^{*+}K^{*-}$	< 141			< 141		< 141
176	$\pi^+\pi^-$	4.8 ± 0.5	$4.7 \pm 0.6 \pm 0.2$	$4.4 \pm 0.6 \pm 0.3$	$4.5^{+1.4+0.5}_{-1.2-0.4}$		4.6 ± 0.4
177	$\pi^0\pi^0$	1.9 ± 0.5	$1.17 \pm 0.32 \pm 0.10$	$2.32^{+0.44+0.22}_{-0.48-0.18}$	< 4.4		1.51 ± 0.28
178	$\eta\pi^0$	< 2.9	< 2.5	< 2.5	< 2.9		< 2.5
179	$\eta\eta$	< 18	< 2.8	< 2.0	< 18		< 2.0
180	$\eta'\pi^0$	< 5.7	< 3.7		< 5.7		< 3.7
181	$\eta'\eta'$	< 47	< 10		< 47		< 10
182	$\eta'\eta$	< 27	< 4.6		< 27		< 4.6
183	$\eta'\rho^0$	< 12	< 4.3	< 14	< 12		< 4.3
184	$\eta\rho^0$	< 10	< 1.5	< 5.5	< 10		< 1.5
–	$\eta\pi^+\pi^-$	New		$16.6^{+3.5+1.4}_{-3.2-1.0}$			$16.6^{+3.8}_{-3.4}$
–	$a_0^\mp(980)\pi^\pm$ †	New	< 5.1	< 3.8			< 3.8
185	$\omega\eta$	< 12	< 2.3		< 12		< 2.3
186	$\omega\eta'$	< 60	< 2.8		< 60		< 2.8
187	$\omega\rho^0$	< 11	< 3.3		< 11		< 3.3
189	$\phi\pi^0$	< 5	< 1.0		< 5		< 1.0
190	$\phi\eta$	< 9	< 1.0		< 9		< 1.0
191	$\phi\eta'$	< 31	< 4.5		< 31		< 4.5
192	$\phi\rho^0$	< 13			< 13		< 13
194	$\phi\phi$	< 12	< 1.5		< 12		< 1.5
196	$\rho^0\pi^0$	< 5.3	< 2.9	$5.1 \pm 1.6 \pm 0.9$	< 5.5		< 2.9
197	$\rho^\mp\pi^\pm$	22.8 ± 2.5	$22.6 \pm 1.8 \pm 2.2$	$29.1^{+5.0}_{-4.9} \pm 4.0$	$27.6^{+8.4}_{-7.4} \pm 4.2$		24.0 ± 2.5
199	$\rho^0\rho^0$	< 2.1	< 1.1		< 18		< 1.1
200	$a_1^-\pi^+$	< 490	$42.6 \pm 4.2 \pm 4.1$				42.6 ± 5.9
203	$\rho^+\rho^-$	< 2200	$30 \pm 4 \pm 5$				30 ± 6
205	$\omega\pi^0$	< 3	< 1.2	< 1.9	< 5.5		< 1.2

†Product BF - daughter BF taken to be 100%

6.2 Radiative and leptonic decays

Table 43: Compilation of B^+ semileptonic and radiative branching fractions (in units of 10^{-6}). Upper limits are at 90% CL. values in red (blue) are new published (preliminary) result since PDG2004 [as of August 25th, 2004].

RPP#	Mode	PDG2004 Avg.	BaBar	Belle	CLEO	New Avg.
160	$K^*(892)^+\gamma$	38 ± 5	$38.7 \pm 2.8 \pm 2.6$	$42.5 \pm 3.1 \pm 2.4$	$37.6^{+8.9}_{-8.3} \pm 2.8$	40.3 ± 2.6
161	$K_1(1270)^+\gamma$	< 99		$42.8 \pm 9.4 \pm 4.3$		42.8 ± 10.3
162	$K^+\phi\gamma$	3.4 ± 1.0		$3.4 \pm 0.9 \pm 0.4$		3.4 ± 1.0
163	$K^+\pi^-\pi^+\gamma$ §	24^{+6}_{-5}		$25 \pm 1.8 \pm 2.2$		25.0 ± 2.8
164	$K^{*0}\pi^+\gamma$ §	20^{+7}_{-6}		$20^{+7}_{-6} \pm 2$		20^{+7}_{-6}
165	$K^+\rho^0\gamma$ §	< 20		< 20		< 20
166	$K^+\pi^-\pi^+\gamma$ (N.R.) §	< 9.2		< 9.2		< 9.2
167	$K_1(1400)^+\gamma$	< 50		< 14.4		< 14.4
168	$K_2^*(1430)^+\gamma$	< 1400	$14.5 \pm 4.0 \pm 1.5$			14.4 ± 4.2
172	$\rho^+\gamma$	< 2.1	< 1.8	< 2.2	< 13	< 1.8
207	$p\overline{\Lambda}\gamma$	New		$2.16^{+0.58}_{-0.53} \pm 0.20$		$2.16^{+0.61}_{-0.57}$
208	$p\overline{\Sigma^0}\gamma$	New		< 3.3		< 3.3
–	$\pi^+\nu\overline{\nu}$	New	< 100			< 100
226	$K^+e^+e^-$	$0.63^{+0.19}_{-0.17}$	$1.05^{+0.25}_{-0.22} \pm 0.07$	$0.63^{+0.19}_{-0.17} \pm 0.03$	< 2.4	0.80 ± 0.15
227	$K^+\mu^+\mu^-$	$0.45^{+0.14}_{-0.12}$	$0.07^{+0.19}_{-0.11} \pm 0.02$	$0.45^{+0.14}_{-0.12} \pm 0.03$	< 3.68	0.34 ± 0.10
229	$K^+\nu\overline{\nu}$	< 240	< 52		< 240	< 52
230	$K^*(892)^+e^+e^-$	< 4.6	$0.20^{+1.34}_{-0.87} \pm 0.28$ ‡	$2.02^{+1.27+0.23}_{-1.01-0.24}$ ‡		$1.29^{+0.90}_{-0.77}$
231	$K^*(892)^+\mu^+\mu^-$	< 2.2	$3.07^{+2.58}_{-1.78} \pm 0.42$ ‡	$0.65^{+0.69+0.14}_{-0.53-0.15}$ ‡		$0.92^{+0.70}_{-0.58}$
238	$\pi^-e^+e^+$	< 1.6			< 1.6	< 1.6
239	$\pi^-\mu^+\mu^+$	< 1.4			< 1.4	< 1.4
240	$\pi^-e^+\mu^+$	< 1.3			< 1.3	< 1.3
241	$\rho^-e^+e^+$	< 2.6			< 2.6	< 2.6
242	$\rho^-\mu^+\mu^+$	< 5.0			< 5.0	< 5.0
243	$\rho^-e^+\mu^+$	< 3.3			< 3.3	< 3.3
244	$K^-e^+e^+$	< 1.0			< 1.0	< 1.0
245	$K^-\mu^+\mu^+$	< 1.8			< 1.8	< 1.8
246	$K^-e^+\mu^+$	< 2.0			< 2.0	< 2.0
247	$K^{*-}e^+e^+$	< 2.8			< 2.8	< 2.8
248	$K^{*-}\mu^+\mu^+$	< 8.3			< 8.3	< 8.3
249	$K^{*-}e^+\mu^+$	< 4.4			< 4.4	< 4.4

§ $M_{K\pi\pi} < 2.4$ GeV/c^2 ‡ Central values are not significant.

Table 44: Compilation of B^0 semileptonic and radiative branching fractions (in units of 10^{-6}). Upper limits are at 90% CL. values in red (blue) are new published (preliminary) result since PDG2004 [as of August 25th, 2004].

RPP#	Mode	PDG2004 Avg.	BaBar	Belle	CLEO	New Avg.
162	$K^*(892)^0\gamma$	43 ± 4	$39.2 \pm 2.0 \pm 2.4$	$40.1 \pm 2.1 \pm 1.7$	$45.5^{+7.2}_{-6.8} \pm 3.4$	40.1 ± 2.0
163	$K^0\phi\gamma$	< 8.3		< 8.3		< 8.3
164	$K^+\pi^-\gamma$ †	4.6 ± 1.4		$4.6^{+1.3+0.5}_{-1.2-0.7}$		4.6 ± 1.4
–	$K^0\pi^+\pi^-\gamma$	New		$24.3 \pm 3.6 \pm 3.4$		24.3 ± 5.0
165	$K^*(1410)^0\gamma$	< 130		< 130		< 130
166	$K^+\pi^-\gamma$ (N.R.) †	< 2.6		< 2.6		< 2.6
169	$K_2^*(1430)^0\gamma$	13 ± 5	$12.2 \pm 2.5 \pm 1.0$	$13 \pm 5 \pm 1$		12.4 ± 2.4
173	$\rho^0\gamma$	< 1.2	< 0.4	< 0.8	< 17	< 0.4
174	$\omega\gamma$	< 1.0	< 1.0	< 0.8	< 9.2	< 0.8
175	$\phi\gamma$	< 3.3	< 0.94		< 3.3	< 0.94
237	$K^0e^+e^-$	< 0.54	$-0.21^{+0.23}_{-0.16} \pm 0.08$ ‡	$0.00^{+0.20+0.02}_{-0.12-0.05}$ ‡	< 8.45	$-0.06^{+0.14}_{-0.10}$
238	$K^0\mu^+\mu^-$	$5.6^{+2.9}_{-2.4}$	$1.63^{+0.82}_{-0.63} \pm 0.14$	$0.56^{+0.29}_{-0.23} \pm 0.05$	< 6.64	$0.73^{+0.28}_{-0.25}$
240	$K^*(892)^0e^+e^-$	< 2.4	$1.11^{+0.56}_{-0.47} \pm 0.11$	$1.29^{+0.57+0.13}_{-0.49-0.10}$		$1.20^{+0.41}_{-0.35}$
241	$K^*(892)^0\mu^+\mu^-$	1.3 ± 0.4	$0.86^{+0.79}_{-0.58} \pm 0.11$	$1.33^{+0.42}_{-0.37} \pm 0.11$		$1.22^{+0.39}_{-0.33}$

† $1.25\ \text{GeV}/c^2 < M_{K\pi} < 1.6\ \text{GeV}/c^2$ ‡ Central values are not significant.

Table 45: Compilation of B semileptonic and radiative branching fractions (in units of 10^{-6}). Upper limits are at 90% CL. values in red (blue) are new published (preliminary) result since PDG2004 [as of August 25th, 2004].

RPP#	Mode	PDG2004 Avg.	BaBar	Belle	CLEO	New Avg.
60	$K_3^*(1780)\gamma$	< 3000		< 34		< 34
67	$s\gamma$	330 ± 40	$388 \pm 36^{+57}_{-46}$	$355 \pm 32^{+30+11}_{-31-7}$	$321 \pm 43^{+32}_{-29}$	352^{+30}_{-28}
–	$s\gamma$ with baryons	New			< 38 †	< 38 †
71	$\rho\gamma$	< 1.9	< 1.2	< 1.4	< 14	< 1.2
–	$K\eta\gamma$	New		$6.9^{+1.7+1.3}_{-1.6-1.0}$		$6.9^{+2.1}_{-1.9}$
101	se^+e^- ‡	5.0 ± 2.6	$6.0 \pm 1.7 \pm 1.3$	$4.04 \pm 1.30^{+0.80}_{-0.76}$	< 57	$4.70^{+1.24}_{-1.23}$
102	$s\mu^+\mu^-$	$7.9^{+3.0}_{-2.6}$	$5.0 \pm 2.8 \pm 1.2$	$4.13 \pm 1.05^{+0.73}_{-0.69}$	< 58	$4.26^{+1.18}_{-1.16}$
103	$s\ell^+\ell^-$ ‡	$6.1^{+2.0}_{-1.8}$	$5.6 \pm 1.5 \pm 1.3$	$4.11 \pm 0.83^{+0.74}_{-0.70}$	< 42	$4.46^{+0.98}_{-0.96}$
104	Ke^+e^-	$0.48^{+0.15}_{-0.13}$	$0.74^{+0.18}_{-0.16} \pm 0.05$	$0.454^{+0.116+0.023}_{-0.104-0.025}$		$0.547^{+0.098}_{-0.095}$
105	$K^*(892)e^+e^-$	1.5 ± 0.5	$0.98^{+0.50}_{-0.42} \pm 0.11$	$1.84^{+0.48}_{-0.44} \pm 0.17$		$1.44^{+0.35}_{-0.34}$
106	$K\mu^+\mu^-$	0.48 ± 0.12	$0.45^{+0.23}_{-0.19} \pm 0.04$	$0.626^{+0.103+0.033}_{-0.064-0.034}$		$0.605^{+0.090}_{-0.064}$
107	$K^*(892)\mu^+\mu^-$	$1.17^{+0.37}_{-0.33}$	$1.27^{+0.76}_{-0.61} \pm 0.16$	$1.81^{+0.30}_{-0.28} \pm 0.11$		$1.73^{+0.30}_{-0.27}$
108	$K\ell^+\ell^-$	5.4 ± 0.8	$0.65^{+0.14}_{-0.13} \pm 0.04$	$0.550^{+0.075}_{-0.070} \pm 0.027$	< 1.7	$0.574^{+0.071}_{-0.066}$
109	$K^*(892)\ell^+\ell^-$	1.05 ± 0.20	$0.88^{+0.33}_{-0.29} \pm 0.10$	$1.65^{+0.23}_{-0.23} \pm 0.10$	< 3.3	1.38 ± 0.20
111	$\pi e^\pm\mu^\mp$	< 1.6			< 1.6	< 1.6
112	$\rho e^\pm\mu^\mp$	< 3.2			< 3.2	< 3.2
113	$Ke^\pm\mu^\mp$	< 1.6			< 1.6	< 1.6
114	$K^*e^\pm\mu^\mp$	< 6.2			< 6.2	< 6.2

† $E_\gamma > 2.0$ GeV; ‡$M(\ell^+\ell^-) > 0.2\ \text{GeV}/c^2$

Table 46: Compilation of B leptonic branching fractions (in units of 10^{-6}). Upper limits are at 90% CL. values in red (blue) are new published (preliminary) result since PDG2004 [as of August 25th, 2004].

RPP#	Mode	PDG2004 Avg.	BaBar	Belle	CLEO	CDF	D0	New Avg.
12	$e^+\nu$	< 15		< 5.4	< 15			< 5.4
13	$\mu^+\nu$	< 21	< 6.6	< 2.0	< 21			< 2.0
14	$\tau^+\nu$	< 570	< 330	< 290	< 840			< 290
15	$e^+\nu_e\gamma$	< 200		< 22	< 200			< 22
16	$\mu^+\nu_\mu\gamma$	< 52		< 23	< 52			< 23
235	e^+e^-	< 0.19	< 0.06	< 0.19	< 0.83			< 0.06
236	$\mu^+\mu^-$	< 0.16	< 0.08	< 0.16	< 0.61	< 0.15		< 0.08
244	$e^\pm\mu^\mp$	< 0.17	< 0.18	< 0.17	< 1.5			< 0.17
247	$e^\pm\tau^\mp$	< 530			< 110			< 110
248	$\mu^\pm\tau^\mp$	< 830			< 38			< 38
–	$\nu\overline{\nu}$	New	< 220					< 220
–	$\nu\overline{\nu}\gamma$	New	< 47					< 47

Table 47: Compilation of B_s leptonic branching fractions (in units of 10^{-6}). Upper limits are at 90% CL. values in red (blue) are new published (preliminary) result since PDG2004 [as of August 25th, 2004].

RPP#	Mode	PDG2004 Avg.	CDF	D0	New Avg.
–	$\mu^+\mu^-$	New	< 0.58	< 0.41	< 0.41

6.3 Baryonic decays

Table 48: Compilation of B^+ baryonic branching fractions (in units of 10^{-6}). Upper limits are at 90% CL. values in red (blue) are new published (preliminary) result since PDG2004 [as of August 25th, 2004].

RPP#	Mode	PDG2004 Avg.	BABAR	Belle	CLEO	New Avg.
201	$p\overline{p}\pi^+$	< 3.7		$3.06^{+0.73}_{-0.62} \pm 0.37$	< 160	$3.06^{+0.82}_{-0.72}$
204	$p\overline{p}K^+$	$4.3^{+1.2}_{-1.0}$	$6.7 \pm 0.9 \pm 0.6$	$5.66^{+0.67}_{-0.57} \pm 0.62$		$6.08^{+0.71}_{-0.68}$
–	$p\overline{p}K^{*+}$	New		$10.31^{+3.62+1.34}_{-2.77-1.65}$		$10.31^{+3.86}_{-3.22}$
206	$p\overline{\Lambda}$	< 1.5		< 0.46	< 1.5	< 0.46
–	$\Lambda\overline{\Lambda}K^+$	New		$2.91^{+0.90}_{-0.70} \pm 0.38$		$2.91^{+0.98}_{-0.80}$
–	$\Lambda\overline{\Lambda}\pi^+$	New		< 2.8		< 2.8
214	$\Lambda_c^- p\pi^+$	210 ± 70		$201 \pm 15 \pm 56$	$240 \pm 60^{+63}_{-62}$	213 ± 48
215	$\Lambda_c^- p\pi^+\pi^0$	1800 ± 600			$1810 \pm 290^{+520}_{-500}$	1810^{+595}_{-578}
216	$\Lambda_c^- p\pi^+\pi^+\pi^-$	2300 ± 700			$2250 \pm 250^{+630}_{-610}$	2250^{+677}_{-659}
218	$\overline{\Sigma}_c^0(2455)p$	< 80		$36.7^{+7.4}_{-6.6} \pm 10.2$	< 80	$36.7^{+12.6}_{-12.1}$
219	$\overline{\Sigma}_c^0(2520)p$	< 46		$12.6^{+5.6}_{-4.9} \pm 3.5$		$12.6^{+6.6}_{-6.0}$
–	$X_c^0(3340)\pi^+$	New		$38.7^{+7.7}_{-7.2} \pm 11.0$		$38.7^{+13.4}_{-13.1}$
220	$\overline{\Sigma}_c^0(2455)p\pi^0$	440 ± 180			$420 \pm 130 \pm 170$	420 ± 214
221	$\overline{\Sigma}_c^0(2455)p\pi^+\pi^-$	440 ± 170			$440 \pm 120 \pm 120$	440 ± 169
222	$\overline{\Sigma}_c^{--}(2455)p\pi^+\pi^+$	280 ± 120			$280 \pm 90 \pm 90$	280 ± 127
223	$\overline{\Lambda}_c^-(2593)p\pi^+$	< 190			< 190	< 190

Table 49: Compilation of B^0 baryonic branching fractions (in units of 10^{-6}). Upper limits are at 90% CL. values in red (blue) are new published (preliminary) result since PDG2004 [as of August 25th, 2004].

RPP#	Mode	PDG2004 Avg.	BABAR	Belle	CLEO	New Avg.
212	$p\overline{p}$	< 1.2	< 0.27	< 0.50	< 1.4	< 0.27
214	$p\overline{p}K^0$	< 7.2		$1.88^{+1.06}_{-0.60} \pm 0.23$		$1.88^{+1.08}_{-0.64}$
–	$p\overline{p}K^{*0}$	New		< 7.6		< 7.6
215	$p\overline{\Lambda}\pi^-$	$4.0^{+1.1}_{-1.0}$		$3.97^{+1.00}_{-0.80} \pm 0.56$	< 13	$3.97^{+1.15}_{-0.98}$
216	$p\overline{\Lambda}K^-$	< 0.82		< 0.82		< 0.82
217	$p\overline{\Sigma}^0\pi^-$	< 3.8		< 3.8		< 3.8
218	$\Lambda\overline{\Lambda}$	< 1.0		< 0.79	< 1.2	< 0.79
224	$\overline{\Lambda}_c^- p\pi^+\pi^-$	1300 ± 400		$1030 \pm 90 \pm 295$	$1670 \pm 190^{+470}_{-460}$	1207 ± 262
225	$\overline{\Lambda}_c^- p$	22 ± 8		$21.9^{+5.6}_{-4.9} \pm 6.5$	< 90	$21.9^{+8.6}_{-8.1}$
229	$\overline{\Sigma}_c^{--}(2520)p\pi^+$	160 ± 70		$104 \pm 23 \pm 30$		104 ± 37
230	$\overline{\Sigma}_c^0(2520)p\pi^+$	< 121		$33 \pm 19 \pm 10$		33 ± 21
231	$\overline{\Sigma}_c^0(2455)p\pi^-$	100 ± 80		$97 \pm 21 \pm 30$	$220 \pm 60 \pm 64$	115 ± 33
232	$\overline{\Sigma}_c^{--}(2455)p\pi^+$	280 ± 90		$115 \pm 22 \pm 33$	$370 \pm 80 \pm 113$	134 ± 38
233	$\overline{\Lambda}_c^-(2593)p$	< 110			< 110	< 110

6.4 Charge asymmetries

Table 50: Compilation of charmless hadronic CP asymmetries for charged B decays. Values in red (blue) are new published (preliminary) result since PDG2004 [as of August 25th, 2004].

RPP#	Mode	PDG2004 Avg.	BABAR	Belle	CLEO	CDF	New Avg.
117	$K^0\pi^+$	0.03 ± 0.08	$-0.087 \pm 0.046 \pm 0.010$	$0.05 \pm 0.05 \pm 0.01$	$0.18 \pm 0.24 \pm 0.02$		-0.020 ± 0.034
118	$K^+\pi^0$	-0.10 ± 0.08	$0.06 \pm 0.06 \pm 0.01$	$0.04 \pm 0.05 \pm 0.02$	$-0.29 \pm 0.23 \pm 0.02$		0.04 ± 0.04
119	$\eta' K^+$	0.009 ± 0.035	$0.037 \pm 0.045 \pm 0.011$	$-0.015 \pm 0.070 \pm 0.009$	$0.03 \pm 0.12 \pm 0.02$		0.022 ± 0.037
121	ηK^+	New	$-0.52 \pm 0.24 \pm 0.01$	$-0.49 \pm 0.31 \pm 0.07$			-0.51 ± 0.19
122	ηK^{*+}	New	$0.13 \pm 0.14 \pm 0.02$	$-0.09^{+0.16}_{-0.15} \pm 0.01$			$0.03^{+0.11}_{-0.10}$
123	ωK^+	$-0.21 \pm 0.28 \pm 0.03$	$-0.09 \pm 0.17 \pm 0.01$	$0.06^{+0.21}_{-0.18} \pm 0.01$			$-0.02^{+0.13}_{-0.12}$
127	$K^+\pi^+\pi^-$	$0.01 \pm 0.07 \pm 0.03$	$0.01 \pm 0.07 \pm 0.03$				0.01 ± 0.08
–	$K^{*0}\rho^+$	New	$-0.14 \pm 0.17 \pm 0.4$				-0.14 ± 0.43
138	$K^{*+}\rho^0$	$0.20^{+0.32}_{-0.29} \pm 0.04$	$0.20^{+0.32}_{-0.29} \pm 0.04$				$0.20^{+0.32}_{-0.29}$
144	$K^+K_SK_S$	New	$-0.04 \pm 0.11 \pm 0.02$				-0.04 ± 0.11
152	$K^+K^-K^+$	$0.02 \pm 0.07 \pm 0.03$	$0.02 \pm 0.07 \pm 0.03$				0.02 ± 0.08
153	ϕK^+	0.03 ± 0.07	$0.054 \pm 0.056 \pm 0.012$	$0.01 \pm 0.12 \pm 0.05$		$-0.07 \pm 0.17^{+0.06}_{-0.05}$	0.038 ± 0.050
156	ϕK^{*+}	0.09 ± 0.15	$0.16 \pm 0.17 \pm 0.03$	$-0.13 \pm 0.29^{+0.08}_{-0.11}$			0.09 ± 0.15
173	$\pi^+\pi^0$	0.05 ± 0.15	$-0.01 \pm 0.10 \pm 0.02$	$-0.02 \pm 0.10 \pm 0.01$			-0.02 ± 0.07
174	$\pi^+\pi^-\pi^+$	$-0.39 \pm 0.33 \pm 0.12$	$-0.39 \pm 0.33 \pm 0.12$				-0.39 ± 0.35
175	$\rho^0\pi^+$	New	$-0.19 \pm 0.11 \pm 0.02$				-0.19 ± 0.11
180	$\rho^+\pi^0$	New	$0.24 \pm 0.16 \pm 0.06$	$0.06 \pm 0.19^{+0.04}_{-0.06}$			0.16 ± 0.13
182	$\rho^+\rho^0$	-0.09 ± 0.16	$-0.19 \pm 0.23 \pm 0.03$	$0.00 \pm 0.22 \pm 0.03$			-0.09 ± 0.16
185	$\omega\pi^+$	-0.21 ± 0.19	$0.03 \pm 0.16 \pm 0.01$	$0.50^{+0.23}_{-0.20} \pm 0.02$	$-0.34 \pm 0.25 \pm 0.02$		0.10 ± 0.11
187	$\eta\pi^+$	New	$-0.44 \pm 0.18 \pm 0.01$	$0.07 \pm 0.15 \pm 0.03$			-0.14 ± 0.12
188	$\eta'\pi^+$	New	$0.24 \pm 0.19 \pm 0.01$				0.24 ± 0.19
190	$\eta\rho^+$	New	$0.07 \pm 0.19 \pm 0.02$	$-0.17^{+0.33}_{-0.29} \pm 0.02$			$0.01^{+0.17}_{-0.16}$

Table 51: Compilation of charmless hadronic CP asymmetries for $B^{\pm}/B^0$ admixtures. Values in red (blue) are new published (preliminary) result since PDG2004 [as of August 25th, 2004].

RPP#	Mode	PDG2004 Avg.	BABAR	Belle	CLEO	CDF	New Avg.
56	$K^*\gamma$	-0.01 ± 0.07	$-0.013 \pm 0.036 \pm 0.010$	$-0.015 \pm 0.044 \pm 0.012$	$0.08 \pm 0.13 \pm 0.03$		-0.010 ± 0.028
67	$s\gamma$	$-0.079 \pm 0.108 \pm 0.022$	$0.025 \pm 0.050 \pm 0.015$	$0.002 \pm 0.050 \pm 0.026$	$-0.079 \pm 0.108 \pm 0.022$		0.005 ± 0.036
103	$s\ell\ell$	New	$-0.22 \pm 0.26 \pm 0.02$				-0.22 ± 0.26

Table 52: Compilation of charmless hadronic CP asymmetries for neutral B decays. Values in red (blue) are new published (preliminary) result since PDG2004 [as of August 25th, 2004].

RPP#	Mode	PDG2004 Avg.	BABAR	Belle	CLEO	CDF	New Avg.
123	$K^+\pi^-$	-0.09 ± 0.04	$-0.133 \pm 0.030 \pm 0.009$	$-0.101 \pm 0.025 \pm 0.005$	$-0.04 \pm 0.16 \pm 0.02$	$-0.04 \pm 0.08 \pm 0.006$	-0.109 ± 0.019
124	$K^0\pi^0$ †						
127	ηK^{*0}	New	$0.02 \pm 0.11 \pm 0.02$	$-0.04^{+0.11}_{-0.10} \pm 0.01$			-0.01 ± 0.08
136	$K^+\rho^-$	0.28 ± 0.19	$0.13^{+0.14}_{-0.17} \pm 0.14$	$0.22^{+0.22+0.06}_{-0.23-0.02}$			$0.17^{+0.15}_{-0.16}$
–	$K_0^*(1430)^+\pi^-$	New	$-0.07 \pm 0.12 \pm 0.08$				-0.07 ± 0.14
–	$K_0^*(1430)^0\pi^0$	New	$-0.34 \pm 0.15 \pm 0.11$				-0.34 ± 0.19
140	$K^{*+}\pi^-$	0.26 ± 0.35	-0.04 ± 0.13		$0.26^{+0.33+0.10}_{-0.34-0.08}$		-0.00 ± 0.12
–	$K^+\pi^-\pi^0$	New		$0.07 \pm 0.11 \pm 0.01$			0.07 ± 0.11
141	$K^{*0}\pi^0$	New	$-0.01^{+0.24}_{-0.22} \pm 0.13$				$-0.01^{+0.27}_{-0.26}$
154	ϕK^{*0}	0.05 ± 0.10	$0.04 \pm 0.12 \pm 0.02$	$0.07 \pm 0.15^{+0.05}_{-0.03}$			0.05 ± 0.10
177	$\pi^0\pi^0$	New	$0.12 \pm 0.56 \pm 0.06$	$0.43 \pm 0.51^{+0.17}_{-0.16}$			0.28 ± 0.39
197	$\rho^+\pi^-$ †						

† Measurements of time-dependent CP asymmetries are listed on the Unitarity Triangle home page. (http://www.slac.stanford.edu/xorg/hfag/triangle/index.html)

Table 53: Brief summary of the world averages as of 2004 summer conferences.

b-hadron lifetimes	
$\tau(B^0)$	1.534 ± 0.013 ps
$\tau(B^+)$	1.653 ± 0.014 ps
$\tau(B_s^0)$	1.469 ± 0.059 ps
$\tau(B_c^+)$	0.45 ± 0.12 ps
$\tau(\Lambda_b^0)$	1.232 ± 0.072 ps
b-hadron fractions	
f^{+-}/f^{00} in $\Upsilon(4S)$ decays	1.026 ± 0.032
$f_d = f_u$ at high energy	0.398 ± 0.010
f_s at high energy	0.104 ± 0.015
$f_{\rm baryon}$ at high energy	0.100 ± 0.017
B^0 and B_s^0 mixing parameters	
Δm_d	0.502 ± 0.006 ps^{-1}
$\|q/p\|_d$	1.0013 ± 0.0034
Δm_s	> 14.5 ps^{-1} at 95% CL
Semileptonic B decay parameters	
$\mathcal{B}(\overline{B}^0 \to D^{*+}\ell^-\overline{\nu})$	$(5.33 \pm 0.20)\%$
$\mathcal{B}(\overline{B}^0 \to D^{+}\ell^-\overline{\nu})$	$(2.13 \pm 0.20)\%$
$\mathcal{B}(\overline{B} \to X\ell\overline{\nu})$	$(10.90 \pm 0.23)\%$
$\|V_{cb}\|$ $(\overline{B}^0 \to D^{*+}\ell^-\overline{\nu})$	$[41.4 \pm 1.0(\text{exp}) \pm 1.8(\text{theo})] \times 10^{-3}$
$\|V_{cb}\|$ $(\overline{B}^0 \to D^{+}\ell^-\overline{\nu})$	$[40.4 \pm 3.6(\text{exp}) \pm 2.3(\text{theo})] \times 10^{-3}$
$\|V_{ub}\|$ (inclusive)	$(4.70 \pm 0.44) \times 10^{-3}$
$CP(t)$ and Unitarity Triangle angles	
$\sin 2\beta(\phi_1)$ (all charmonium)	0.726 ± 0.037
$\sin 2\beta(\phi_1)_{\rm eff}$ (all $b \to s$ penguin)	0.41 ± 0.07
Rare B decays	
$A_{CP}(B^0 \to K^+\pi^-)$	-0.109 ± 0.019 $(5.7\,\sigma)$

7 Summary

This article provides the updated world averages for b-hadron properties as of 2004 summer conferences (ICHEP04 and FPCP04). A brief summary of the results described in Secs. 3-6 is given in Table 53.

The HFAG provided the first averages at 2003 winter conferences and have given updates at summer and winter conferences, as well as annual PDG averages.

The accuracies of b-hadron lifetimes and B^0 mixing parameters have been considerably improved with the asymmetric B factory results compared to the previous LEP working group averages [2]. In 2004 summer, the *BABAR* and Belle collaborations reported the simultaneous measurements of B lifetime and Δm_d with improved precision using increased data samples. Because of correlation between lifetime and Δm_d which complicates the average procedures, these new results are not included in current averages and there are no substantial changes from

previous averages at 2004 winter. It is planned to incorporate them in the next update. In the previous update, new results of b-hadron fractions from CDF are included and they remain the same in this update. The average of f^{+-}/f^{00} was newly added to HFAG average items from the previous update. With new results from *BABAR*, the accuracy has been improved to $\sim 3\%$ and the average value is consistent with 1. In this update, the average of $|q/p|_d$ is newly added.

For $|V_{cb}|$ and $|V_{ub}|$ average values, various new measurements have been available from CLEO, *BABAR*, and Belle. Accordingly, the statistical uncertainties of averages are significantly reduced from LEP working group averages [2]. Considerable progress has been also made in theoretical side, but the reduction of uncertainty is somewhat slower in some cases (*e.g.* $|V_{cb}|$ in exclusive modes). The determination of $|V_{cb}|$ from the inclusive semileptonic branching fraction in combination with hadronic mass and lepton energy moments is under discussion and foreseen in the future update. The average of $|V_{ub}|$ using inclusive $b \to u\ell\overline{\nu}$ is provided from the previous update. In this update, a substantial change has occurred with the usage of the Belle photon spectrum measurement in $b \to s\gamma$ decays. This is used for the determination of shape function parameters which enter the $|V_{ub}|$ calculation in inclusive charmless semileptonic B decays. The new shape function parameters result in substantially smaller error in $|V_{ub}|$ than previous one.

Measurements by *BABAR* and Belle of the time-dependent *CP* violation parameter $S_{b\to c\bar{c}s}$ in B decays to charmonium and a neutral kaon have established *CP* violation in B decays, and allow a precise extraction of the Unitarity Triangle parameter $\sin 2\beta/\sin 2\phi_1$. The B factories have also provided various measurements of time-dependent *CP* asymmetries in hadronic $b \to s$ penguin decays, establishing *CP* violation in these modes. Intriguingly, the measured parameters exhibit deviations from the Standard Model expectation. The significance of this effect depends on the treatment of the theoretical error. Results from time-dependent analyses with the decays $B^0 \to \pi^+\pi^-, \rho^\pm\pi^\mp$ and $\rho^+\rho^-$ allow, via various methods, constraints on the Unitarity Triangle angle α/ϕ_2. Constraints on the third Unitarity Triangle angle γ/ϕ_3 have been obtained by *BABAR* and Belle, using $B^- \to D^{(*)}K^-$ decays with Dalitz plot analysis of the subsequent $D \to K^0_S\pi^+\pi^-$ decay.

For the rare B decays, branching fractions and charge asymmetries of many new decay modes have been measured recently, mostly by *BABAR* and Belle. Since there are several hundred measurements in the tables in Sec. 6, we highlight only the measurement of $A_{CP}(B^0 \to K^+\pi^-)$, which provides the observation of direct *CP* violation ($5.7\,\sigma$) in in the B meson system.

Acknowledgements

We would like to thank collaborators of *BABAR*, Belle, CDF, CLEO, DØ, LEP, and SLD experiments who provided fruitful results on b-hadron properties and cooperated with the HFAG for averaging. These results are thanks to the excellent operations of the accelerators and collaborations with experimental groups by the accelerator groups of PEP-II, KEKB, CESR, Tevatron, LEP, and SLC. Some of the averages have been obtained based on the discussions between theorists for better understanding and improvement on the theoretical uncertainties.

References

[1] N. Cabibbo, Phys. Rev. Lett. 10, 531 (1963); M. Kobayashi and T. Maskawa, Prog. Theor. Phys. **49**, 652 (1973).

[2] ALEPH, CDF, DELPHI, L3, OPAL, and SLD collaborations, "Combined results on b-hadron production rates and decay properties", CERN-EP-2000-096, hep-ex/0009052 (2000); updated in CERN-EP-2001-050, hep-ex/0112028 (2001).

[3] S. Eidelman *et al.* (Particle Data Group Collaboration), Phys. Lett. B **592**, 1 (2004).

[4] J.P. Alexander *et al.* (CLEO Collaboration), Phys. Rev. Lett. **86**, 2737 (2001).

[5] B. Aubert *et al.* (*BABAR* Collaboration), Phys. Rev. D **65**, 032001 (2002).

[6] S.B. Athar *et al.* (CLEO Collaboration), Phys. Rev. D **66**, 052003 (2002).

[7] N.C. Hastings *et al.* (Belle Collaboration), Phys. Rev. D **67**, 052004 (2003).

[8] B. Aubert *et al.* (*BABAR* Collaboration), Phys. Rev. D **69**, 071101 (2004).

[9] B. Aubert *et al.* (*BABAR* Collaboration), BABAR-CONF-04/21, SLAC-PUB-10618, hep-ex/0408022, submitted to ICHEP04, August 2004.

[10] B. Barish *et al.* (CLEO Collaboration), Phys. Rev. Lett. **76**, 1570 (1996).

[11] P. Abreu *et al.* (DELPHI Collaboration), Phys. Lett. B **289**, 199 (1992);
P.D. Acton *et al.* (OPAL Collaboration), Phys. Lett. B **295**, 357 (1992);
D. Buskulic *et al.* (ALEPH Collaboration), Phys. Lett. B **361**, 221 (1995).

[12] P. Abreu *et al.* (DELPHI Collaboration), Z. Phys. C **68**, 375 (1995).

[13] R. Barate *et al.* (ALEPH Collaboration), Eur. Phys. J. C **2**, 197 (1998).

[14] P. Abreu *et al.* (DELPHI Collaboration), Z. Phys. C **68**, 541 (1995).

[15] D. Buskulic *et al.* (ALEPH Collaboration), Phys. Lett. B **384**, 449 (1996).

[16] R. Barate *et al.* (ALEPH Collaboration), Eur. Phys. J. C **5**, 205 (1998).

[17] J. Abdallah *et al.* (DELPHI Collaboration), Phys. Lett. B **576**, 29 (2003).

[18] T. Affolder *et al.* (CDF Collaboration), Phys. Rev. Lett. **84**, 1663 (2000).

[19] F. Abe *et al.* (CDF Collaboration), Phys. Rev. D **60**, 092005 (1999).

[20] This value was obtained by the LEP Electroweak Working Group for the 2004 edition of the Review of Particle Physics. It is one of the 18 parameters determined from the so-called "Heavy Flavour fit" performed on all LEP and SLD data. Details on the combination procedures can be found in: LEP collaborations ALEPH, CDF, DELPHI, L3, OPAL, LEP Electroweak Working Group, SLD Electroweak and Heavy Flavour Working Groups, "A combination of preliminary electroweak measurements and constraints on the Standard Model", CERN-EP/2003-091, hep-ex/0312023, December 2003.

[21] D. Acosta *et al.* (CDF Collaboration), Phys. Rev. D **69**, 012002 (2004).

[22] M.A. Shifman and M.B. Voloshin, Sov. Phys. JETP **64**, 698 (1986);
J. Chay, H. Georgi and B. Grinstein, Phys. Lett. B **247**, 399 (1990);
I.I. Bigi, N.G. Uraltsev and A.I. Vainshtein, Phys. Lett. B **293**, 430 (1992), erratum ibid. B **297**, 477 (1993).

[23] I. Bigi, UND-HEP-95-BIG02 (1995);
G. Bellini, I. Bigi, and P. Dornan, Phys. Reports **289**, 1 (1997).

[24] F. Gabbiani, A. Onischenko and A. Petrov, Phys. Rev. D **70**, 094031 (2004).

[25] M. Ciuchini, E. Franco, V. Lubicz, and F. Mescia, Nucl. Phys. B **625**, 211 (2002);
E. Franco, V. Lubicz, F. Mescia, and C. Tarantino, Nucl. Phys. B **633**, 212 (2002).

[26] C. Tarantino, Eur. Phys. J. C **33**, s895 (2004), hep-ph/0310241;
F. Gabbiani, A. Onishchenko, and A. Petrov, Phys. Rev. D **68**, 114006 (2003).

[27] L. Di Ciaccio *et al.*, internal note by former B lifetime working group (1996),
`http://lepbosc.web.cern.ch/LEPBOSC/lifetimes/ps/final_blife.ps`

[28] D. Buskulic *et al.* (ALEPH Collaboration), Phys. Lett. B **314**, 459 (1993).

[29] P. Abreu *et al.* (DELPHI Collaboration), Z. Phys. C **63**, 3 (1994).

[30] P. Abreu *et al.* (DELPHI Collaboration), Phys. Lett. B **377**, 195 (1996).

[31] P. Abreu *et al.* (DELPHI Collaboration), Eur. Phys. J. C **33**, 307 (2004).

[32] M. Acciarri *et al.* (L3 Collaboration), Phys. Lett. B **416**, 220 (1998).

[33] K. Ackerstaff *et al.* (OPAL Collaboration), Z. Phys. C **73**, 397 (1997).

[34] K. Abe *et al.* (SLD Collaboration), Phys. Rev. Lett. **75**, 3624 (1995).

[35] D. Buskulic *et al.* (ALEPH Collaboration), Phys. Lett. B **369**, 151 (1996).

[36] P.D. Acton *et al.* (OPAL Collaboration), Z. Phys. C **60**, 217 (1993).

[37] F. Abe *et al.* (CDF Collaboration), Phys. Rev. D **57**, 5382 (1998).

[38] CDF Collaboration, contrib. to Int. Europhysics Conf. on High-Energy Physics (EPS 2003), Aachen, Germany (2003).

[39] R. Barate *et al.* (ALEPH Collaboration), Phys. Lett. B **492**, 275 (2000).

[40] D. Buskulic *et al.* (ALEPH Collaboration), Z. Phys. C **71**, 31 (1996).

[41] F. Abe *et al.* (CDF Collaboration), Phys. Rev. D **58**, 092002 (1998).

[42] D. Acosta *et al.* (CDF Collaboration), Phys. Rev. D **65**, 092009 (2003).

[43] P. Abreu *et al.* (DELPHI Collaboration), Z. Phys. C **68**, 13 (1995).

[44] W. Adam *et al.* (DELPHI Collaboration), Z. Phys. C **68**, 363 (1995).

[45] P. Abreu *et al.* (DELPHI Collaboration), Z. Phys. C **74**, 19 (1997).

[46] M. Acciari *et al.* (L3 Collaboration), Phys. Lett. B **438**, 417 (1998).

[47] R. Akers *et al.* (OPAL Collaboration), Z. Phys. C **67**, 379 (1995).

[48] G. Abbiendi *et al.* (OPAL Collaboration), Eur. Phys. J. C **12**, 609 (2000).

[49] G. Abbiendi *et al.* (OPAL Collaboration), Phys. Lett. B **493**, 266 (2000).

[50] K. Abe *et al.* (SLD Collaboration), Phys. Rev. Lett. **79**, 590 (1997).

[51] B. Aubert *et al.* (*BABAR* Collaboration), Phys. Rev. Lett. **87**, 201803 (2001).

[52] B. Aubert *et al.* (*BABAR* Collaboration), Phys. Rev. Lett. **89**, 061801 (2002).

[53] B. Aubert *et al.* (*BABAR* Collaboration), Phys. Rev. D **67**, 072002 (2003).

[54] B. Aubert *et al.* (*BABAR* Collaboration), Phys. Rev. D **67**, 091101 (2003).

[55] K. Abe *et al.* (Belle Collaboration), Phys. Rev. Lett. **88**, 171801 (2002).

[56] CDF Collaboration, CDF note 7409,
`http://www-cdf.fnal.gov/physics/new/bottom/040428.blessed-lft/`

[57] B. Aubert *et al.* (*BABAR* Collaboration), BABAR-CONF-04/15, hep-ex/0408039, submitted to ICHEP04.

[58] K. Abe *et al.* (Belle Collaboration), hep-ex/0408111, submitted to Phys. Rev. D.

[59] V.M. Abazov *et al.* (DØ Collaboration), hep-ex/0410052, submitted to Phys. Rev. Lett.

[60] D. Buskulic *et al.* (ALEPH Collaboration), Phys. Lett. B **377**, 205 (1996).

[61] F. Abe *et al.* (CDF Collaboration), Phys. Rev. D **59**, 032004 (1999).

[62] P. Abreu *et al.* (DELPHI Collaboration), Eur. Phys. J. C **16**, 555 (2000).

[63] K. Ackerstaff *et al.* (OPAL Collaboration), Phys. Lett. B **426**, 161 (1998).

[64] D. Buskulic *et al.* (ALEPH Collaboration), Eur. Phys. J. C **4**, 367 (1998).

[65] P. Abreu *et al.* (DELPHI Collaboration), Eur. Phys. J. C **18**, 229 (2000).

[66] P. Abreu *et al.* (DELPHI Collaboration), Z. Phys. C **71**, 11 (1996).

[67] K. Ackerstaff *et al.* (OPAL Collaboration), Eur. Phys. J. C **2**, 407 (1998).

[68] V.M. Abazov *et al.* (DØ Collaboration), hep-ex/0409043, submitted to Phys. Rev. Lett.

[69] Y. Keum and U. Nierste, Phys. Rev. D **57**, 4282 (1998);
M. Beneke, G. Buchalla, and I. Dunietz, Phys. Rev. D **54**, 4419 (1996);
M. Beneke *et al.*, Phys. Lett. B **459**, 631 (1999).

[70] F. Abe *et al.* (CDF Collaboration), Phys. Rev. Lett. **81**, 2432 (1998).

[71] V.M. Abazov *et al.* (DØ Collaboration), DØ Note 4539, contribution 11-0559 to ICHEP04, August 2004.

[72] A preliminary result of 5620 ± 1.6 (stat) ± 1.2 (sys) MeV/c^2 exists from CDF, CDF Note 6557, 15 July 2003, consistent with the world average. The PDG value is used for scaling, and its precision is not the dominant common systematic uncertainty.

[73] D. Buskulic *et al.* (ALEPH Collaboration), Phys. Lett. B **365**, 437 (1996).

[74] F. Abe *et al.* (CDF Collaboration), Phys. Rev. Lett. **77**, 1439 (1996).

[75] M. Paulini *et al.* (CDF Collaboration), FERMILAB-CONF-04/013-E, proc. Advanced Studies Institute "Physics at LHC" (LHC-Praha-2003), Prague, Czech Republic, July 2003; see also
`http://www-cdf.fnal.gov/physics/new/bottom/030710.blessed-lambdab-lifetime/`

[76] V.M. Abazov *et al.* (DØ Collaboration), hep-ex/0410054, submitted to Phys. Rev. Lett.

[77] P. Abreu *et al.* (DELPHI Collaboration), Eur. Phys. J. C **10**, 185 (1999).

[78] P. Abreu *et al.* (DELPHI Collaboration), Z. Phys. C **71**, 199 (1996).

[79] R. Akers *et al.* (OPAL Collaboration), Z. Phys. C **69**, 195 (1996).

[80] M.B. Voloshin, Phys. Rep. **320**, 275 (1999);
B. Guberina, B. Melic, and H. Stefancic, Phys. Lett. B **469**, 253 (1999);
M. Neubert, and C.T. Sachrajda, Nucl. Phys. B **483**, 339 (1997).

[81] J. Bartelt *et al.* (CLEO Collaboration), Phys. Rev. Lett. **71**, 1680 (1993).

[82] B.H. Behrens *et al.* (CLEO Collaboration), Phys. Lett. B **490**, 36 (2000).

[83] D.E. Jaffe *et al.* (CLEO Collaboration), Phys. Rev. Lett. **86**, 5000 (2001).

[84] F. Abe *et al.* (CDF Collaboration), Phys. Rev. D **55**, 2546 (1997).

[85] K. Ackerstaff *et al.* (OPAL Collaboration), Z. Phys. C **76**, 401 (1997).

[86] R. Barate *et al.* (ALEPH Collaboration), Eur. Phys. J. C **20**, 431 (2001).

[87] B. Aubert *et al.* (*BABAR* Collaboration), Phys. Rev. Lett. **92**, 181801 (2004).

[88] B. Aubert *et al.* (*BABAR* Collaboration), Phys. Rev. Lett. **88**, 231801 (2002).

[89] K. Abe *et al.* (Belle Collaboration), BELLE-CONF-0451, hep-ex/0409012, submitted to ICHEP04, August 2004.

[90] G. Abbiendi *et al.* (OPAL Collaboration), Eur. Phys. J. C **12**, 609 (2000).

[91] M. Beneke, G. Buchalla and I. Dunietz, Phys. Lett. B **393**, 132 (1997);
I. Dunietz, Eur. Phys. J. C **7**, 197 (1999).

[92] D. Buskulic *et al.* (ALEPH Collaboration), Z. Phys. C **75**, 397 (1997).

[93] P. Abreu *et al.* (DELPHI Collaboration), Z. Phys. C **76**, 579 (1997).

[94] J. Abdallah *et al.* (DELPHI Collaboration), Eur. Phys. J. C **28**, 155 (2003).

[95] M. Acciarri *et al.* (L3 Collaboration), Eur. Phys. J. C **5**, 195 (1998).

[96] G. Alexander *et al.* (OPAL Collaboration), Z. Phys. C **72**, 377 (1996).

[97] K. Ackerstaff *et al.* (OPAL Collaboration), Z. Phys. C **76**, 401 (1997).

[98] K. Ackerstaff *et al.* (OPAL Collaboration), Z. Phys. C **76**, 417 (1997).

[99] G. Abbiendi *et al.* (OPAL Collaboration), Phys. Lett. B **493**, 266 (2000).

[100] F. Abe *et al.* (CDF Collaboration), Phys. Rev. Lett. **80**, 2057 (1998) and Phys. Rev. D **59**, 032001 (1999).

[101] F. Abe *et al.* (CDF Collaboration), Phys. Rev. D **60**, 051101 (1999).

[102] F. Abe *et al.* (CDF Collaboration), Phys. Rev. D **60**, 072003 (1999).

[103] T. Affolder *et al.* (CDF Collaboration), Phys. Rev. D **60**, 112004 (1999).

[104] CDF Collaboration, CDF note 7176, August 6, 2004, submitted to ICHEP04 conference.

[105] CDF Collaboration, CDF note 7187, August 12, 2004, submitted to ICHEP04 conference.

[106] DØ Collaboration, DØ Note 4578-CONF, August 30, 2004, submitted to DPF 2004 conference.

[107] B. Aubert *et al.* (*BABAR* Collaboration), Phys. Rev. Lett. **88**, 221802 (2002) and Phys. Rev. D **66**, 032003 (2002).

[108] B. Aubert *et al.* (*BABAR* Collaboration), Phys. Rev. Lett. **88**, 221803 (2002).

[109] T. Tomura *et al.* (Belle Collaboration), Phys. Lett. B **542**, 207 (2002).

[110] K. Hara *et al.* (Belle Collaboration), Phys. Rev. Lett. **89**, 251803 (2002).

[111] Y. Zheng *et al.* (Belle Collaboration), Phys. Rev. D **67**, 092004 (2003).

[112] H. Albrecht *et al.* (ARGUS Collaboration), Z. Phys. C **55**, 357 (1992); Phys. Lett. B **324**, 249 (1994).

[113] H.-G. Moser and A. Roussarie, Nucl. Instrum. Methods A **384**, 491 (1997).

[114] A. Heister *et al.* (ALEPH Collaboration), Eur. Phys. J. C **29**, 143 (2003).

[115] F. Abe *et al.* (CDF Collaboration), Phys. Rev. Lett. **82**, 3576 (1999).

[116] P. Abreu *et al.* (DELPHI Collaboration), Eur. Phys. J. C **16**, 555 (2000).

[117] J. Abdallah *et al.* (DELPHI Collaboration), Eur. Phys. J. C **35**, 35 (2004).

[118] G. Abbiendi *et al.* (OPAL Collaboration), Eur. Phys. J. C **11**, 587 (1999).

[119] G. Abbiendi *et al.* (OPAL Collaboration), Eur. Phys. J. C **19**, 241 (2001).

[120] K. Abe *et al.* (SLD Collaboration), Phys. Rev. D **67**, 012006 (2003).

[121] K. Abe *et al.* (SLD Collaboration), Phys. Rev. D **66**, 032009 (2002).

[122] SLD Collaboration, SLAC-PUB-8568, contrib. to 30th Int. Conf. on High-Energy Physics, Osaka, Japna (2000).

[123] K. Hartkorn and H.-G. Moser, Eur. Phys. J. C **8**, 381 (1999).

[124] R. Barate *et al.* (ALEPH Collaboration), Phys. Lett. B **486**, 286 (2000).

[125] R. Aleksan, Phys. Lett. B **316**, 567 (1993).

[126] See for example M. Beneke, G. Buchalla, and I. Dunietz, Phys. Rev. D **54**, 4419 (1996).

[127] CDF Collaboration, CDF note 7715,
`http://www-cdf.fnal.gov/physics/new/bottom/040708.blessed-dgog-bsjpsiphi/`

[128] M. Artuso and E. Barberio, on page 786-793 of S. Eidelman *et al.* (Particle Data Group Collaboration), Phys. Lett. B **592**, 1 (2004).

[129] M. Battaglia and L. Gibbons, on page 793-802 of S. Eidelman *et al.* (Particle Data Group Collaboration), Phys. Lett. B **592**, 1 (2004).

[130] J. E. Duboscq *et al.* (CLEO Collaboration), Phys. Rev. Lett. **76**, 3898 (1996).

[131] D. Buskulic *et al.* (ALEPH Collaboration), Phys. Lett. B **395**, 373 (1997).

[132] G. Abbiendi *et al.* (OPAL Collaboration), Phys. Lett. B **482**, 15 (2000).

[133] P. Abreu *et al.* (DELPHI Collaboration), Phys. Lett. B **510**, 55 (2001).

[134] K. Abe *et al.* (Belle Collaboration), Phys. Lett. B **526**, 247 (2002).

[135] N. E. Adam *et al.* (CLEO collaboration), Phys. Rev. D **67**, 032001 (2003).

[136] J. Abdallah *et al.* (DELPHI Collaboration), Eur. Phys. J. C **33**, 213 (2004).

[137] B. Aubert *et al.* (*BABAR* Collaboration), hep-ex/0408027.

[138] M. Battaglia *et al.*, proceedings of the 1st workshop on CKM Unitarity Triangle, Feb. 2002, hep-ph/0304132.

[139] J. Bartelt *et al.* (CLEO Collaboration), Phys. Rev. Lett. **82**, 3746 (1999).

[140] K. Abe *et al.* (Belle Collaboration), Phys. Lett. B **526**, 258 (2002).

[141] For recent introductions, see, *e.g.*, Z. Ligeti, eConf **C020805**, L02 (2002) hep-ph/0302031; G. Buchalla, hep-ph/0202092; N. Uraltsev, hep-ph/9804275.

[142] LEP Electroweak working group, hep-ex/0412015.

[143] H. Albrecht *et al.* (ARGUS Collaboration), Phys. Lett. B **318**, 397 (1993).

[144] U. Langenegger (*BABAR* Collaboration), in proceedings of EPS 2001, hep-ex/0204001.

[145] K. Abe *et al.* (Belle Collaboration), Phys. Lett. B **547**, 181 (2002).

[146] B. Aubert *et al.* (*BABAR* Collaboration), Phys. Rev. D **67**, 031101 (2003).

[147] Talk given by A. Sugiyama at Moriond EW, March 2003, France.

[148] A. H. Mahmood *et al.* (CLEO Collaboration), Phys. Rev. D **70**, 032003 (2004).

[149] C. J. Stepaniak, Ph.D. thesis, University of Minnesota, 2004.

[150] M. Battaglia *et al.*, Phys. Lett. B **556**, 41 (2003).

[151] B. Aubert *et al.* (*BABAR* Collaboration), Phys. Rev. Lett. **93**, 011803 (2004).

[152] C. W. Bauer, Z. Ligeti, M. Luke, A. V. Manohar and M. Trott, hep-ph/0408002.

[153] B. H. Behrens *et al.* (CLEO Collaboration), Phys. Rev. D **61**, 052001 (2000).

[154] B. Aubert *et al.* (*BABAR* Collaboration), Phys. Rev. Lett. **90**, 181801 (2003).

[155] C. Schwanda *et al.* (Belle Collaboration), Phys. Rev. Lett. **93**, 131803 (2004).

[156] S. B. Athar *et al.* (CLEO Collaboration), Phys. Rev. D **68**, 072003 (2003).

[157] K. Abe *et al.* (Belle Collaboration), hep-ex/0408145.

[158] D. del Re (*BABAR* Collaboration), talk presented at ICHEP 2004, Beijing.

[159] M. Luke, Nucl. Phys. Proc. Suppl. **115**, 272 (2003).

[160] Z. Ligeti, eConf **C030603**, JEU10 (2003).

[161] M. Acciarri *et al.* (L3 Collaboration), Phys. Lett. B **436**, 174 (1998); R. Barate *et al.* (ALEPH Collaboration), Eur. Phys. J. C **6**, 555 (1999); P. Abreu *et al.* (DELPHI Collaboration), Phys. Lett. B **478**, 14 (2000); G. Abbiendi *et al.* (OPAL Collaboration), Eur. Phys. J. C **21**, 399 (2001).

[162] A. H. Hoang, Z. Ligeti and A. V. Manohar, Phys. Rev. D **59**, 074017 (1999).

[163] N. Uraltsev, Int. J. Mod. Phys. A **14**, 4641 (1999).

[164] A. Limosani and T. Nozaki (of the Belle Collaboration for the Heavy Flavor Averaging Group), hep-ex/0407052.

[165] `http://www.slac.stanford.edu/xorg/hfag/semi/summer04/summer04.xls`

[166] F. De Fazio and M. Neubert, JHEP **9906**, 017 (1999).

[167] S. Chen *et al.* (CLEO Collaboration), Phys. Rev. Lett. **87**, 251807 (2001).

[168] L. Gibbons (CLEO Collaboration), in proceedings of Beauty 2002, hep-ex/0402009.

[169] S. W. Bosch, B. O. Lange, M. Neubert and G. Paz, hep-ph/0402094.

[170] M. Neubert, Phys. Lett. B **543**, 269 (2002).

[171] C. N. Burrell, M. E. Luke and A. R. Williamson, Phys. Rev. D **69**, 074015 (2004).

[172] C. W. Bauer, Z. Ligeti and M. E. Luke, Phys. Rev. D **64**, 113004 (2001).

[173] A. Bornheim *et al.* (CLEO Collaboration), Phys. Rev. Lett. **88**, 231803 (2002).

[174] H. Kakuno *et al.* (Belle Collaboration), Phys. Rev. Lett. **92**, 101801 (2004).

[175] K. Abe *et al.* Belle Collaboration, BELLE-CONF-0325.

[176] B. Aubert *et al.* (*BABAR* Collaboration), hep-ex/0408075.

[177] B. Aubert *et al.* (*BABAR* Collaboration), hep-ex/0408068.

[178] B. Aubert *et al.* (*BABAR* Collaboration), hep-ex/0408045.

[179] K. Abe *et al.* (Belle Collaboration), hep-ex/0408115.

[180] C. W. Bauer and A. V. Manohar, Phys. Rev. D **70**, 034024 (2004).

[181] L.L. Chau and W.Y. Keung, Phys. Rev. Lett. **53**, 1802 (1984).

[182] L. Wolfenstein, Phys. Rev. Lett. **51**, 1945 (1983).

[183] A.J. Buras, M.E. Lautenbacher and G. Ostermaier, Phys. Rev. D **50**, 3433 (1994).

[184] D. Atwood, M. Gronau and A. Soni, Phys. Rev. Lett **79**, 185 (1997).

[185] D. Atwood, T. Gershon, M. Hazumi and A. Soni, hep-ph/0410036 (submitted to Phys. Rev. D).

[186] M. Gronau and D. London, Phys. Lett. B **253**, 483 (1991), M. Gronau and D. Wyler, Phys. Lett. B **265**, 172 (1991).

[187] D. Atwood, I. Dunietz, and A. Soni, Phys. Rev. Lett. **78**, 3257 (1997), Phys. Rev. D **63**, 036005 (2001).

[188] A. Giri, Y. Grossman, A. Soffer and J. Zupan, Phys. Rev. D **68**, 054018 (2003); A. Poluektov *et al.* (Belle Collaboration), Phys. Rev. D **70**, 072003 (2004).

[189] A. Bondar and T. Gershon, Phys. Rev. D **70**, 091503(R) (2004).

[190] B. Aubert *et al.* (*BABAR* Collaboration), BABAR-PUB-04/030, hep-ex/0411016, submitted to Phys. Rev. D

[191] K. Abe *et al.* (Belle Collaboration), BELLE-CONF-0438, hep-ex/0408104.

[192] B. Aubert *et al.* (*BABAR* Collaboration), BABAR-CONF-04/38, hep-ex/0408127, submitted to Phys. Rev. Lett.

[193] R. Barate *et al.* (ALEPH Collaboration), Phys. Lett. B **492**, 259 (2000).

[194] K. Ackerstaff *et al.* (OPAL Collaboration), Eur. Phys. J C **5**, 379 (1998).

[195] T. Affolder *et al.* (CDF Collaboration), Phys. Rev. D **61**, 072005 (2000).

[196] `http://www.slac.stanford.edu/xorg/ckmfitter/`

[197] `http://utfit.roma1.infn.it/`

[198] D. Aston *et al.* (LASS Collaboration), Nucl. Phys. B **296**, 493 (1988).

[199] M. Suzuki, Phys. Rev. D **64**, 117503 (2001).

[200] K. Abe *et al.* (Belle Collaboration), Phys. Rev. Lett. **91**, 261602 (2003).

[201] B. Aubert *et al.* (*BABAR* Collaboration), BABAR-CONF-04/033, hep-ex/0408072.

[202] K. Abe *et al.* (Belle Collaboration), BELLE-CONF-0435, hep-ex/0409049.

[203] B. Aubert *et al.* (*BABAR* Collaboration), BABAR-CONF-04/040, hep-ex/0408090.

[204] B. Aubert *et al.* (*BABAR* Collaboration), BABAR-CONF-04/019, hep-ex/0408095.

[205] B. Aubert *et al.* (*BABAR* Collaboration), BABAR-CONF-04/030, hep-ex/0408062.

[206] B. Aubert *et al.* (*BABAR* Collaboration), BABAR-CONF-04/025, hep-ex/0408076.

[207] K. Abe *et al.* (Belle Collaboration), BELLE-CONF-0475, hep-ex/0411056.

[208] B. Aubert *et al.* (*BABAR* Collaboration), Phys. Rev. Lett. **91**, 061802 (2003).

[209] S.U. Kataoka *et al.* (Belle Collaboration), Belle-Preprint-2004-23, hep-ex/0408105, to appear in Phys. Rev. Lett.

[210] B. Aubert *et al.* (*BABAR* Collaboration), Phys. Rev. Lett. **91**, 131801 (2003).

[211] K. Abe *et al.* (Belle Collaboration), BELLE-CONF-0453.

[212] B. Aubert *et al.* (*BABAR* Collaboration), Phys. Rev. Lett. **90**, 221801 (2003).

[213] T. Aushev, Y. Iwasaki *et al.* (Belle Collaboration), Phys. Rev. Lett. **93**, 201802 (2004).

[214] B. Aubert *et al.* (*BABAR* Collaboration), Phys. Rev. Lett. **93**, 201801 (2004).

[215] K. Abe *et al.* (Belle Collaboration), BELLE-CONF-0475, hep-ex/0411056.

[216] CKMfitter Group (J. Charles *et al.*), LAL-04-21, hep-ph/0406184.

[217] A.E. Snyder and H.R. Quinn, Phys. Rev. D **48**, 2139 (1993).

[218] B. Aubert *et al.* (*BABAR* Collaboration), BABAR-CONF-04/047, hep-ex/0408089.

[219] K. Abe *et al.* (Belle Collaboration), Phys. Rev. Lett. **93**, 021601 (2004).

[220] L. Roos, BABAR-PROC-04-012, hep-ex/0407051.
See also talk given by C. Dallapiccola at ICHEP'04, Aug. 2004, Beijing, China.
`http://www.slac.stanford.edu/BFROOT/www/Public/ichep2004/7733_ICHEP04-rhorho.pdf`

[221] B. Aubert *et al.* (*BABAR* Collaboration), Phys. Rev. Lett. **91**, 201802 (2003).

[222] B. Aubert *et al.* (*BABAR* Collaboration), BABAR-CONF-04/038, hep-ex/0408099.

[223] C.C. Wang *et al.* (Belle Collaboration), Belle-Preprint 2004-21, hep-ex/0408003, submitted to Phys. Rev. Lett.

[224] M. Gronau and J.L. Rosner, Phys. Rev. D **65**, 093012 (2002).

[225] B. Aubert *et al.* (*BABAR* Collaboration), BABAR-CONF-04/037, hep-ex/0408061.

[226] B. Aubert *et al.* (*BABAR* Collaboration), Phys. Rev. Lett. **91**, 171802 (2003).

[227] J. Zhang *et. al.* (Belle Collaboration), Phys. Rev. Lett. **91**, 221801 (2003).

[228] M. Gronau and D. London, Phys. Rev. Lett. **65**, 3381 (1990).

[229] B. Aubert *et al.* (*BABAR* Collaboration), BABAR-CONF-04/029, hep-ex/0408059.

[230] T. Sarangi *et al.* (Belle Collaboration), Phys. Rev. Lett. **93**, 031802 (2004); Erratum-ibid. **93**, 059901 (2004).

[231] B. Aubert *et al.* (*BABAR* Collaboration), BABAR-CONF-04/018, hep-ex/0408038.

[232] K. Abe *et al.* (Belle Collaboration), BELLE-CONF-0448, hep-ex/0408106.

[233] O. Long, M. Baak, R.N. Cahn, D. Kirkby, Phys.Rev. D **68**, 034010 (2003).

[234] R. Fleischer, Nucl. Phys. B **671**, 459 (2003).

[235] B. Aubert *et al.* (*BABAR* Collaboration), BABAR-CONF-04/039, hep-ex/0408082.

[236] K. Abe *et al.* (Belle Collaboration), BELLE-CONF-0443.

[237] B. Aubert *et al.* (*BABAR* Collaboration), BABAR-CONF-04/049, hep-ex/0408060.

[238] B. Aubert *et al.* (*BABAR* Collaboration), BABAR-CONF-04/012, hep-ex/0408069.

[239] K. Abe *et al.* (Belle Collaboration), BELLE-CONF-0316, hep-ex/0307074.

[240] B. Aubert *et al.* (*BABAR* Collaboration), BABAR-CONF-04/13, hep-ex/0408028.

[241] K. Abe *et al.* (Belle Collaboration), BELLE-CONF-0444, hep-ex/0408129.

[242] B. Aubert *et al.* (*BABAR* Collaboration), BABAR-CONF-04/13, hep-ex/0408088.

[243] K. Abe *et al.* (Belle Collaboration), BELLE-CONF-0476, hep-ex/0411049.